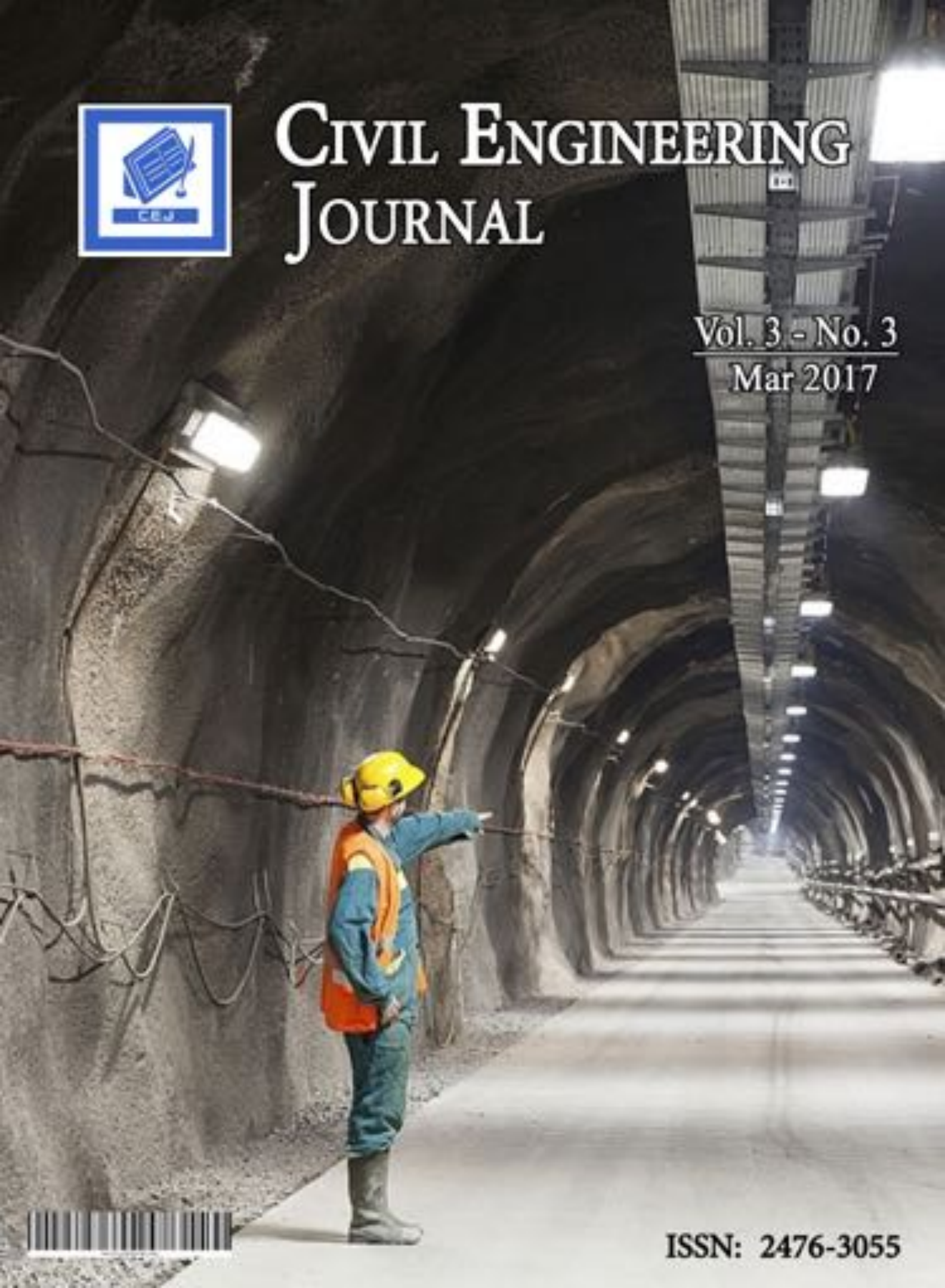

Civil Engineering Journal

Vol. 3 - No. 3
Mar 2017

ISSN: 2476-3055

Civil Engineering Journal (ISSN: 2476-3055)

3rd Issue 2017

www.CivileJournal.org

Contents

Vol. 3, No. 3, March, 2017

Phone: +98-21-88779475-ext. 258
Fax: +98-21-88779674
E-mail: office@civilejournal.com
Website: www.CivileJournal.org

Mailing Address: Dr. Kavianpour office, 3rd Floor of Civil Engineering Faculty, K.N.Toosi University of Technology, No. 1346, ValiAsr St, Mirdamad Intersection, Tehran, Iran

Civil Engineering Journal

Focus and Scope

Civil Engineering Journal (C.E.J) is a multidisciplinary, an open-access, internationally double-blind peer-reviewed journal concerned with all aspects of civil engineering, which include but are not necessarily restricted to:

- Building Materials and Structures
- Coastal and Harbor Engineering
- Constructions Technology
- Constructions Economy and Management
- Earthquake Engineering
- Environmental Engineering
- Renovation of Buildings
- Geotechnical Engineering
- Highway Engineering
- Hydraulic and Hydraulic Structures
- Road and Bridge Engineering
- Structural Engineering
- Surveying and Geo-Spatial Engineering
- Transportation Engineering
- Tunnel Engineering
- Urban Engineering and Economy
- Water Resources Engineering
- Urban Drainage

Special Issues

Special Issues deal with more focused topics with high current interest falling within the scope of the journal in which they are published. Special Issue proposals are welcome at any time during the year.

For most of the civil engineering conferences it is possible to submit papers presented at the conference for subsequent publication in special issues of the C.E.J.

- **Civil Engineering Journal (C.E.J) is published monthly.**
- **Civil Engineering Journal (C.E.J) has fast peer review process (3-4 weeks).**

Civil Engineering Journal (C.E.J) Indexing & Abstracting

Available online at www.CivileJournal.org

Civil Engineering Journal

Vol. 3, No. 3, March, 2017

Evaluation of the Performance of Rainwater Harvesting Systems for Domestic Use in Tlalpan, Mexico City

Niall Nolan [a*], Cecilia Lartigue [b]

[a] *Engineers Without Borders - UK, The Foundry, Oval Way, London SE11 5RR, UK.*

[b] *National Autonomous University of Mexico (UNAM), Programa de Manejo, Uso y Reuso del Agua (PUMAGUA), Circuito Escolar S/N Torre de, Ingeniería, Cd. Universitaria, 04510 Ciudad de México, D.F.*

Received 30 November 2016; Accepted 14 March 2017

Abstract

Rainwater harvesting (RWH) as an alternative means of providing water in domestic contexts, is viewed as an effective supply option worldwide. In Mexico City, the water situation is critical and the provision of water services to the population represents a formidable challenge for the city's water utilities. The main objective of this study is to evaluate the potential for RWH to supply domestic properties in Tlalpan, 1 of 16 delegations in the city with one of the highest percentages of homes unconnected to the distribution network. Results show RWH can meet 88% of household water demand during the 6 month wet season, with an annual saving of 55%. Modelling a World Health Organisation minimum demand of 20 l/p/d as a means of resilience management in the event of a water crisis, 6-month and annual savings were 99% and 80% respectively. The minimum tank size to achieve wet season savings of 90% was 6 m^3 in two precipitation bands and tank sizes of 13,000 – 17,000 L were sufficient in 3 out of 4 to prevent overspill. The report concludes RWH is a viable method of providing water in the south of the city and should be part of an integrated water management solution.

Keywords: Isla Urbana; Mexico City; Pipas; Rainwater Harvesting; Water Crisis; Water Supply.

1. Introduction

The issue of water scarcity is a significant and increasing threat to the environment, human health, development, energy security and the global food supply. Growing populations with increased wealth and consumptive behaviour, combined with current water management policies, will see the demand for water rise exponentially, while supply becomes more erratic and uncertain [1].

In Mexico, a country of 125 million people [2], the population quadrupled during the period 1950 to 2010. The migration was from mostly rural to predominantly urban areas with now more than 75% of the population living in urban zones, while the availability of water in the country during this time has been significantly reduced [3].

Mexico City suffers from multiple and inter-related problems regarding the quality and availability of its water supply, which so far the Government has failed in addressing adequately [4, 5]. It is the capital of the country and also one of the most vulnerable areas to water scarcity. Currently the water situation is critical, with projections to 2030 indicating that the availability of water per capita in the Valley of Mexico (where the city is located) is only going to get much worse, necessitating the search for additional, sustainable sources to help redress the problem now [6].

In addition to water scarcity; land subsidence as a result of aquifer overexploitation, inefficient water use, concerns about the reuse of wastewater in agriculture, low share of wastewater treatment, child mortality linked to gastroenteric diseases and limited cost recovery, are all problems which seriously affect the city [7]. As a result of the ageing infrastructure and land subsidence, the thousands of kilometers of primary and secondary pipes in the supply system

* Corresponding author: niall_nolan99@hotmail.com

leak almost 40% of the water they are tasked with distributing [7]. Government initiatives thus far been unable to keep up with repairing these leaks, which results in more water being pumped to meet the demand and further exacerbating the unsustainable feedback loop. Water policies have favoured large-scale infrastructure projects such as the Lerma-Cutzamala system, responsible for supplying the metropolitan area with approximately 31.4% of its water [8]. These solutions are incredibly energy intensive, equivalent to the entire energy demands of the nearby city of Puebla, as the water must be pumped 1000 m vertically over mountains before reaching the population of the metropolitan area [7].

Somewhat counter-intuitively, while Mexico City's residents lack access to water, the urban area also receives a significant amount of precipitation during the well-defined rainy season, from late May through to early October [9]. A United Nations Environment Programme [10] report advocated for the inclusion of rainwater harvesting as an important resource in water management policies and one that can reduce negative impacts on water-stressed basins. Studies globally have shown RWH is an effective means of augmenting existing supply capabilities and can produce significant water savings in various contexts all over the world [11-13].

In the Valley of Mexico, frustratingly from a RWH perspective, the rain that falls in the urban area is currently not valued or utilised to such an extent that it currently expels more rain water from the basin than it manages to recharge in the main aquifers [14]. The geography of the city, located on the flat bed of what was once a series of lakes, has no natural drainage outlet meaning that the rainwater does not flow into streams or rivers to replace surface and ground water sources. Only 10% [15] is estimated to find its way back to the aquifer while the remainder is collected in the drains, mixed with sewage and pumped straight out of the valley.

A unique feature of Mexico City compared to other global contexts where RWH has been adopted is that most of the residents already have an existing cistern or form of water tank at their property due to the year-round intermittent supply [16]. As this is generally the most expensive component of a RWH system, connecting this through an effective conveyance and filtering system could be an achievable solution. In light of the confirmed need to find additional water sources to supply the city, RWH should be a part of an integrated solution to the water crisis which is given serious consideration [4, 5].

1.1. Study Area

One of the delegations with the lowest connectivity to the network is Tlalpan located in the south of the city. Large parts of the delegation are peri-urban and contain many informal settlement areas where connection to centralised water distribution infrastructure is difficult. It has an estimated population of 646,715 and of the 175,983 private dwellings, 27.5% do not have access to piped water from the network inside their homes [17]. These communities must rely almost solely on water delivery trucks, colloquially known as pipas, for their supply. These pipas can either be a public or private service and the price range can vary greatly depending on government subsidy rate and the type and quality of vendor. Reliability and speed of service can also vary, with some households having to request another pipas delivery almost immediately after they have received one due to the slow turnaround time between request and delivery [18]. Safety is also a great concern as in the under-developed areas of the delegation; road quality is poor with surfaces and sizes insufficient for large and heavy vehicles trying to navigate to their delivery point. To date, publically available information on the pipas program is scarce or non-existent and no serious attempts have been made to evaluate how rainwater harvesting could help mitigate against reliance on these during the rainy season in Mexico City.

1.2. Objective

The main objective of this study then is to determine the amount of rainwater available throughout Tlalpan and subsequently the potential for RWH to meet potable water demand and mitigate against pipas reliance in the area. In addition, as cisterns are the most expensive component of a RWH system, the study will estimate the smallest tank size which will still provide 90% demand satisfaction during the rainy season. A method of estimating the tank size required to prevent any overspill during the rainy season is also presented.

For these objectives, the study will use systems designed and installed by Isla Urbana, a social enterprise based in Mexico City who has carried out a significant number of installations of RWH systems, particularly in the south of the city. Figure 1. shows a typical system as designed by Isla Urbana.

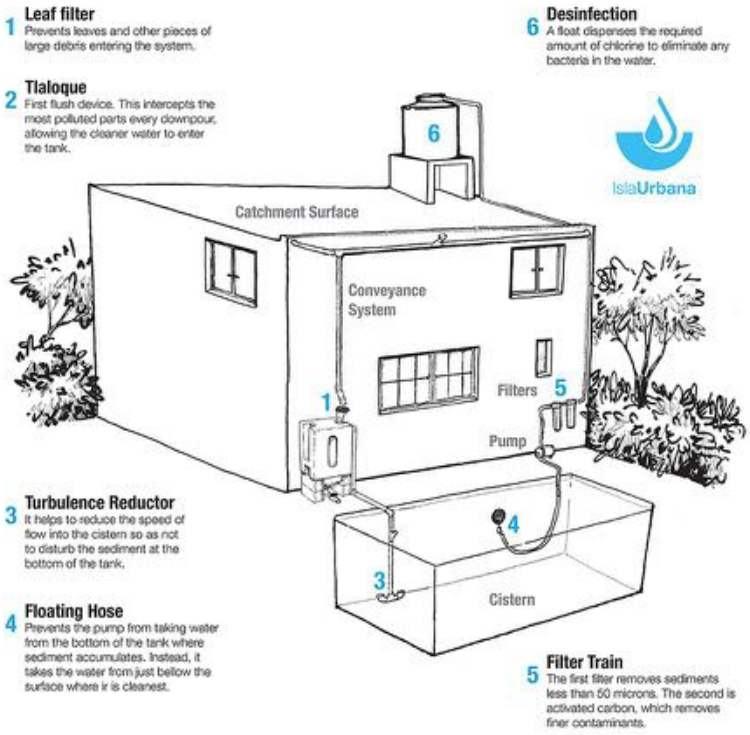

Figure 1. Typical RWH system as designed by Isla Urbana. The components as installed by Isla Urbana system are numbered 1-6 and the more general components labelled. Source: Author's compilation based on existing Isla Urbana graphic design

2. Method

To model the potential for RWH in Tlalpan where Isla Urbana has installed a number of systems, a survey of 1186 properties was carried out at the time of installation. The data was later analysed to ascertain information relating to catchment surface, number of occupants per household and tank size. The data was filtered to remove incomplete entries or properties that were non-domestic, leaving a sample size of 1034 properties. A further survey of 10 properties was carried out at a later date in Tlalpan to ascertain a figure for average potable water demand per person per day.

The properties, within their colonias (neighbourhoods), were approximately divided into four precipitation bands relating to their location and proximity to the four weather stations based on data mapped in Google Maps. From here, the data was filtered to obtain averages for the different inputs for each precipitation band: rainfall data; catchment surface; runoff and filter coefficient; average household occupancy and tank size.

To model the system performance and to determine the ideal rainwater tank capacity, a computer model developed by Ghisi, Tres & Kotani [19] called Netuno was used. This tool has previously been applied in the south-east of Brazil to estimate the potential for water savings using RWH. Information about its validation can be found in Rocha [20]. The model takes into account daily rainfall data, catchment surface, household water demand, number of people per dwelling, coefficient for losses and tank size.

2.1. Rainfall Data

Daily rainfall data was obtained from the National Water Commission (CONAGUA), across four weather stations in Tlalpan: Calvario 61; Al Pedregal; Ajusco and El Guarda. Figure 2. shows the different precipitation bands within Mexico City and the approximate location of the weather stations within Tlalpan. Figure 3. shows a satellite view of Tlalpan, with the urban and peri-urban areas visible. The daily rainfall data ranged from 1961-2008 but did not cover the same period for all stations and some records were missing, meaning consecutive daily data was not possible for all of this period. To include change in precipitation due to climate change, it was decided to only include the most recent 20 years (El Guarda, 15 years) where full daily rainfall data was available.

Figure 2. Precipitation bands of the Federal District with the sixteen delegations labelled.

(Tlalpan is in the south of the city, with four different precipitation bands visible. Source: Author's compilation based on existing Isla Urbana graphic design)

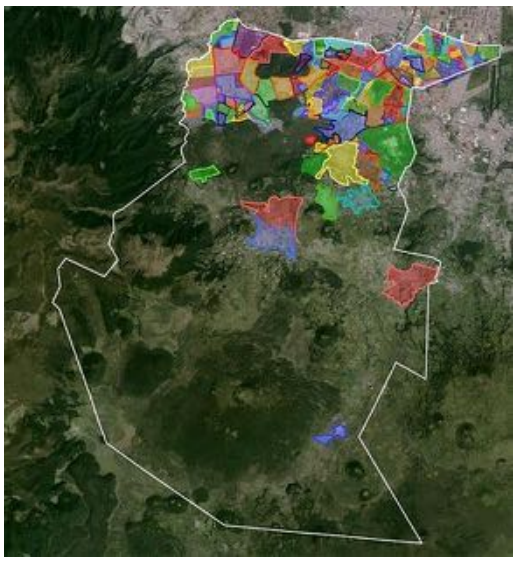

Figure 3. Satellite image of Tlalpan delegation in the south of the city.

(The Al Pedregal precipitation band in the north is the most urbanised zone, generally with better connection to grid water. As we move further south to the Ajusco and El Guarda precipitation bands, the numbers of properties connected to the grid is reduced. Properties in these bands rely most on water from the pipas trucks. Source: Map of colonies of the Delegation)

2.2. Catchment Surface

Values were obtained for average catchment surfaces across the properties within the different precipitation bands. It is important to note that the initial survey of 1034 properties only included the catchment surface where the RWH system was installed and not the total roof area available to the property. The modelled results therefore could underestimate the potential for water savings which a property could achieve.

2.3. Average Number of People per Dwelling

The modal number of people per dwelling was calculated for each precipitation band from the properties surveyed.

2.4. Coefficient for Losses

The coefficient for losses takes into account water losses between the roof and cistern, including evaporation and first flush. In the literature, values for roof runoff coefficients used in modelling typically range from 0.7-0.95 [21] In a study carried out by KANRRC [22] it was suggested that roof absorption losses dominated for rainfall events less than 3 mm, resulting in a low runoff coefficient. Roof material was therefore included in the survey and any day with less than 3 mm rainfall was taken as a zero precipitation day.

2.5. Tank Size

From the survey in Tlalpan, the median tank sizes (lower tank) across the precipitation bands were calculated to model current average hydraulic performance. No data was available on the size of the roof tanks and so these were not included in the model.

2.6. Water Availability

The total volume of rainwater V available for capture in each precipitation band was estimated using Equation 1. where: R equals monthly rainfall amount; an average roof size and R_c runoff coefficient.

$$V = R \times A \times R_c \quad (1)$$

2.7. Water Demand

This study assumes a single value for water demand for daily time-steps, as applied by a number of similar studies [12, 23]. In addition, the study assumed that water from the cistern was only used for internal purposes. Rainwater demand was modelled as 100% of potable water demand, i.e. it is used for all internal purposes. It should also be noted

again that this investigation for potable water savings is primarily for houses which are unconnected to the main water network or have extremely intermittent supply (1-2 days a week) and rely largely on pipas. They therefore are extremely conscientious and efficient water users (using informal greywater systems to flush toilets etc.) and so demand is typically lower than for properties in other parts of the city where water availability is much greater. Tortajada [7] refers to 20 litres per capita per day as being typical in some of the poorer areas of Mexico City, and which the World Health Organisation (WHO) quotes as a minimum to meet a person's basic cooking and hygiene needs.

This was taken into consideration before carrying out a water demand survey of 10 properties within the Ajusco and Al Pedgreal precipitation bands, which represent peri-urban and urban areas respectively. Participants were asked three different questions relating to their demand: 1. How long it took them to use all the water in their cistern? 2. How frequently they had to request a pipas delivery? 3. How often they used their pump to supply their roof tank per week? In this way, it is possible to obtain three values for water demand which participants estimate they use and from this, take an average to obtain one more reliable figure for the water demand. The figure could then be divided by the number of people living at the property to discern a figure for the daily amount of litres used per person (l/p/d). Participants were also asked if they used the water for any external uses, to test the assumption that water is solely for internal end-uses.

2.8. Ideal Tank Size

As Mexico City has a rainy season approximately 6 months in length, it was deemed most pertinent to calculate the smallest possible tank size which will still give a demand satisfaction of 90% over the 6 months June to November. In this way performance can be balanced with cost, as cisterns are generally the most expensive component of the system.

3. Results

3.1. Rainfall Data

Figure 4. shows that across the four weather stations there is a large amount of rainfall available, ranging from 870 mm per year in Calvario 61 to 1484 mm per year in El Guarda. This represents a 52% difference within the delegation, justifying the need to divide the delegation into precipitation bands.

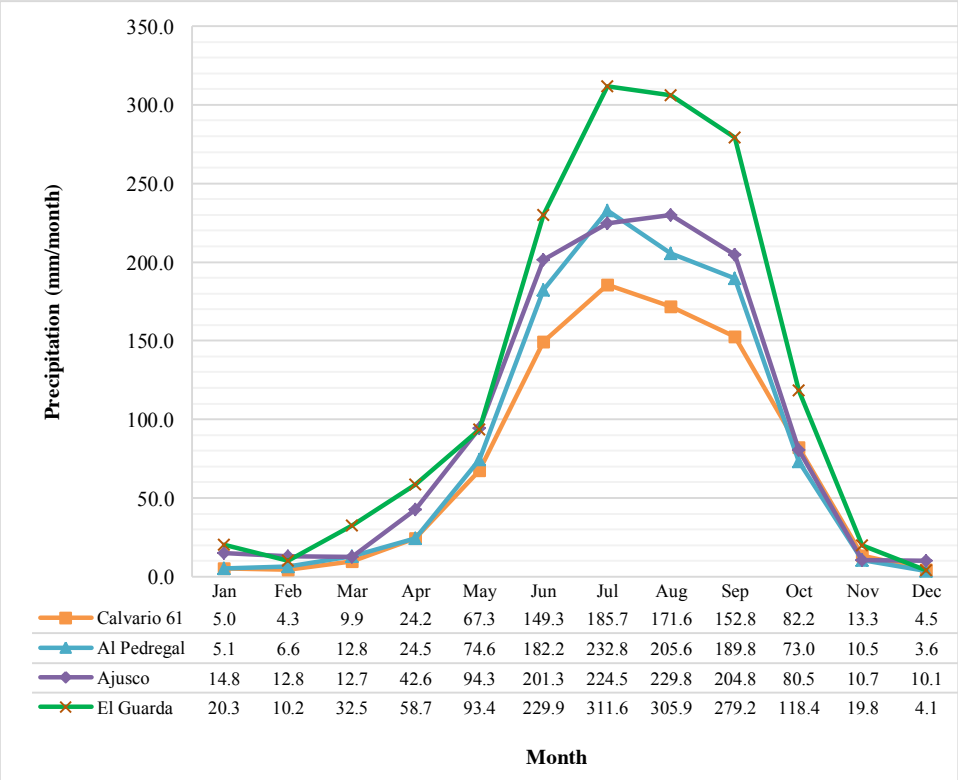

	Jan	Feb	Mar	Apr	May	Jun	Jul	Aug	Sep	Oct	Nov	Dec
Calvario 61	5.0	4.3	9.9	24.2	67.3	149.3	185.7	171.6	152.8	82.2	13.3	4.5
Al Pedregal	5.1	6.6	12.8	24.5	74.6	182.2	232.8	205.6	189.8	73.0	10.5	3.6
Ajusco	14.8	12.8	12.7	42.6	94.3	201.3	224.5	229.8	204.8	80.5	10.7	10.1
El Guarda	20.3	10.2	32.5	58.7	93.4	229.9	311.6	305.9	279.2	118.4	19.8	4.1

Figure 4. Monthly rainfall of the four weather stations in Tlalpan

A summary of the different inputs within the four different precipitation bands is summarised in Table 1.

Table 1. Summary of hydraulic details

Weather station	Sample size	Rainfall (mm/yr)	Catchment surface (m^2)	No. of people per household	Tank size (m^3)	Runoff & filter coefficient[a]
Calvario 61	333	870	60	5	10	0.72
Al Pedregal	416	1021	60	5	8	0.72
Ajusco	272	1139	55	4	10	0.72
El Guarda	13	1484	70	5	12	0.72

[a] Based on the properties surveyed, concrete slabs are the most common roof material in Tlalpan, which has a high runoff coefficient compared to other roof materials. A value therefore of 0.80 and 0.90 was chosen to account for roof and first-flush losses and filter losses respectively

3.2. Water Availability

Table 2. shows the monthly volume of rainwater that is available for each household to harvest based on the methodology already described and hydraulic details in Table 1.

Table 2. Average volume of rainwater that is available to harvest in each precipitation band

Month	Calvario 61		Al Pedregal		Ajusco		El Guarda	
	Rainfall (mm/month)	Volume (L)	Rainfall (mm/month)	Volume (L)	Rainfall (mm/month)	Volume (L)	Rainfall (mm/month)	Volume (L)
Jan	5	217	5	222	15	640	20	1022
Feb	4	188	7	285	13	553	10	514
Mar	10	427	13	553	13	549	32	1637
Apr	24	1043	25	1056	43	1838	59	2960
May	67	2907	75	3222	94	4074	93	4707
Jun	149	6452	182	7870	201	8695	230	11586
Jul	186	8020	233	10057	225	9698	312	15705
Aug	172	7415	206	8882	230	9926	306	15416
Sep	153	6599	190	8200	205	8847	279	14070
Oct	82	3551	73	3155	81	3479	118	5967
Nov	13	573	11	455	11	460	20	998
Dec	5	193	4	157	10	435	4	207
Total	870	37586	1021	44115	1139	49196	1484	74788

3.3. Potable Water Demand

Based on the 10 properties surveyed, water demand ranged from 22 l/p/d to 60 l/p/d with an average of 41 l/p/d, and no significant variation across the precipitation bands. In addition, all of the participants said the water was for internal end-uses only. It should be noted here the distinction between the total daily water demand and what is actually drawn from the cistern (which should be less). As explained previously, occupants in these underserved areas typically use informal greywater systems such as water collected from the shower to wash clothes, with this collected again and used to flush toilets. In this way, occupants may be using more than the figures listed above (as they recycle the water), but what they actually draw from the cistern ranges between 22 – 60 l/p/d. In this context, system performance was modelled across the bands for potable water demands 41 and 60 l/p/d representing expected and high daily consumption amounts respectively. In addition, a demand of 20 l/p/d was modelled representing the low demand as surveyed and in accordance with the WHO minimum amount to meet basic cooking and hygiene needs. This was modelled to see the potential for RWH in times of severe water crisis as part of a possible resilience management strategy in the city.

3.4. Potential for Potable Water Savings

An estimate for potential for potable water savings was estimated by comparing the monthly volume of rainwater that could be harvested with the different potable water demands in each of the precipitation bands. Figures 5 and 6. show the potential for potable water savings for 41 l/p/d and 60 l/p/d demand. The average annual volumetric savings for 41 l/p/d demand was 55%, with a range 45% to 66% in Calvario 61 and El Guarda respectively. Significantly though, during the six wet months June to November, average savings of 88% could be observed across the four precipitation bands for this demand. This indicates that under current conditions, RWH can effectively supply a

household their entire water needs for the whole wet season. When the demand was increased to 60 l/p/d, the annual and 6-month average potential savings fall to 43% and 73% respectively across the regions.

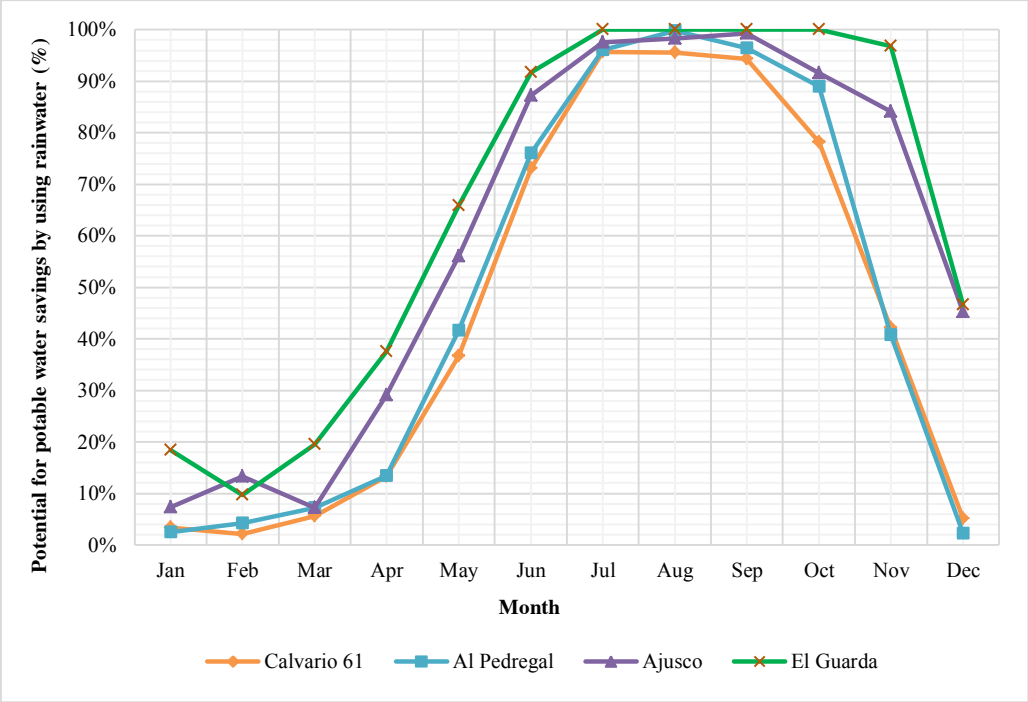

Figure 5. Potential potable water savings 41 l/c/d

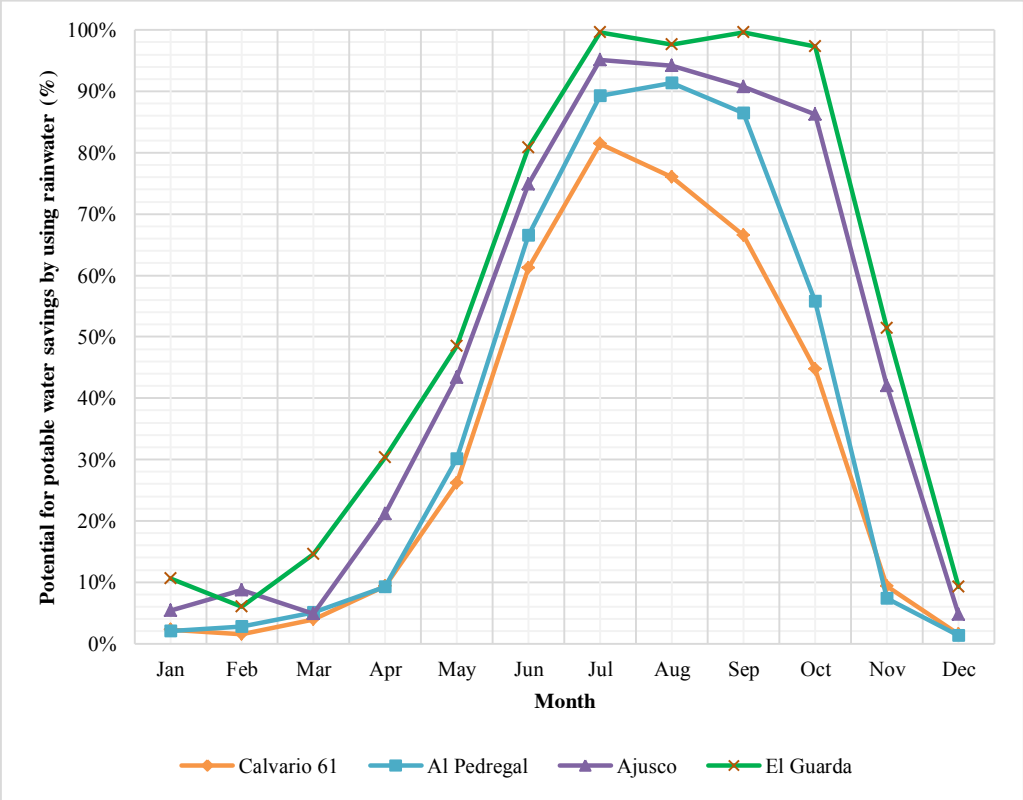

Figure 6. Potential potable water savings 60 l/c/d

3.5. Potential for Potable Water Savings Including Overspill

During the wet months, the results showed significant overspill at these demands. Figures 7 and 8. show the results for water savings including the overspill. During the months June to November, El Guarda, Ajusco and Al Pedregal

spilled on average approximately 42% of the water they could have potentially captured at 41 l/p/d demand. During the three wettest months of the year (Jul – Sep), potential for water savings including overspill ranged from 241% in El Guarda to 108% in Calvario 61, with an average of 186% across El Guarda, Ajusco and Al Pedregal. During these wet months therefore, properties in these bands could increase their consumption in line with the water which is available to them.

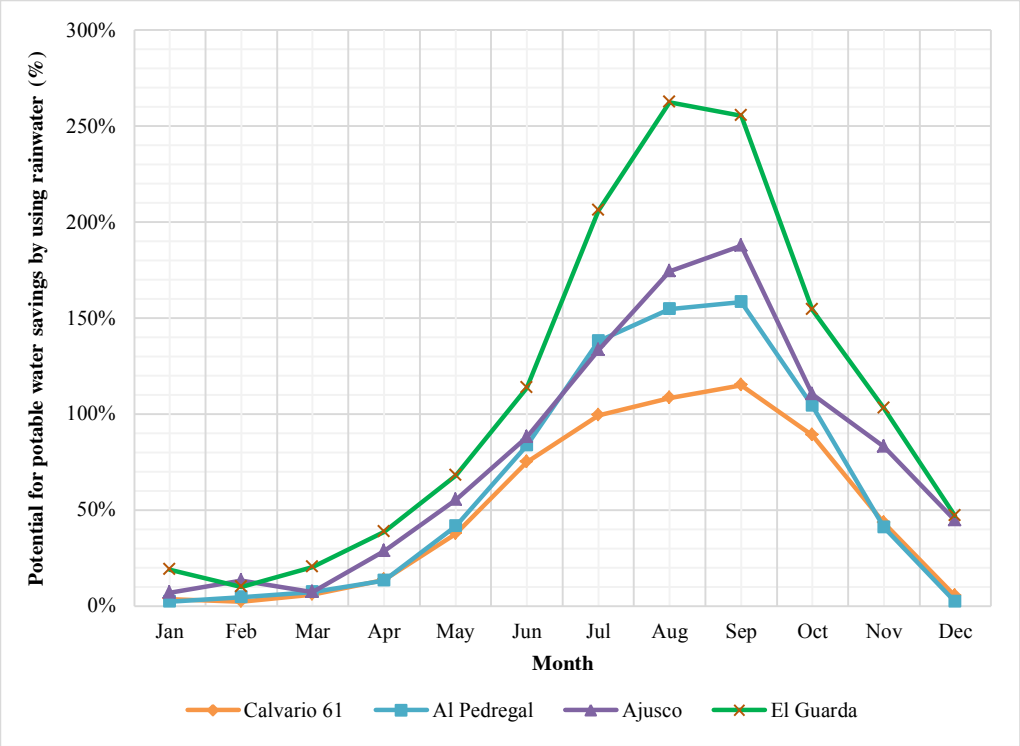

Figure 7. Water savings including overspill 41 l/c/d

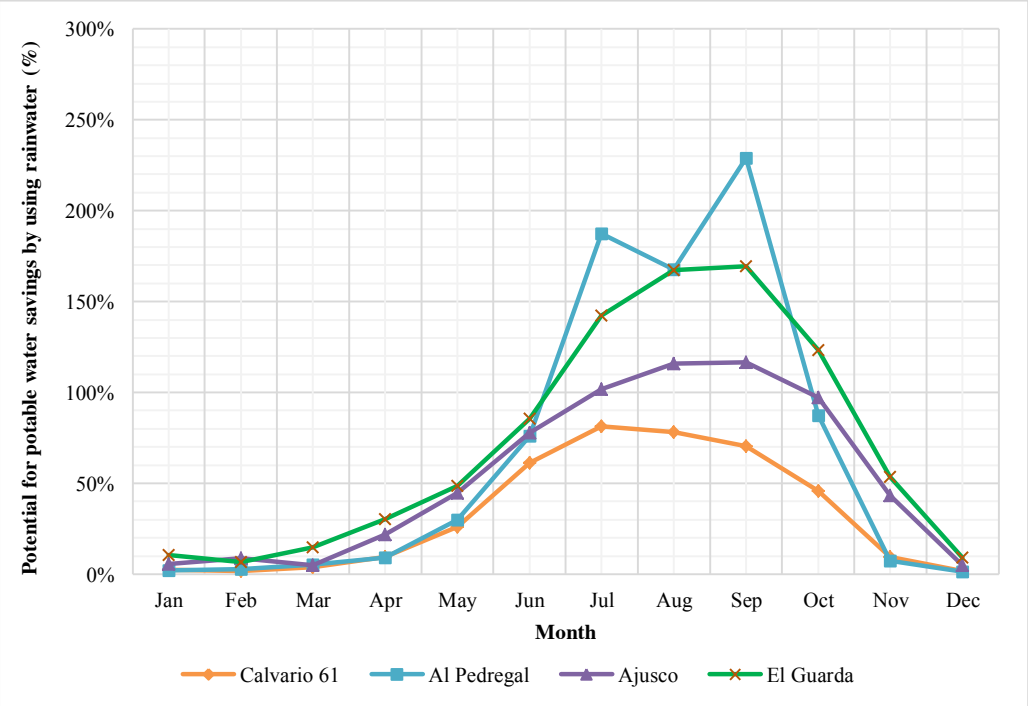

Figure 8. Water savings including overspill 60 l/c/d

3.6. Resilience Management

Figure 9. shows the results for a demand of 20 l/p/d and Figure 10. the water savings including overspill. The 6-month average potential for water savings across all bands was 99%. Significantly for this demand, annual averages ranged from 72% in Calvario 61 to 89% in El Guarda, with an average of 80% across all bands, meaning households can almost go an entire year solely on rainwater at this demand with existing average tank sizes and catchment surfaces.

As Figure 10. shows, at this demand households will be spilling a significant amount during the wet months and so it would not be necessary to manage consumption to such a low level for the entire year.

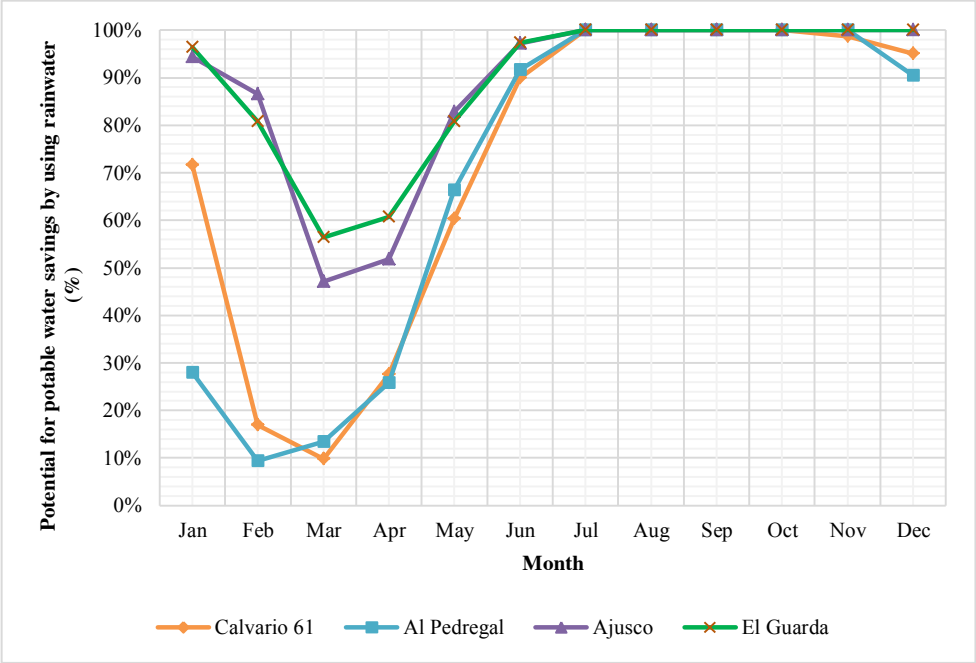

Figure 9. Potential potable water savings 20 l/c/d

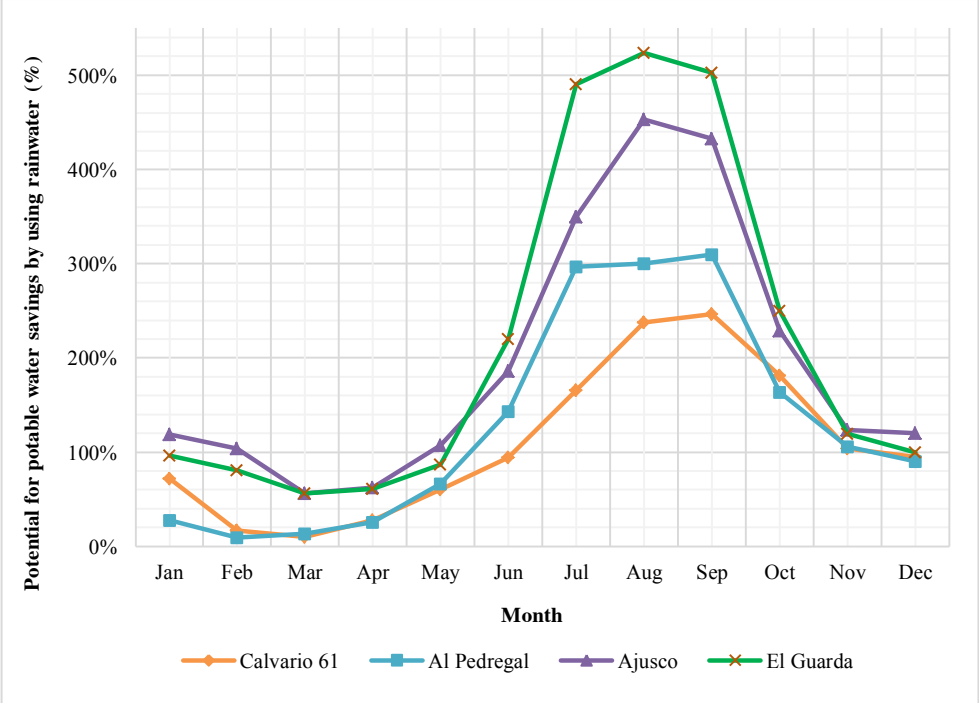

Figure 10. Water savings including overspill 20 l/c/d

3.7. Rainwater Tank Size

Ideal rainwater tank capacities to maximise performance were determined for households in the different precipitation bands, across the expected demand of 41 l/p/d using the computer simulation Netuno. Tank sizes were modelled between 5 m^3-15 m^3 representing the smallest tank size Isla Urbana install (if there is not an existing one) and the maximum commercially available size from a leading supplier. Figure 11. shows the 6-month average potential potable water savings for the expected demand of 41 l/p/d, across the precipitation bands with the 90% satisfaction line displayed. As can be observed, for the bands Ajusco and El Guarda, 6-month average savings of 90% with a tank size of 6 m^3 can be achieved. This is entirely achievable when we consider that this tank size is lower than the existing average cistern size in households as obtained in Table 1.

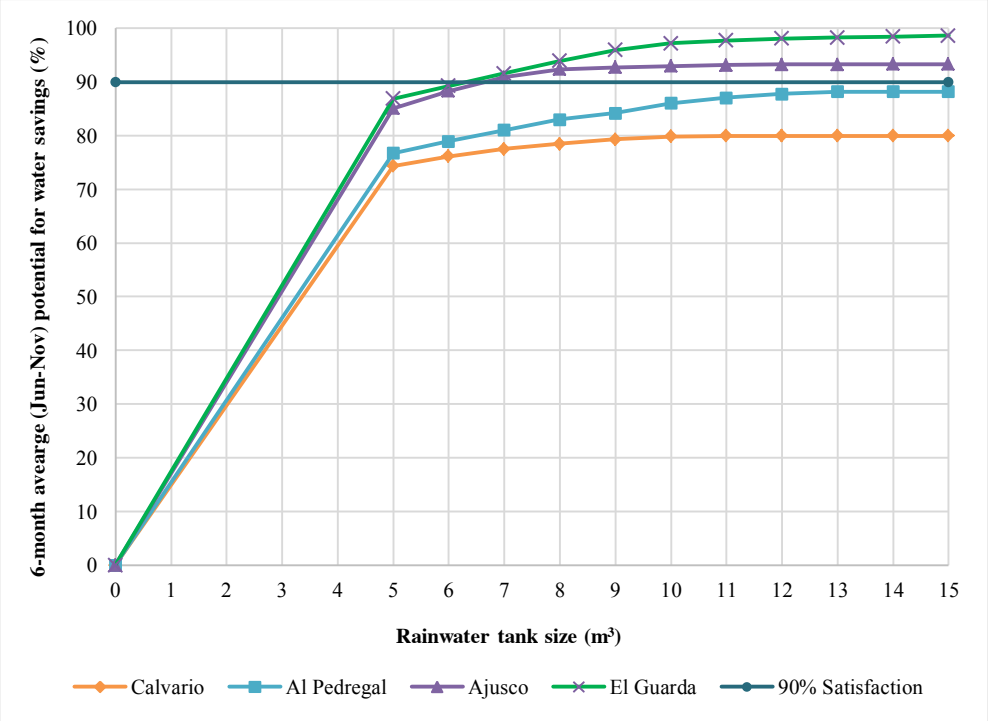

Figure 11. 6-Month average potential potable water savings with varying tank sizes

Given the significant amount of overspill observed in the results, it was deemed salient to investigate the tank size which would be sufficiently large to prevent any overspill so that all water could be (in theory) captured during the rainy season. As demand is a factor in overspill, the calculation assumes households will increase their demand to the higher limit of 60 l/p/d during the rainy season. From this, the tank sizes were increased in intervals of 1,000 L beginning from a 10,000 L tank (Figure 12.), until no overspill was observed as a function of captured rainwater. Due to the significant rainfall in the El Guarda band, a tank size of 20,000 L was still not sufficient to prevent any overspill at this demand. Tank sizes of 13,000-17,000 litres in the other bands were sufficient to prevent any overspill and wastage of water.

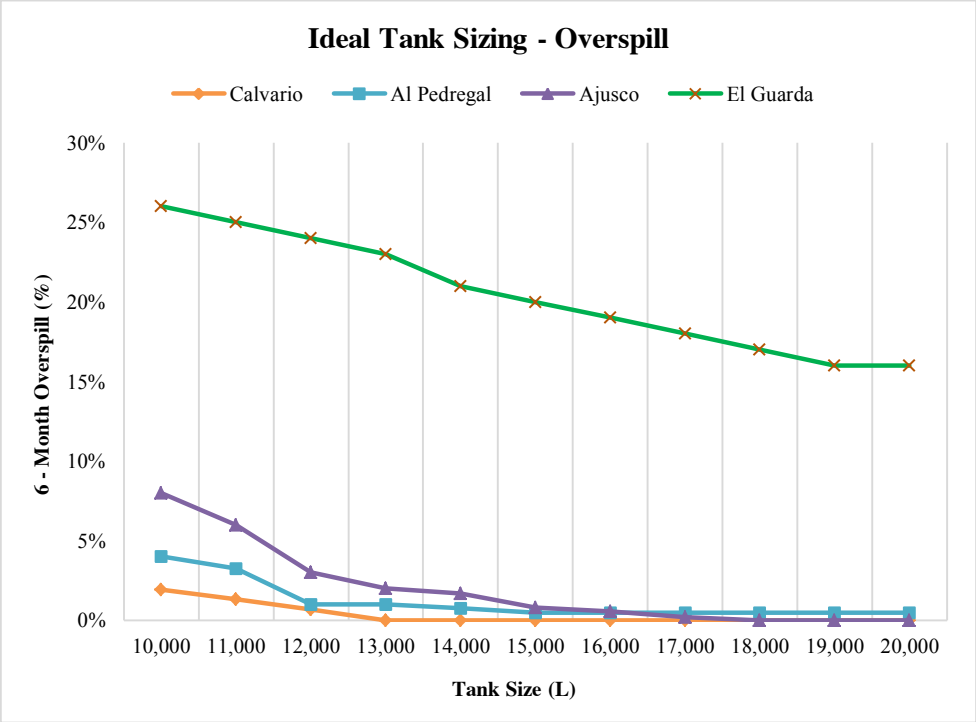

Figure 12. Tank sizes to prevent overspill

3.8. Potential for Rainwater Harvesting to Mitigate Reliance on Pipas

Assuming it is possible to install a RWH system in the 27.5% of homes in Tlalpan with no piped water inside their homes, it was estimated how many litres of water could be harvested and how many pipas trucks this would keep off the road in the entire delegation over a ten year analysis period. No data was available on the percentage of homes in each precipitation band with no access to piped water, so an average of the different inputs (Table 3) across the precipitation bands was deemed appropriate to model the whole delegation. When the figures were tested through the model, annual potable water savings of 55% and 6-month savings of 90% could be observed, with the total annual volume of water harvested 41m^3. Taking 27.5% of the 175,983 domestic homes in Tlalpan with no access to piped water inside of their homes, leaves 48,395 unconnected households. If each of these had an average RWH system as above, they could collectively harvest 1,979,300 m^3 (1m^3 = 1000 L) of water annually, with ten years savings of 19,793,000 m^3. The average number of people per household is 5 as above, meaning RWH systems could benefit almost a quarter of a million people if they were installed. In terms of savings in pipas journeys, taking the average delivery amount as one tank full i.e. 10 m^3 as above, over a ten year period, almost 2 million pipas could be kept off the road. This is a hugely significant figure from just one delegation when the issues of pollution, greenhouse emissions relating to pollution and road safety which affect the city are considered.

Table 3. Average of the hydraulic details across the precipitation bands

Input	Value
Rainfall	Ajusco
Roof area (m^2)	60
Tank size (L)	10000
No. of people per household	5
Runoff Coefficient	0.72
Demand (l/p/d)	41

3.9. Sensitivity Analysis

A sensitivity analysis was carried out to ascertain the effect of the four key variables on the annual yield in each precipitation band. As the distribution of the data was known, low and high values were taken as a standard deviation either side of the mean or median values (depending on the measure of central tendency used). The base case annual yield was estimated using the average values already obtained from Table 1. in each precipitation band. Each variable was then individually set to the corresponding high and low estimates to develop the 'tornado chart' (Figure 13). The

sensitivity of the results to changes in each variable could then be individually identified. Each band showed different sensitivity to the various variables. Roof area and number of occupants were two characteristics in each band which showed large variation in yield when the values were adjusted from low to high around the base case (all other variables were held constant). In the worst performing areas (Al Pedregal and Calvario 61), an increase in roof size of 18 m^2 and 20 m^2 could increase the yield by 28% and 48% respectively. Given that the original survey included only connected roof area and not total roof area, it is possible households in these bands could potentially avail of these extra potential water savings if all the roof was connected.

3.10. Discussion

3.10.1. Current RWH Policies in Mexico City

Currently, the Mexico City water authority SACMEX, has not invested in any large-scale rainwater harvesting programme, either for domestic rooftop harvesting or aquifer recharge. This is despite the Water Law of 2003 which calls for rainwater harvesting to be installed in new buildings and encourages its implementation in existing constructions [24]. Rainwater was also included in the Law for Climate Change Adaptation and Mitigation of 2012 but has yet to materialise into a structured RWH implementation plan. Existing literature and accepted opinion on the water situation in Mexico City has acknowledged the fact that the "availability of water has already reached its maximum viable point in spite of all technological innovations and large infrastructure development" [4]. One of the most common disadvantages cited globally against RWH is the significant space requirement for the storage tank [25]. However, in Mexico City where the majority of the population already own a cistern, this is less of an issue and presents the city with a unique, currently unexploited opportunity.

3.10.2. Comparison of RWH Policies throughout the World

In Brazil, the government has launched several rainwater harvesting programs for small-scale and domestic agriculture. Around 700, 000 cisterns have been built for this purpose in semi-arid regions of the country [26]. A study by Ghisi et al. [12] in south-eastern Brazil, found RWH to be a potentially very significant source of water to meet the demand. In Australia, rainwater harvesting is commonplace with many state governments making them mandatory in new housing developments [11, 27]. In Germany, local governments in many towns award grants and subsidies for construction of rainwater tanks and seepage wells [28]. In countries with less water availability such as Spain, RWH is being looked at as an option although uptake so far has been slow. Morales-Pinzón et al. [29] found RWH to be undervalued in Cataluña, Spain where systems have only been installed in low density areas and in individual houses. In Singapore, RWH schemes have included high-rise buildings, airports, and integrated systems using the combined run-off from industrial complexes, aquaculture farms and educational institutions [28]. In India, rooftop rainwater harvesting systems are now compulsory for new buildings in 18 of India's 28 states and four of its seven federally-administered union territories [30].

3.10.3. Opportunities for Future Study

The ideas and methods presented in this study can be used in similar contexts throughout the Mexico City metropolitan area and further studies may look to carry out a larger survey of water demand, breaking it down at a Delegational level as currently figures range from 20-600 L [7] which make it difficult to scale-up and estimate the potential to supply demand across the city. The authors also recommend additional studies into the potential for RWH to offset aquifer overexploitation if implemented on a much larger scale, in both domestic and commercial contexts. There also exists fertile ground for research into the potential for RWH to delay the construction of further large-scale infrastructure projects (extending the Cutzamala system for example) and for its ability to mitigate against flooding in high-risk areas.

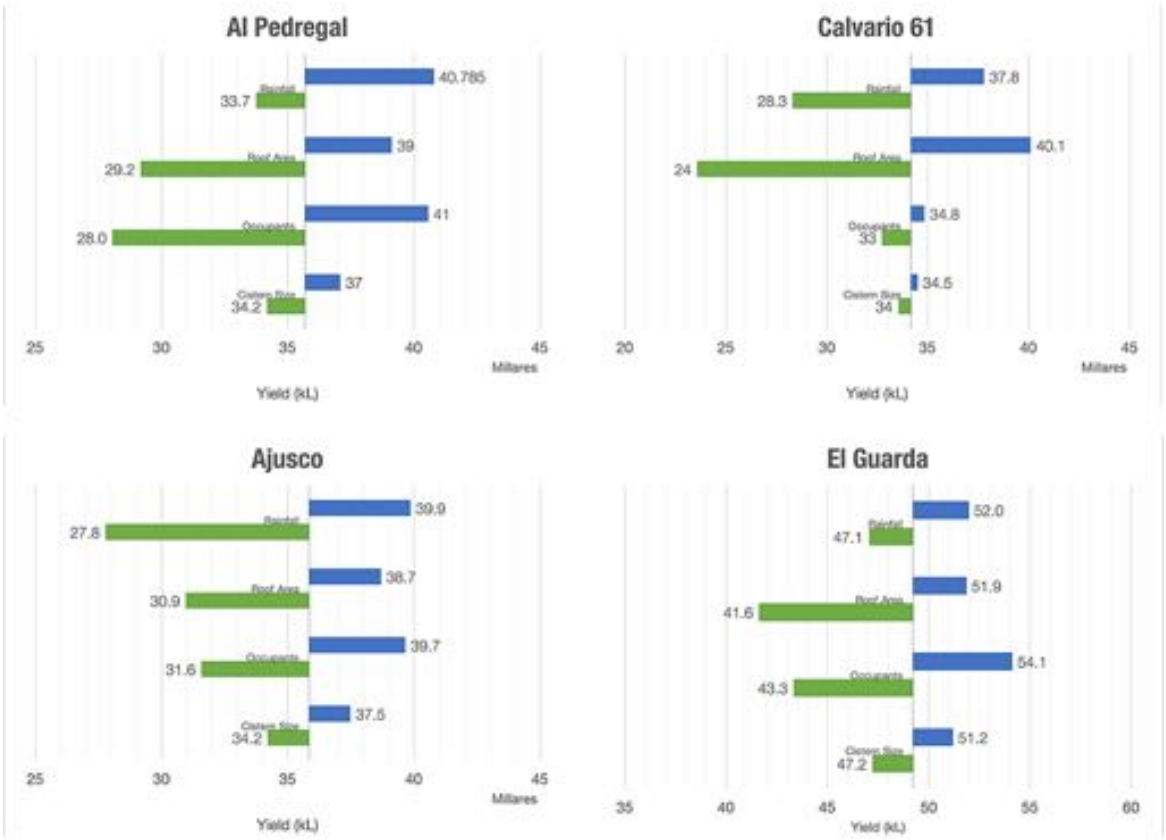

Figure 13. Annual yield varied by key factors

4. Conclusion

The availability of water for households in some areas of Mexico City is severely limited, with families unconnected to the network having to rely on pipas for delivery. In Tlalpan, where there is a high percentage of people not connected to the network, the potential for potable water savings by using rainwater was assessed across different precipitation bands. Results of the research performed indicate there is a large amount of annual rainfall available in the delegation, ranging from 870-1484 mm, with significant variation in amount across areas. The average 6-month saving for the expected and above average demands of 41 and 60 l/p/d across the bands was 81%. The annual saving across the bands and demands was 49%. The overspill graphs showed that demand could be increased during the wetter months. A tank size of 6 m^3 could still provide 90% of potable water to families in two of the bands during the wet months. The report also found that large-scale implementation of RWH could positively impact a large number of people in Tlalpan and dramatically reduce the need for pipas, resulting in much fewer journeys made per year, helping with traffic, safety and pollution issues in the city.

5. Acknowledgment

The authors thank Engineers Without Borders – UK for providing funding for the placement during which the majority of the research was conducted and to Isla Urbana for providing access to their dataset, relating to actual installed systems in the south of Mexico City.

6. References

[1] World Bank. High and Dry: Climate Change, Water, and the Economy. World Bank, Washington, DC. (2016).

[2] Consejo Nacional de Población (CONAPO). (2010). Proyecciones De La Población 2010 - 2050. [Projection of the Population 2010 – 2050].

[3] Comisión Nacional del Agua (CONAGUA). (2010). Statistics on Water in Mexico. 2010 Edition, 1-15.

[4] Delgado-Ramos, Gian Carlo. "Water and the political ecology of urban metabolism: the case of Mexico City." Journal of Political Ecology 22, no. 9 (2015).

[5] Jiménez, Blanca. "The unintentional and intentional recharge of aquifers in the Tula and the Mexico Valleys: The Megalopolis

needs Mega solutions." In Rosenberg Symposium, Buenos Aires, Argentina. 2010.

[6] SEMARNAT. (2012). Informe de la situación del medio ambiente en México [Report of the situation of the environment in Mexico]. Retrieved from http://app1.semarnat.gob.mx/dgeia/informe_12/06_agua/cap6_1.html.

[7] Tortajada, Cecilia. "Water management in Mexico City metropolitan area." Water Resources Development 22, no. 2 (2006): 353-376. doi.org/10.1080/07900620600671367

[8] Romero Lankao, Patricia. "Water in Mexico City: what will climate change bring to its history of water-related hazards and vulnerabilities?." Environment and Urbanization 22, no. 1 (2010): 157-178. doi.org/10.1177/0956247809362636

[9] Magaña, Víctor, Joel Pérez, and Matías Méndez. "Diagnosis and prognosis of extreme precipitation events in the Mexico City Basin." GEOFISICA INTERNACIONAL-MEXICO- 42, no. 2 (2003): 247-260.

[10] Barron, Jennie. Rainwater harvesting: a lifeline for human well-being. UNEP/Earthprint, 2009.

[11] Coombes, Peter J., John R. Argue, and George Kuczera. "Figtree Place: a case study in water sensitive urban development (WSUD)." Urban Water 1, no. 4 (2000): 335-343. doi.org/10.1016/S1462-0758(00)00027-3

[12] Ghisi, Enedir, Diego Lapolli Bressan, and Maurício Martini. "Rainwater tank capacity and potential for potable water savings by using rainwater in the residential sector of southeastern Brazil." Building and Environment 42, no. 4 (2007): 1654-1666. doi.org/10.1016/j.buildenv.2006.02.007

[13] Hajani, Evan, and Ataur Rahman. "Reliability and cost analysis of a rainwater harvesting system in peri-urban regions of Greater Sydney, Australia." Water 6, no. 4 (2014): 945-960. doi.org/10.3390/w6040945

[14] Labadie, J.L, Valdivia, J.M., Sánchez, A.G., Hermosillo, O.M., Orozco, M.F., Llana, C.V.P., Barragán, P.M. Repensar La Cuenca: La Gestión De Ciclos Del Agua En El Valle De México, 1, no. 1 (2010): 1–26.

[15] Burns, E. "¿De Dónde Vendrá Nuestra Agua?" Guía hacia la Sustentabilidad en la Cuenca de México. Guardianes de los Volcanes y Fondo Mexicano para la Conservación de la Naturaleza. México, Comisión Ambiental Metropolitana-Programa, UAM. (2006).

[16] Instituto Nacional de Estadística y Geografía [Institute of Nacional Statistics and Geography] (INEGI) (2010a). Retrieved from http://www3.inegi.org.mx/sistemas/sisept/default.aspx?t=mamb287&s=est&c=32905

[17] Instituto Nacional de Estadística y Geografía (INEGI) (2010b). Panorama sociodemográfico del Distrito Federal [Socio-Demographic Outlook of the Federal District]. Retrieved from http://documents.mx/documents/delegaciones-panorama-df.html.

[18] Isla Urbana. (2015). Encuestas de Seguimiento en la delegación Tlalpan [Questionnaire in the delegation Tlalpan]. August 2015.

[19] Ghisi E, Tres ACR, Kotani M. Netuno—aproveitamento de aguas pluviais no setor residencial [Neptune—a computer programme to evaluate potable water savings and rainwater tank capacity in the residential sector] (In Portuguese). (2004).

[20] Rocha, V.L. Validação do algoritmo do programa Netuno para avaliação do potencial de economia de água potável e dimensionamento de reservatórios de aproveitamento de água pluvial em edificações. (2009). [Validation of the Algorithm of the Netuno Computer Programme to Assess the Potential for Potable Water Savings and Sizing of Rainwater Tanks for Rainwater Usage in Buildings]. Master's Dissertation. School of Civil Engineering, Federal University of Santa Catarina, Florianópolis, Brazil, 2009.

[21] Sharma, Ashok K., Donald Begbie, and Ted Gardner, eds. Rainwater Tank Systems for Urban Water Supply. Iwa Publishing, 2015. 1-18. doi.org/10.2166/9781780405360

[22] KRANRRC. Harvesting For Sustainable Water Resources Development and Climate Change Adaptation in an Arid Region (N-E of Iran), Khorasan Razavi Agricultural & Natural Resources Research Center and The Institute For Global Environmental Strategies. (2011).

[23] Palla, A., I. Gnecco, and L. G. Lanza. "Non-dimensional design parameters and performance assessment of rainwater harvesting systems." Journal of Hydrology 401, no. 1 (2011): 65-76. doi.org/10.1016/j.jhydrol.2011.02.009.

[24] Ley de Aguas Nacionales. (2003). [National Water Law].

[25] Islam, Kamal Ziaul, Md Sirajul Islam, Jean O. Lacoursière, and Lisa Dessborn. "Low cost rainwater harvesting: An alternate solution to salinity affected coastal region of Bangladesh." American Journal of Water Resources 2, no. 6 (2014): 141-148. doi.org/10.12691/ajwr-2-6-2

[26] Heijnen, H. Enhancing economic resilience in North Eastern Brazil by harnessing rain. Rainwater Harvesting Implementation Network (RAIN), Amsterdam. (2013).

[27] Associates, M. J. (2007). The cost-effectiveness of rainwater tanks in urban Australia. Waterlines (Vol. 2008).

[28] Rainwater Harvesting Organisation. Rainwater Harvesting in Germany. Centre for Science and Environment. (2017).

[29] Morales-Pinzón, Tito, Rodrigo Lurueña, Joan Rieradevall, Carles M. Gasol, and Xavier Gabarrell. "Financial feasibility and environmental analysis of potential rainwater harvesting systems: A case study in Spain." Resources, Conservation and Recycling 69 (2012): 130-140. doi.org/10.1016/j.resconrec.2012.09.014

[30] Walton, B. India Cities Focus on Rainwater Harvesting to Provide Clean Drinking Water. Circle of blue. (2010).

Available online at www.CivileJournal.org

Civil Engineering Journal

Vol. 3, No. 3, March, 2017

Parametric Study on the Post-Tensioned Steel Connecting Components

Ahmadreza Torabipour [a*], Mahmodreza Shiravand [a]

[a] *Department of Civil Engineering, Qazvin Branch, Islamic Azad University, Qazvin, Iran.*

Received 18 January 2017; Accepted 15 March 2017

Abstract

One of the newest steel beam-column joints to replace conventional welded connections, post-tensioned connection steel is with the upper and lower angles. In this connection are high-strength steel strands that parallel beam web and angles between beams and column. Actually high resistance strands and upper and lower angles respectively are provider centralization properties and energy dissipation capacity of the connection. The benefits of post-tensioned steel can be used in connection with the centralization and lack of relative displacement (drift) persistent, stay elastic core components such as connecting beams, columns and fountains connection, appropriate initial stiffness and joint manufacture with materials and traditional skills. . In this study, numerical modelling in Abaqus software, the results of the analysis were compared with the results of laboratory samples and the results showed that the two together are a perfect match. After validation, parameters influential centrist connection then pulled the thick angles in three numerical models were evaluated. The results show that by increasing the thickness of the angles, increase energy dissipation capacity and ductility connection and the β_1 value does not experience tangible changes with changes in angle thickness.

Keywords: Post-Tensioned Connection; Centralized Bending-Resistant Frame; Sensitivity Analysis.

1. Introduction

Since the 1994 Northridge and 1995 Kobe earthquake, many efforts to improve seismic design, strength and performance steel building was carried out. When the earthquake affected buildings are large and powerful forces that are building these forces would enter the field of non-linear behaviour in the area of nonlinear behaviour. Today, the new framework is expected moment frames with non-elastic deformation large pile of Weston to withstand major earthquakes. Non-elastic deformations in structures oriented center of attention remains Drift are in connection with the opening of the beam can be removed Weston so it seems structures oriented center can be no harm in main structural members after earthquake is restored the initial position. Unlike conventional steel frame structural members based on ductility materials, behaviour-oriented center ductility with high strength is based on the behaviour of post-tensioned strands with bars. In general these strands and connectivity junctions foot of the column is in Weston Mercury application of steel structures for the construction. In this connection property to maintain its centralization post-tensioned strands and main components must remain elastically connection.

Another form of post-tensioned connections by Christopoulos et al. [3] was examined experimental and numerical analysis. This circuit consists of high-strength steel bars and rods enclosed for energy dissipation by submission in tension and compression, respectively. The results showed that the relative movement of the top floor, the frame has this connection to its original position without causing damage to the beams and columns, returns. Once again Christopoulos et al. [4] it has drawn seismic behaviour of connections after centralization with hysteretic behaviour flag shape compared with conventional seismic behaviour of welded joints. This comparison was made only for a single degree of freedom. For this study were used 20 record earthquakes and in the end it was observed that hysteretic

* Corresponding author: Iran.torabipour.a@gmail.com

response hysteretic elastic flag shaped like an even better response is achieved.

Garlock and colleagues [5] of the angles of the upper and lower fittings published in the lab under cyclic loading. The aim of the present study, the size and spacing of the holes on the corners to heel stiffness, strength and energy dissipation capacity of the connection. The results showed that corners even after the surrender, their efficiency are preserved. Also, much of the energy dissipation mechanism connecting the corners of performance and surrendered linked. Garlock et al [6] 6 examples of rigid beam to column connections under cyclic loading post-tensioned steel with 4% drift to simulate the effects of the earthquake.

In this connection the upper and lower corners bolted to beams and columns and also are used resister strands parallel to web beam. Bending moment resistant strands for service loads, high beam to column flange pressure the day. The parameters in this study were strengthened that consists of the initial strain, the number of post-tensioned strands and the sheets. The results showed that the binding post-tensioned steel has good ductility and energy dissipation capacity and are also subject to drift beam and column 4% remain elastic and will not have any harm. Only members of the upper and lower angles were damaged, causing energy dissipation as well. Garlock [7] a series of studies on the cyclic behaviour of a limited number of components of the proposed post-tensioned connections Ricles [1], carried out. They laboratory sample results with the results of the numerical model and found that the results were compared and validated numerical models corresponded with the results of laboratory samples.

Rojas et al [18] studied a PT connection for a steel moment resisting frame with post-tensioned friction damped connections (PFDC) to increase the energy dissipation capacity. The results represented that the response of a PT frame exceeds that of a frame with a rigid connection and also good strength, ductility and energy dissipation observed. Wolski et al. [19] performed an experimental study on connections with top and seat angles combined with post-tensioned strands which indicated that such post-tensioning concentrates inelastic deformation on angles. They concluded that the combination of post-tensioned strands and energy dissipating devices results in self-centering behaviour by eliminating residual drifts of system. Hadianfard et al. [20] made numerical studies on the effects of angle geometry on a PT connection behaviour. The results showed that the energy dissipation capacity and post-yielding stiffness of a PT connection increase by increasing the angle thickness or decreasing the angle gage length.

Shiravand [9] the development of centralized post-tensioned connections, stiffeners to the upper and lower corners for improved energy dissipation capacity of the connection, were added. They are using numerical analysis, a series of theory to predict the behaviour of post-tensioned connections with the upper and lower corners reinforced with stiffeners have suggested. Finally, by adding hardware to connect the corners of increased resistance against high drift (4%). This paper is to model the experimental sample and then to validate the results of the numerical simulation of the laboratory samples deals. Then, the numerical modelling of principal and interest, explains. Number ٣is investigated numerically. The characteristics of the three models are post-tensioned connection with three thick steel angles (17.5, 22 and 25.5 mm).

2. Numerical Simulation

Sample name is 36S-20-P. Sample is consist of the two beams and a column crosswise, high-strength strand, beam flange reinforcement sheets, plates and sheets continuity forehead. Sample 36S-20-P simulated in Abaqus finite element software [10]. This section summarizes the modelling centralized connection point is then drawn.

All the models in this paper have been made in SIMULIA Abaqus FEA software. Figure 1. shows the three-dimensional solid model springs mode. Because of the complexity of the model and the massive computing, assumptions have been considered in order to solve these problems. Due to the symmetrical shape of sections and connecting components such as beams, columns, plates and sheets of strengthening the beams, the conditions and numerical simulation is used in the symmetry properties, in other words, half the beam-column connection is made in the application [7, 11].

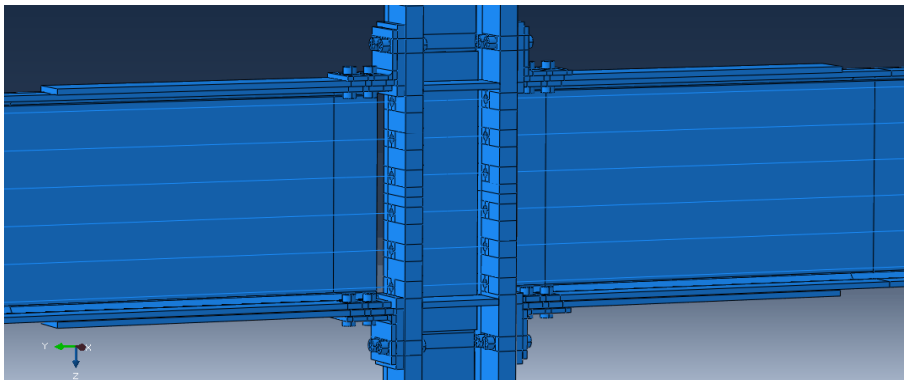

Figure 1. The placement of components in the springs' area

2.1. Specification Materials

Steel material properties connectivity components are given in Table 1. The values of tensile testing in the laboratory components are calculated in accordance with ASTM standard [12]. All of the components except the angles in the analysis are just a stretch, but for material properties angles are loaded on a cross. Materials have been tested twice and values of yield stress and ultimate been achieved of average tensions. For all materials is considered the behaviour of stress - strain that approximated as bilinear (Isotropic). For bilinear stress-strain curve definition is need to yield and ultimate stress and strain failure. Also, Young modulus, and thermal expansion coefficient strands and respectively is 199 GPA, 12e-6, 266 KN is considered of according to the force-displacement curve of strand 85% yield stress and tensile stress [13].

Table 1. Profile of steel materials [7]

Components	Yield Stress	Ultimate Stress
Beam Flange	362	498
Beam Web	414	527
Reinforce Plate	397	574
Column Flange	356	499
Column Web	345	496
Angle	383	545
Strand	1620	1900

2.2. Meshing

main components of connection such as beams, columns, plates, sheets strengthened, screws and sheet forehead of elements volumetric 3D solid 8 node with integral dropped (C3D8R) have been made, but to simulate cable, Germans beam (B31) been selected. Nearby areas Springs has a grid (mesh) smaller than other places like between the sheets are strengthening to the free end. Figure 2. shows the meshed model is assembled. Beams in areas adjacent columns, elements smaller markets. Also column in areas adjacent angles elements smaller markets and in other areas is elements elder. About strand and pitch can be notice that in areas adjacent holes are elements smaller and others area elements elder. (Table 2)

Table 2. Number elements for components

Components	Number elements
beam	4008
column	5567
Reinforce beam	611
Plate double	812
angle	828
strand	1579
Column pitch	1728
Beam pitch	1288

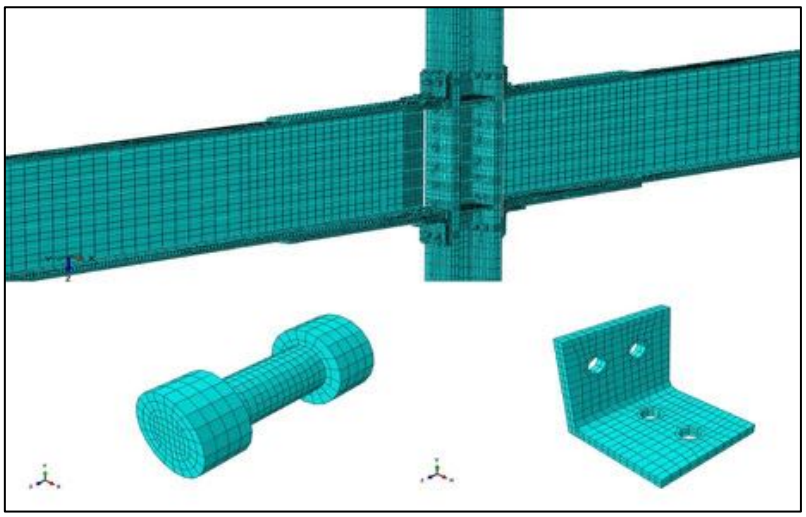

Figure 2. Details meshing simulation model

2.3. Interaction

The interaction between the main components of structural surfaces that are in contact with each other, have a huge impact on the accuracy of numerical model nonlinear analysis. In order to model the behaviour of welded components is used from the TIE. The interaction between other components (not boiling), is defined in two directions tangential and vertical. In a vertical direction, for all parts, components influence each other to prevent interaction is determined into HARD CONTACT. Two types of contact defined without friction and friction tangential to the characteristics. In order to simulate have been used forehead frictionless contact and friction contact between the body of the screw and strand holes in walls and head of bolts with angles, beams and columns angles with sheets and sheets of strengthening the beams. The coefficient of friction between steel surfaces is selected 0.33 [14].

2.4. Boundary Conditions

Connecting the boundary conditions, such as low-articular bearing columns, beams and maintenance support roller end side (side controls) connection, accurately modelled in the software. Fulcrum joint to simulate the coupling beam and columns, the points under the wing of the beam vertically and move around the bottom of the column were bound in three directions.

2.5. Pattern Cyclic Load

The load on the model of displacement such as displacement or relocation of the number and size of each load cycle under the Protocol SAC is shown in Table 3.

Table 3. Drift and the number of cycles loading protocol [15]

Load Step	1	2	3	4	5	6	7	8
Number of Cycles	0.00375	0.005	0.0075	0.01	0.015	0.02	0.03	0.04
θ (rad)	0.005	6	6	4	2	2	2	2

3. Verification of Finite Element Model

Solver of choice to simulate the performance cycle post-tensioned connections called Static-General. In this analysis to considered the effect of large deformations and nonlinear geometric. According to Moradi [7] and Shiravand [9] found that the use of finite element method in assessing the cyclical behaviour of post-tensioned connections is very convenient and accurate. For validation, the results of finite element model post-tensioned connection were compared with the results of laboratory samples Garlock [2 and 6]. Built-in software model is simulated exactly like laboratory specimens.

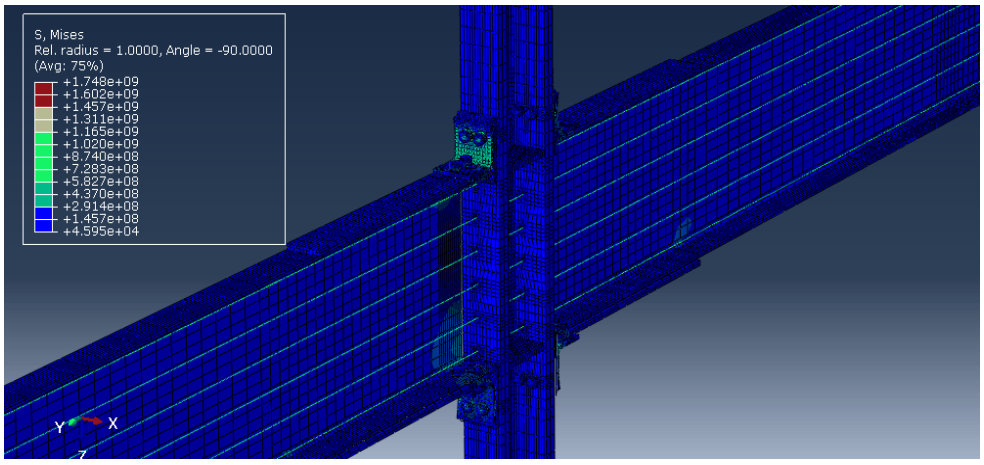

Figure 3. Typical stress distribution 36S-20-P

Compare the response force - displacement connection after laboratory sample drawn numerical example is shown in Figure 4. It turns out that the hysteresis curve as shown in laboratory samples hysteresis curve with a minimum number of errors matches.

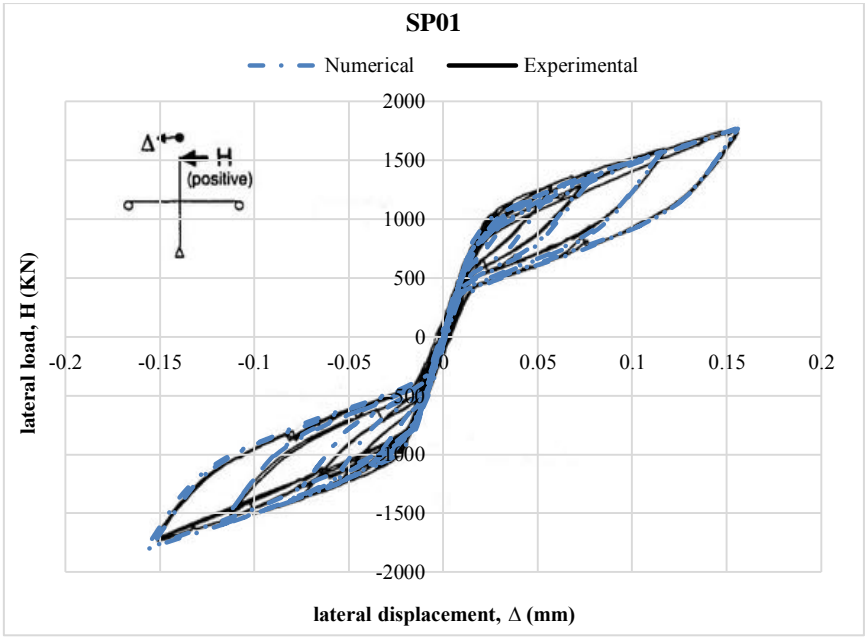

Figure 4. compares the response force - displacement experimental and numerical examples

The values in Table 4. is calculated that results of experimental and numerical analysis of the samples were compared with the percentage of error between two values, and observed that the maximum error between experimental and numerical results is less than 5%.

The values of this tables include of T_0 total initial post-tensioning force, T_u ultimate post-tensioned strands, T_{max} maximum post-tensioned strands in drift 4%, M_d moment or anchor detachment threshold, M_{max} maximum bending moment in the beam in drift 4% and have to say that plastic hinges is visible in the upper and lower angles.

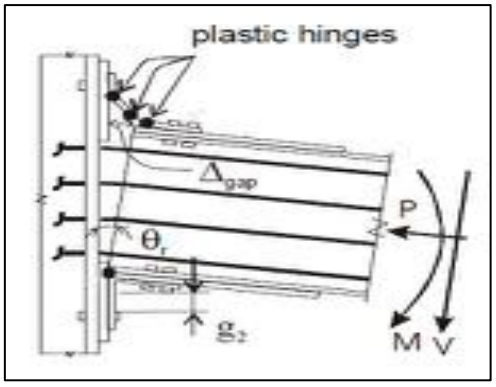

Figure 5. Plastic hinges and the final transformation of post-tensioned steel connection [16]

Table 4. Comparison of experimental and numerical analysis

Sample Model	T_0 (KN)	θ_{max} (rad)	$\frac{M_d}{M_{pn}}$	$\frac{M_{max}}{M_{pn}}$	$\frac{T_{max}}{T_u}$	θ_{rmax} (rad)
Experimental Model	3194	4%	0.47	0.96	0.55	0.033
Numerical Model (SP1)	3123	4%	0.487	0.995	0.0551	0.0325
Error Percent	2%	0	3.62%	3.65%	0.18%	1.5%

4. Numerical Models

Numerical simulation model validation is named SP1. After validation of 36S-20-P, turn to build three other models to assess the effect of the thickness of the angles, the behaviour of post-tensioned steel connection arrives. Specifications models are given in Table 5. where T_0 = total initial post-tensioning force, N_s = Number of PT strands, L_{rp} = length of the beam flange reinforcing plates, g_2 = distance from the fillet to the washer plate edge.

Table 5. Profile models

Sample Model	T_0 (mm)	N_s	L_{rp} (mm)	g_2 (mm)	Angle Thickness (mm)
SP01	3123	36	1372	137	19.05
SP02	3123	36	1372	137	17.5
SP03	3123	36	1372	137	22
SP04	3123	36	1372	137	25.5

5. The Results of the Analysis of Numerical Models

M − θ Curves are obtained from the force-displacement of each connection, by increasing the thickness of angles in connection, the induced initial stiffness from post-tensioned strands decrease. Also by increasing the thickness of angles, energy dissipation of connections increases.

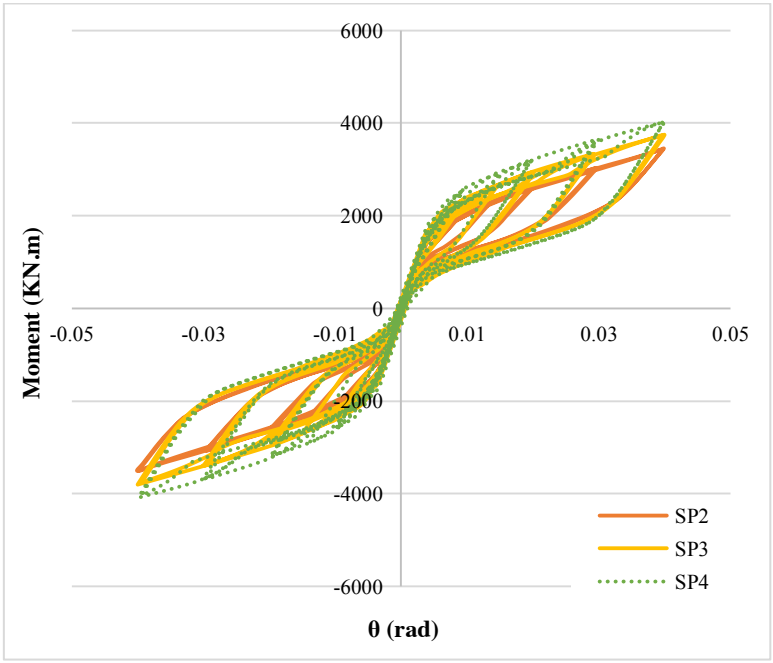

Figure 6. Curves $M - \theta$ samples SP2, SP3 and SP4

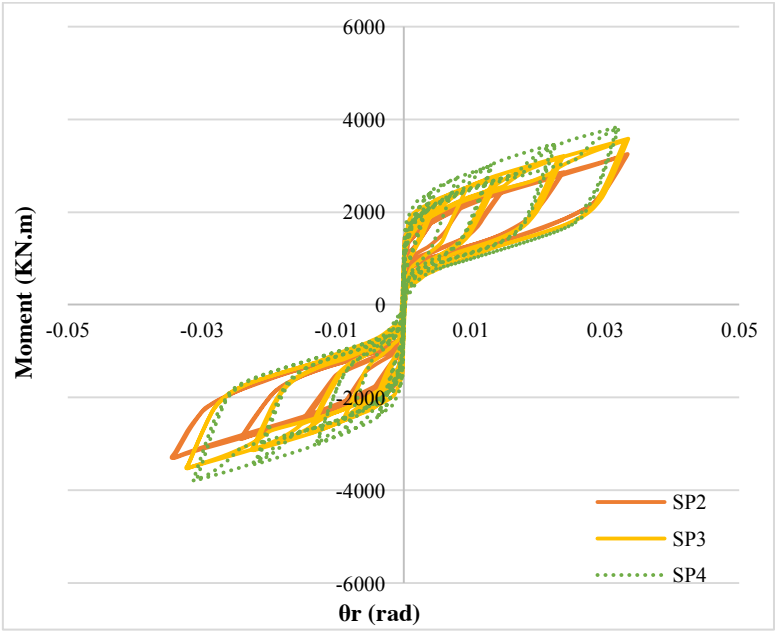

Figure 6. Curves M − θr samples SP2, SP3 and SP4

6. Ductility

To determine the seismic design standards of steel structures, the ductility of the connection is of great importance. The ductility of connection is, indeed, the ability of the connection in tolerating non-resilient transformations so that the connections in the changes do not show considerable resistance reduction. The requirements of ductility in average and special frames must be considered. The moment-rotation curve has been used to express the ductility. The angles of relative and absolute rotation of the connections are considered as an important quantity in ductility classification. For example, final rotation of θ_u connection or relative ductility index $\frac{\theta_u}{\theta_y}$ with elastic rotation limit of θ_y is often used. T_0 Compute the elastic rotation limit, the M_y yield moment is calculated by $M_y = C_y \times M_u$ [17], where M_u is ultimate connection moment (Table 6).

Table 6. Form factor of the modelled sample

Sample Model	Ductility Factor
SP01	1.99
SP02	2.25
SP03	2.06
SP04	1.85

7. Analysis of Sensitivity

Shiravand [13] provided equations for calculating the coefficients. The values of this article have been calculated using the proposed equations. In fact, it is only dependent on the geometry of the angles. Table 7. is displayed Correction factors for all models.

Table 7. Values β_1

Sample Model	β_1
SP01	0.497
SP02	0.494
SP03	0.496
SP04	0.495

Table 7. by analysing samples SP01 to SP04 values obtained from the analysis as shown are available in Table 8. Δ_{gap} Parameter which it shows the gap opening and closing at the beam-column interface under cyclic loading. By increasing the thickness of angles, tolerate the bending moment in beam, 4.5 to 13.8 percent .maximum the opening connections SP02 (angles connection with a thickness of 17.5) and the lowest is belong to SP04.

Table 8. The numerical values of the analysed samples

Sample Model	$\frac{M_{max}}{M_u}$	$\frac{T_{max}}{T_u}$	θ_{rmax} (mm)	Δ_{gap} (mm)
SP01	0.995	0.551	0.0325	28.71
SP02	1.006	0.54	0.0334	29.5
SP03	1.07	0.53	0.03226	28.5
SP04	1.2	0.53	0.03192	28.2

8. Conclusion

In this study, a connection with the real dimensions of post-tensioned steel beams, columns, upper and lower angles, strands resistance and stiffeners examined and analysed under cyclic loading cyclic connect SAC to assess response (curve M-θ and M-θ_r) and location of plastic hinges forming the desired connection, M-θ Curves is obtained from the force-displacement of each connection, The results showed that by increasing the thickness of angles in connection, the induced initial stiffness from post-tensioned strands decrease. Also by increasing the thickness of angles, energy dissipation of connections increases. By increasing the thickness of the angles bear the bending moment in beam, 4.5 to 13.8% increase. The β_1 value does not experience tangible changes with changes in angle thickness. And also values of the opening distance between beams and column (Δ_{gap}) in 4 models are near to 28.5 mm.

9. References

[1] Ricles, J.M., et al., Posttensioned seismic-resistant connections for steel frames. Journal of Structural Engineering, 2001. 127(2): p. 113-121.

[2] Garlock, M., Full-scale testing, seismic analysis, and design of post-tensioned seismic resistant connections for steel frames, in Civil and Environmental Engineering Dept., Lehigh University. 2002.

[3] Christopoulos ,C., et al., Posttensioned energy dissipating connections for moment-resisting steel frames. Journal of Structural Engineering, 2002. 128(9): p. 1111-1120.

[4] Christopoulos, C., A. Filiatrault, and B. Folz, Seismic response of self-centring hysteretic SDOF systems. Earthquake engineering & structural dynamics, 2002. 31(5): p. 1131-1150.

[5] Garlock, M.M., J.M. Ricles, and R. Sause, Cyclic load tests and analysis of bolted top-and-seat angle connections. Journal of structural Engineering, 2003. 129(12): p .1615-1625.

[6] Garlock, M.M., J.M. Ricles, and R. Sause, Experimental studies of full-scale posttensioned steel connections. Journal of Structural Engineering, 2005. 131(3): p. 438-448.

[7] Moradi, S. and M.S. Alam, Finite-Element Simulation of Posttensioned Steel Connections with Bolted Angles under Cyclic Loading. Journal of Structural Engineering, 2015. 142(1): p. 04015075.

[8] Pirmoz, A. and M.M. Liu, Finite element modeling and capacity analysis of post-tensioned steel frames against progressive collapse. Engineering Structures, 2016. 126: p. 446-456.

[9] Shiravand, M. and S. Mahboubi, Behavior of post-tensioned connections with stiffened angles under cyclic loading. Journal of Constructional Steel Research, 2016 .116 :p. 183-192.

[10] Simulia, D., Analysis User Manual, in Abaqus/Standard. 2014, Simulia: USA.

[11] Moradi, S. and M.S. Alam. ANSYS MODELING OF POST-TENSIONED STEEL BEAM-COLUMN CONNECTIONS UNDER CYCLIC LOADING. In 5th International Structural Specialty Conference, CSCE, London, ON. 2016.

[12] ASTM, Standard methods for tension testing of metallic materials, in ASTM Designation E8-91. 1991: Philadelphia.

[13] ASTM, Standard specification for steel strand, uncoated seven-wired for prestessed concrete, in ASTM Designation NO. A416-94. 1997: Philadelphia.

[14] ANSI, A., AISC 341-10 (2010). ‘‘Seismic provisions for structural steel buildings.’’American Institute of Steel Construction. Inc.: Chicago, IL.

[15] Venture, S.J., Protocol for fabrication, inspection, testing, and documentation of beam-column connection tests and other experimental specimens, in Rep. No. SAC/BD-97. 1997.

[16] Garlock, M., J.M. Ricles, and R. Sause. Experimental studies on full-scale post-tensioned steel moment connections. in 13th World Conference on Earthquake Engineering. 2004.

[17] Venture, S.J. and G.D. Committee, Recommended seismic design criteria for new steel moment-frame buildings. 2000: Federal Emergency Management Agency.

[18] P. Rojas, J. Ricles, R. Sause, Seismic performance of post-tensioned steel moment Resisting frames with friction devices, J. Struct. Eng. ASCE 131 (4) (2005) 529–540.

[19] M. Wolski, J. Ricles, R. Sause, Experimental study of a self-centering beam–column Connection with bottom flange friction device, J. Struct. Eng. ASCE 135 (5) (2009) 479–488.

[20] M.A. Hadianfard, R. Sharbati, A. Lashkari, Cyclic behavior of post-tensioned energy Dissipating steel connections, 14th international conf. on computing in civil and Building engineering, Moscow, Russia, 27–29 June, 2012.

Available online at www.CivileJournal.org

Civil Engineering Journal

Vol. 3, No. 3, March, 2017

The Effects of Using Different Seismic Bearing on the Behavior and Seismic Response of High-Rise Building

Saman Mansouri [a*], Amin Nazari [a]

[a] *Department of Civil Engineering, Dezful Branch, Islamic Azad University, Dezful, Iran.*

Received 7 February 2017; Accepted 23 March 2017

Abstract

The effects of using different seismic bearings were investigated to reduce the seismic response of buildings by assuming the vulnerability of 20-story regular RC building in this paper. The method of this study was that the studied building was studied in three different models in terms of its connection to the foundation. In the first model, the structures were placed on the rigid bearing and in the second and third models; lead-rubber bearings and friction pendulum bearings were placed at the counter between the structure and foundation, respectively. Then, the dynamic analysis was used to assess the behaviour and seismic response of the mentioned models. The results of the study showed that the structures in the first model functioned like cantilever column that would become uniaxial and biaxial bending under the effects of earthquake around the vertical axis of structure. Due to the tensile (tension) weakness in concrete, seismic loads caused major cracks in the tension part of the structures according to the place of the neutral axis that could lead to the collapse of structure. In addition, the use of mentioned seismic bearings under the earthquake caused the structure like a semi-rigid box slid on this equipment that reduced the structure's stiffness and increased the period of the structure in comparison with the first model. Using the studied seismic bearings caused the displacement of the roof of the first and twentieth stories of the structure become approximately equal and prevented the creation of the bending moment in the first model. The results of non-linear time history analysis showed that using the studied seismic bearings caused the response of the structure reduced significantly when the structure was placed on rigid bearings. It could be very valuable regarding the limitation of the capacity of the structure's members.

Keywords: Seismic Retrofit; High-Rise Building; Lead-Rubber Bearings; Friction Pendulum Bearings.

1. Introduction

One of the important issues in the existing buildings is their design in accordance with codes that are developed many years ago and these codes have been revised several times so far. By investigating the behavior of existing buildings against recent earthquakes and assessing the vulnerability of structures (especially in areas that earthquake accrued less during these years), it has been observed that these buildings are vulnerable to the earthquakes.

With the advancement of computers and consequently structural analysis-design softwares, great change happened in the civil engineering sciences that lead to the correction and permanent promotion of the codes. Besides, with the progress and development of seismographs, it was revealed that a significant number of earthquakes (especially earthquakes occurred near fault) had significant acceleration components which were much larger than the normal values stated in the codes (0.35 g - 0.4 g) respectively. The design of structures with high importance against accelerations much greater than the code's values is costly in terms of economic and very space-occupying and improper design. Because of the mentioned causes, using energy dissipation devices in structures due to the significant dissipation of energy caused by earthquake is one of the solutions against acceleration of bedrock in seismic design of structures.

* Corresponding author: samanmansouri@ymail.com (S. Mansouri).

2. Background Research

Recently, using energy dissipation devices for retrofitting structures against earthquake is common in the academic research. In a comprehensive study, kinds of equipment and methods of increasing dissipating energy in structural systems were investigated. It was shown the use of dampers in the discussed structures has the property that in all cases even in the most severe earthquakes caused a significant reduction in imposed forces on the structure. This phenomenon is valuable due to the limitation of capacity of structure members [1]. In another study on seismic behavior of based-isolated building by seismic isolators, it was found that their periods increased in comparison with the structures with fixed bearing and on the other hand, the values of response of isolated system reduced significantly [2]. The researchers showed that applying dampers and seismic isolators in bridge could reduce the damages caused by lateral forces several times and the correct design of the equipment would guarantee the high performance of the bridge [3]. In another research, applying friction pendulum bearing and lead-rubber bearings could reduce the base shear of a building significantly compared with when the building bearing was rigid [4].

In a case study, the results of the study indicated that the use of friction pendulum bearings could reduce the seismic response of the structure significantly compared to the case where the bearing of structures was rigid [5]. In a detailed study, it was found that by increasing the radius concavity of the foundation, the impact of reflecting mechanism of structure under its own weight, especially at 5-storey models, was reduced and possibly the structure did not return to its original location after occurring earthquake. The best way to solve this problem was the use of displacement limiter or mechanism that returned the structure to its original place after the earthquake. The nonlinear response of displacement and base shear in the modeled 2-story building and 5-story building equipped with common friction pendulum isolators (first model) and isolation system with pendulum movement mechanism for whole structure (second model) showed the reduction in the values of base shear structure in the second model in comparison with the first model [6]. In another detailed study, the seismic behavior of multiple-span RC bridges was evaluated at the different states of using the lead-rubber bearings, friction pendulum bearing at the counter between the deck with cab beam and abutments. It was found that the mentioned operation could reduce the seismic response of structures significantly in comparison with the rigid connection state of deck to cab beam and abutments [7]. Some researchers found that the seismic response of the RC short building could be reduced by using of seismic bearings [8]. The researchers showed that linear analysis is not recommended for the analysis of the isolated structures [9].

Despite extensive studies, a worthy research has not done about the seismic retrofitting of RC high-rise building using lead rubber bearing and friction pendulum bearing so far. Therefore, the seismic response of RC high-rise building has been investigated using seismic bearing in this study. The method of study is that the studied building at the first state with the fixed support has been introduced as the first model. In the second and third models, the states are investigated in order that lead rubber bearing and friction pendulum bearing are used at the counter between foundation and structure. These three models have been studied by the non-linear time-history analysis and Eigen vector analysis.

3. The Studied Equipment

3.1. Lead Rubber Bearing

This bearing consists of a lead core that is enclosed in a relatively thick rubber band. The Rubber isolators are not able to provide high damping and energy absorption. The combination of lead core with rubber bands not only provides primary stiffness of structure but also resist isolated structures against lateral loads such as wind or earthquake.

Figure 1. Lead-rubber bearings with different dimension

The reason of selecting the lead for this isolator is its crystal structure. This kind of structure changes by displacement but immediately returns to the original state and thus consecutive yielding under lateral vibrated dynamic loads does not cause to the fatigue phenomenon. The rubber section of this equipment is like rubber isolators with steel plate and has the function of providing reflecting force to the starting point after the end of structure's vibration [10]. The lead rubber bearings are modeled by SAP2000 software with following characteristics [4]:

Element = Rubber isolator
U1 → Linear effective stiffness= 1500000 KN/M
U2=U3 → Linear effective stiffness= 800 KN/M , U2=U3 → Nonlinear stiffness=2500 KN/M
U2=U3 → Yield strength= 80 , U2=U3 → Post yield stiffness ratio= 0.1

3.2. Friction Pendulum Bearing

This bearing contains a concave surface at the bottom part and a steel flat surface at the top part and a globe with high resistance and low friction at the middle part. Due to the exerting considerable lateral force, the top section of the structure moves on this bearing. The curvature radius of the bottom part of this bearing specifies period of the isolation system. The reflecting force in this bearing is provided by gravity and the weight of the structure. The following figure shows a view of the bearings.

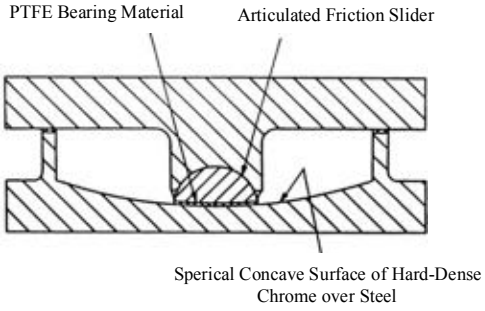

Figure 2. A view of friction pendulum bearing [11]

Friction pendulum bearings with three-dimensional behavior are modeled in SAP2000 software using the following characteristics [4]:
Element= Friction isolator
U1 → Linear effective stiffness= 15000000 KN/M , U1→Nonlinear effective stiffness= 15000000 KN/M
U2=U3 → Linear effective stiffness= 750 KN/M , U2=U3 → Nonlinear stiffness=15000 KN/M
U2=U3 → Friction coefficient slow= 0.03 , U2=U3 → Friction coefficient fast= 0.05
U2=U3 → Rate parameter= 40 , U2=U3 → Radius of sliding surface= 2.23

4. The Studied Building

In this study, a 20-story reinforced concrete building is investigated in which the connections of beams and columns are rigid. The dimensions of the considered structure on each side are 12 m (square plan) and there are four rows of columns in each side at equal distance of 4 m. The used sections and models of structure are based on the following forms:

Table 1. The dimensions of the studied building based on the centimeter

Floor	Dimension	
	Column	Beam
1, 2, 3	70×70	25×60
4, 5, 6	65×65	25×60
7, 8, 9	60×60	25×60
10, 11, 12	55×55	25×60
13, 14, 15	50×50	25×60
16, 17, 18	45×45	25×60
19, 20	40×40	25×60

Figure 3. shows the view of the studied model in the SAP2000 software.

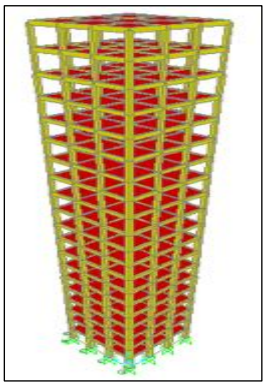

Figure 3. The view of the studied model in the SAP2000 software

According to Figure 4, Mander model is used in order to model the nonlinear behaviour of materials.

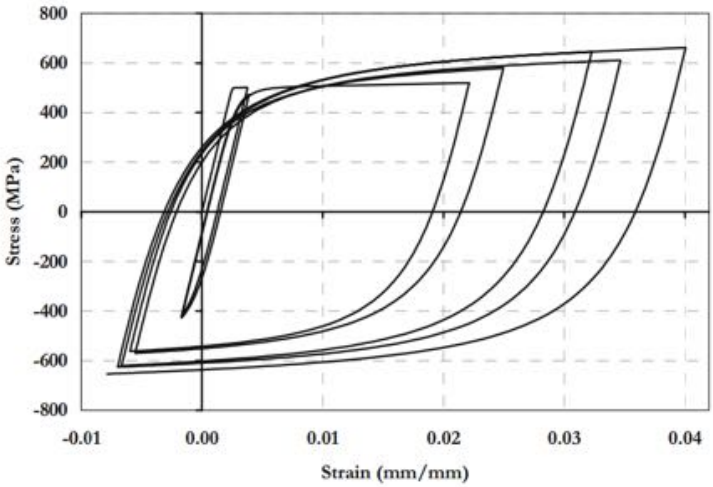

Figure 4-a. Nonlinear behaviour model of steel

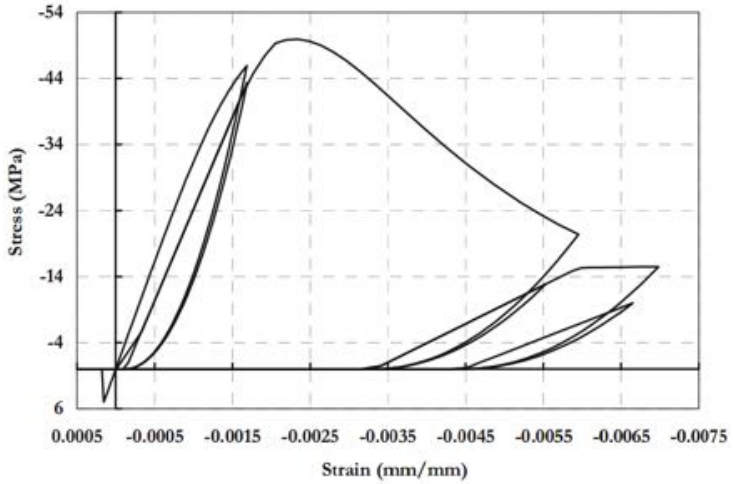

Figure 4-b. Nonlinear behaviour model of concrete

Figure 4. behaviour's models of material [12]

Figures 5 and 6. show a view of how to use seismic bearings in the second and third models.

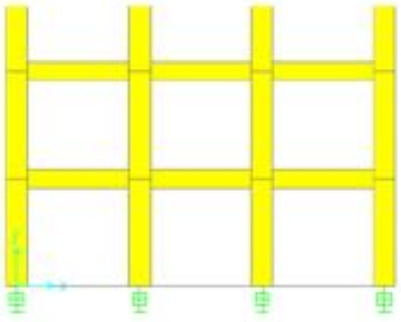

Figure 5. The view of using the lead rubber bearings in the second model

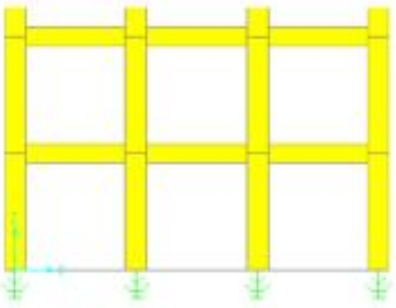

Figure 6. The view of using the friction pendulum bearings in the third model

5. The Features of Selected Earthquakes

In this study, the horizontal components of selective accelerogram elated to the Landers, Loma Prieta, Manjil, Tabas, New Zealand, Northridge and Park Field earthquakes are combined by using SRSS method in order to obtain one spectrum of each earthquake. Then, the Average of the spectra of the seven mentioned earthquakes is obtained and is scaled with 1.3AB spectrum (acceleration spectrum of 2800 standard [13]) within the period of 0.2 T and 1.5 T. Specifications of the earthquakes are presented in the following table.

Table 2. The specifications of the selected earthquakes

Accelerogram	Station
Landers 1992 LCN 260, 345	SCE 24 Lucerne
Loma Prieta WVC 000, 270	CDMG 58235 Saratoga- W vally Coll
Manjil, Iran 1990-06-20-L,T	BHRC 99999 Abbar
New Zealand A-MAT 0.83-353	99999 Matahina Dam
Northridge-01 1994 ORR 090,360	CDMG 24278 Castaic- OLD Ridge Route
Park Field TMB	CDMG 1438 Temblor Pre- 1969
Tabas DAY- LN,TR	9102 Dayhook

6. Eigen Vectors Analysis

Free vibration is the vibration free from any dynamic excitation (such as applying external dynamic forces or the motion of structure base) that begins by disturbing the balance state of the structure by applying the deformation and or the initial speed. The natural vibration (frequency and period) depend only on the mass and rigidity of the structure. The period of natural vibration has an inverse relationship with the natural vibration frequency. N determines the root of characteristic equation ($det[k-\omega_n^2 m]=0$), the natural frequency, and the natural period of frequency. The roots of mentioned equation are known as Eigen Value (characteristic values or normal values). There is an independent vector φ_n for each of the N natural frequency of a system with N freedom degrees that represents mode vibration shape and is called "The vector of vibration natural mode" or "The shape of vibration natural mode". As a result, there are N vectors of φ_n for an N-degree freedom system that is called eigen vector. The number of selective modes for eigen vector analysis is considered so that the minimum modal mass participation factors reaches to the minimum of the value mentioned in 2800 code (90%). The periods of the first mode of vibration at x and y (horizontal directions) is as follows:

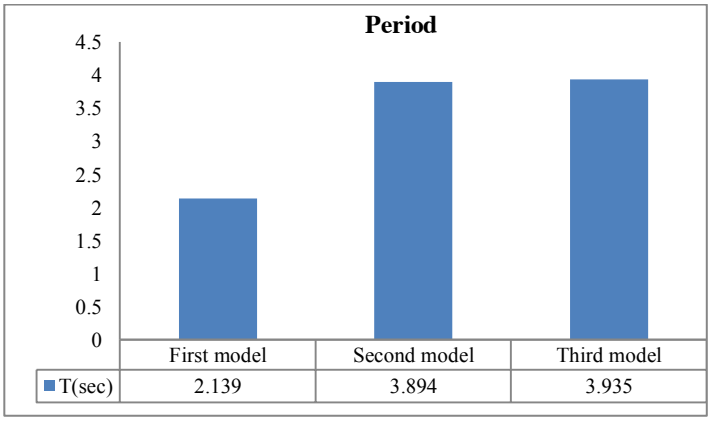

Figure 7. The periods' values of different models of structure

Based on Figure 7, it is shown that the use of mentioned equipment cause to reduce the structure's stiffness and increase its period. The period of structure increases from 2.139 seconds in the first model where the structure is fixed on bearing and to 3.894, 3.935 seconds in the second, third and fourth models by using lead rubber bearing and friction pendulum bearing, respectively.

7. The Non-Linear Time History Analysis and Presenting the Results

The non-linear time history analysis by modal method was done with the zero initial conditions and the definition of the Ritz vectors and specifications of Tabas earthquake with the scale factor of 1.7g. The main model was turned to the three models in order to study the effects of the studied energy dissipation device. The first model was the connection of the structure to the foundation that was rigid and in the second, third, and fourth models at three distinct models, lead-rubber bearing and friction pendulum bearing at the interface between structure and foundation was s used respectively. It should be noted that united system of all figures was ton-m.

Graphs of the displacement of the different point's structure at the longitudinal and transverse directions with respect to time:

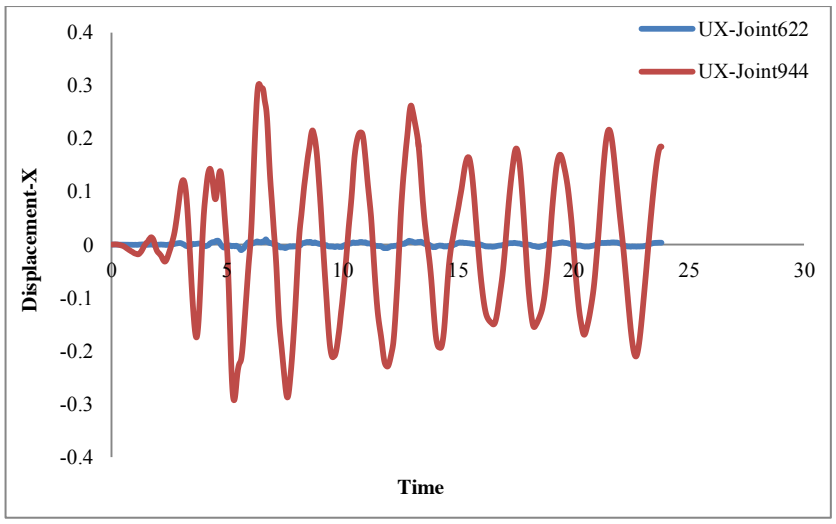

Figure 8-a. Displacement-X direction

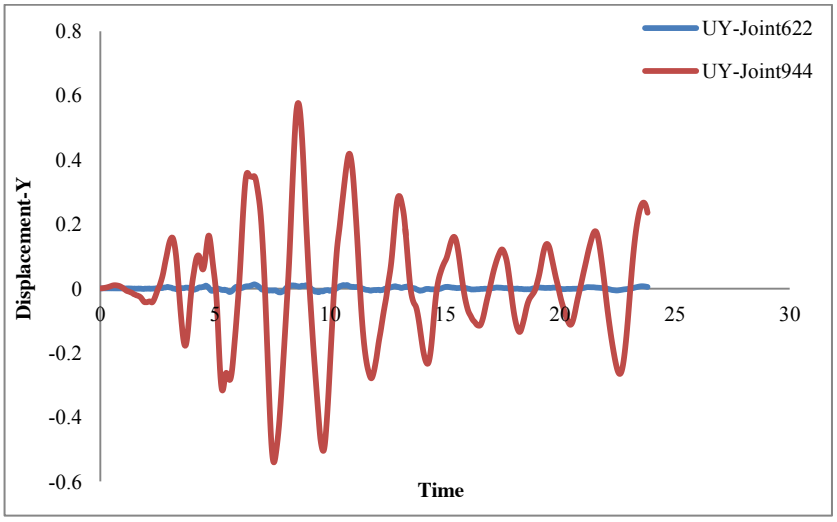

Figure 8-b. Displacement- Y direction

Figure 8. The horizontal displacement of different points of the first model at x direction and y direction

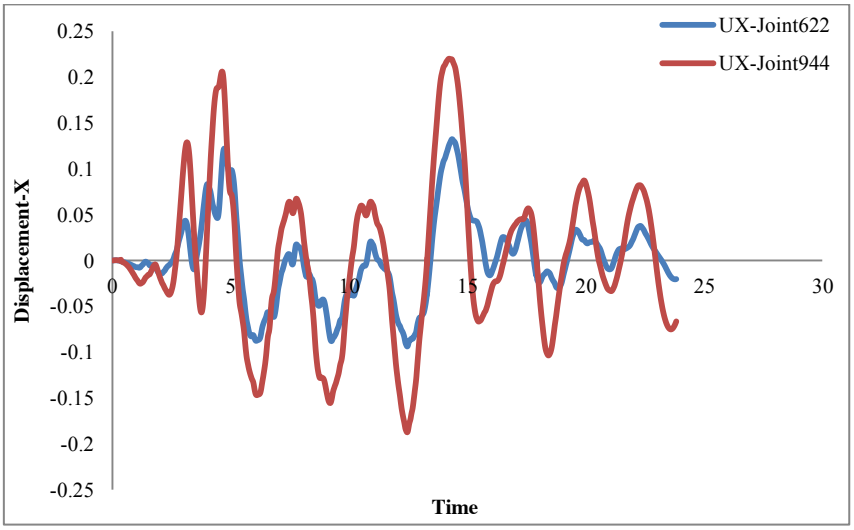

Figure 9-a. Displacement-X direction

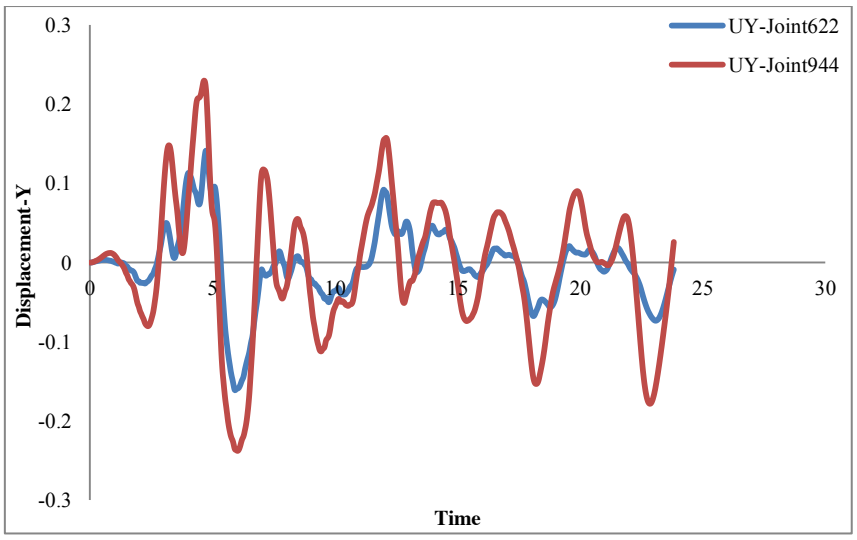

Figure 9-b. Displacement-Y direction

Figure 9. The horizontal displacement of different points of the second model at x direction and y direction

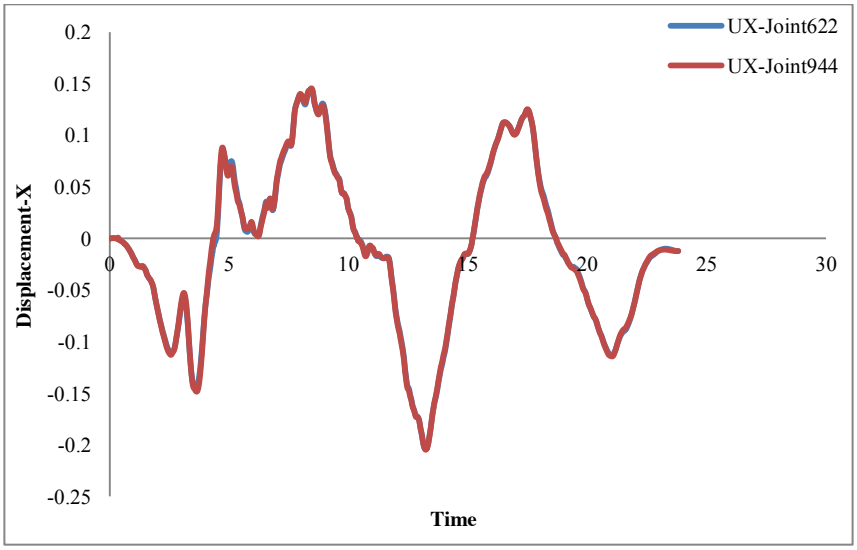

Figure 10-a. Displacement-X direction

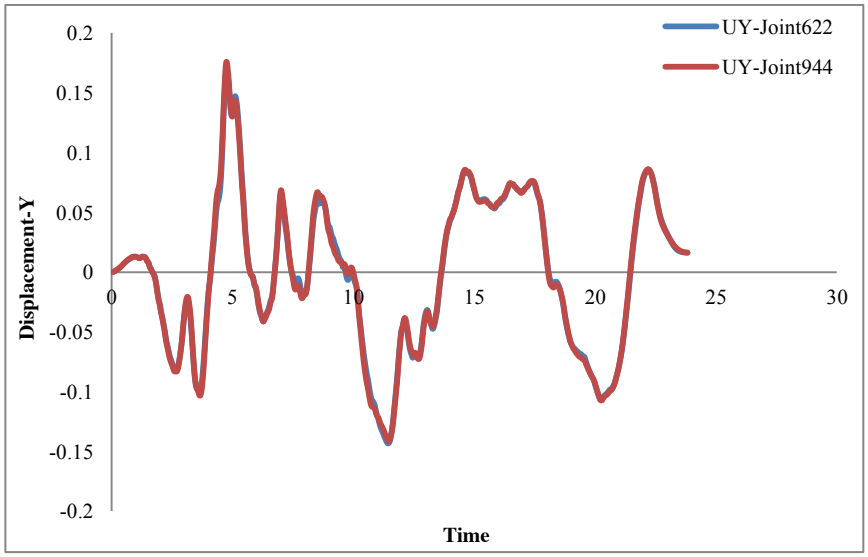

Figure 10-b. Displacement-Y direction

Figure 10. The horizontal displacement of different points of the third model at x direction and y direction

Based on the Figure 8, the rigid connection of structure to the foundation causes that the lower stories of structures closer to foundation affected by an earthquake have a very trivial horizontal shift about zero. Due to the openness of the roof of the twentieth story without any constraint, and of course the considerable height of the structure, the considered building acts somewhat similar to a cantilever column, so that the displacement of the considered point (point 622) on the roof the first story at horizontal direction is almost equal to zero and the maximum horizontal displacement of the roof of twentieth story (point 944) at X and Y directions is equal to 30 and 57 cm respectively.

The mentioned points show this fact that the studied building affected by lateral forces such as an earthquake on the lower story are almost fixed and on the upper story becomes bend and causes to create the substantial bending moment in bearing and increases the seismic response of structure. Nonetheless, the existence lead-rubber bearing and friction pendulum bearing between structure and foundation make the structure slides on the equipment under the effect of the earthquake and behave like rigid box on seismic bearing. Therefore, based on the Figures 9 and 10, the displacement of specified point on the floor of first story with the displacement of similar point on twentieth story is almost equal at the both X and Y directions.

The maximum displacement of roof on the twentieth story at X and Y directions is equal to 22 cm and 22 cm for second model and for third model 20 and 17, respectively. The following figure shows a view of schematic two-dimension of structure behavior in different states:

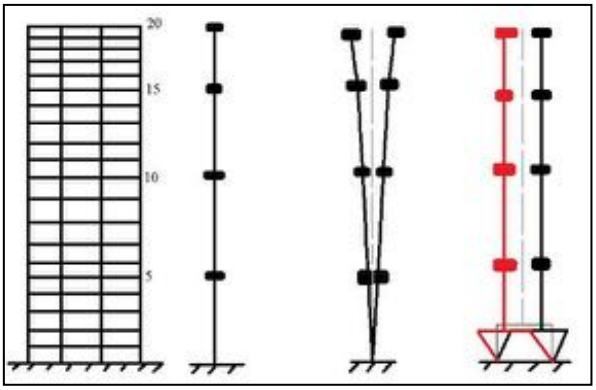

Figure 11. The dynamic model of the studied structure

Figure 11. (A) shows the studied building and the Figure 11. (B) shows a simplified dynamic model. Forms Figure 11. (C) and (D) show the behaviour of structures against lateral loads (e.g. earthquake's load) in rigid connection states of structure to the foundation and the use of seismic bearings between structure and foundation. Considering the deformation of the three-dimensional forms of studied structure in a rigid connection state of the building to the foundation, it is determined that the structure became under uniaxial and biaxial bending in the cross-section of its plan. Considering neutral fibre in any mode of deformation, almost the half of the structure was under tension and the other half was under pressure.

Due to the general weakness of concrete against tension, in the case of non-application of the necessary arrangements for strengthening of structure against the bending phenomenon, the possibility of severe seismic damage and creation of diagonal and tension cracks would increase, which eventually can lead to the destruction or non-usable of structure.

The figures of base shear of longitudinal and transversal directions of different models with the respect to the time:

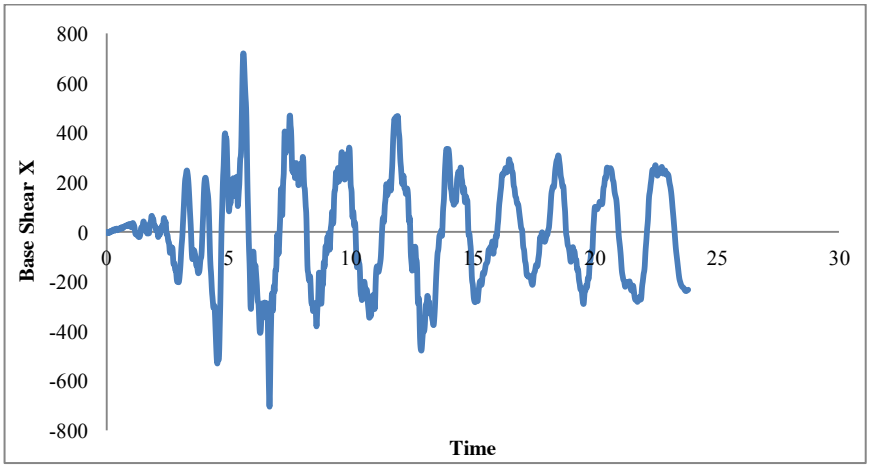

Figure 12-a. Base shear X

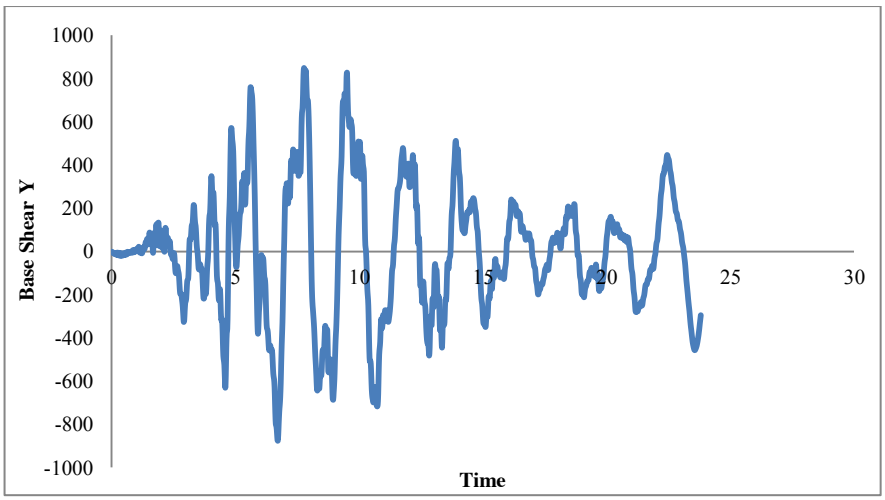

Figure 12-b. Base shear Y

Figure 12. The figures of base shear of structure at horizontal directions of first model

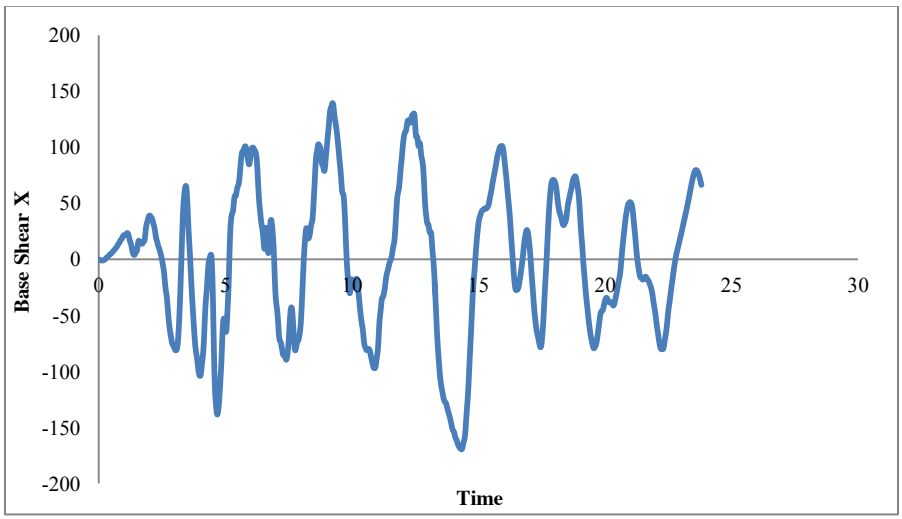

Figure 13-a. Base shear X

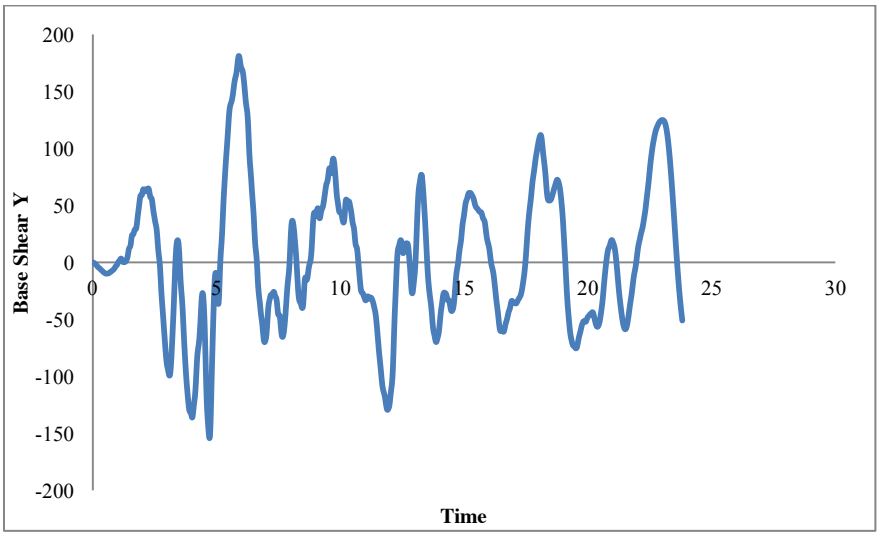

Figure 13-b. Base shear Y

Figure 13. The figures of base shear of structure at horizontal directions of second model

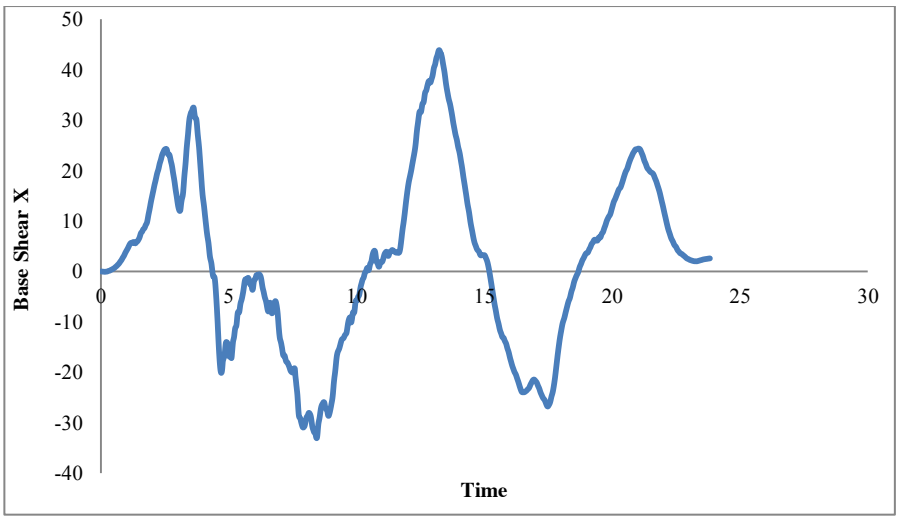

Figure 14-a. Base shear X

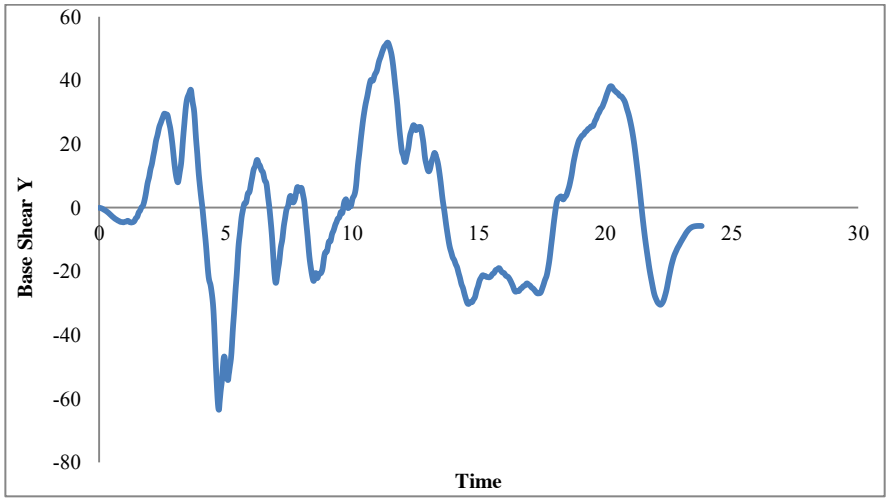

Figure 14-b. Base shear Y

Figure 14. The figures of base shear of structure at horizontal directions of third model

By investigating the results of non-linear time history analysis as shown in Figures 12 to 14, it is obvious that utilizing the studied seismic bearings could reduce the base shear force in comparison with the rigid connection of structure to the foundation, So that the base shear force of the studied building in rigid connection state to foundation at the X and Y directions are 720.1 and 876 tons respectively and these values are reduced to 169.4 and 181.3 tons in use of lead rubber bearings, 43.89 and 63.41 tons in the use of the friction pendulum bearings.

8. Conclusion

The use of the studied seismic bearings could reduce structure's stiffness and subsequently increase its period in comparison with the rigid connection of the structure to the foundation. The period of structure increases from 2.139 seconds in the first model that structure is fixed on bearing and for the second and third models (using lead rubber bearing and friction pendulum bearing) 3.894, 3.935 seconds, respectively.

The base shear force of the studied building in rigid connection state to foundation at the X and Y directions were 720.1 and 876 tons respectively and these values were reduced to 169.4 and 181.3 tons in use of lead rubber bearings, 43.89 and 63.41 tons in the use of the friction pendulum bearings.

In comparison with the first model, using the seismic bearing in second and third models reduces the stiffness of the studied structures and increases its period. Using this equipment has improved the seismic behaviour of the studied structures so that the difference of lateral displacement between the first and the last roofs of the structure has minimized in the case of using this equipment compared to the initial state (first model). This seismic behaviour leads to significant reduction of base shear of the structure in the second and third model than the first model. This result indicates that using lead-rubber bearings and friction pendulum bearings lead to the seismic retrofitting of the studied structure than its initial state.

The results of the study showed that using the studied seismic bearings caused the response of the structure

reduced significantly when the structure was placed on rigid bearings. It could be very valuable regarding the limitation of the capacity of the structure's members.

The use of the studied seismic bearings caused that the structure slid on this equipment that finally lead to the dissipation of the transmitted inertia forces to the foundation in comparison with rigid connection state of structure to the foundation. This function prevented the possible seismic damage at the interface between the structure and foundation and also falling equipment and devices inside the building (such as a closet, refrigerator and pictures). Falling of equipment in the building was a common cause of life and property damage at the time of earthquake that this equipment could be handled with bolts or other suitable connectors to structure, of course.

Computer modelling and theoretical design of these bearings for suitable application of them was necessary for reducing the seismic response of structures, however, not sufficient. The use of the mentioned equipment in the different structures enquires urgent need of computer modelling in the finite element method and theoretical design and experimental results requires much experience, talent, and genius designer particularly in the utilizing of them in the existing structure retrofitting.

In the case of existing structures such as buildings and bridges the different kinds of energy dissipation devices could be used in these places by cutting and separating of the different parts of the structure. According to the results of this study, the mentioned function could lead to a considerable reduction of seismic responses in the structure. Doing this action needs high force of plan's implementers, since it is necessary the upper part of the structure could be controlled by providing special arrangements such as jacking below the structure so that the considered seismic bearings could be put in this place.

Due to the behaviour of the studied energy dissipation devices that are inherently nonlinear in this research, their effects could not be evaluated properly using linear analysis. By proper designing and optimal use of seismic bearing, the seismic response of structure could be reduced significantly in comparison with the rigid connection state of structure to the foundation and the dimensions of structure could be designed in small and optimal dimension that could compensate for the cost of using of the equipment slightly.

Generally, the isolation function of different parts of structure from each other or different parts of structure from foundation and placing seismic bearings in these places could lead to the improvement of structure's behavior and dissipating of imposed seismic forces. Therefore, the selection of appropriate seismic bearing is essential and considerable that could be different in any case study based on the type of structure, place of its use and the condition of the site, ground movement.

Feasibility study of structure instability equipped with seismic bearings is essential due to the various reasons including extreme movements of ground, the weakness of properties in the mentioned equipment affected by various reasons.

It is necessary that some restraints should be created in different parts of the structures in order to prevent the excessive shift of the whole or some parts of the structure that were on the seismic bearings and the instability of the structure due to the excessive displacement.

In addition to the essential requirement for designing of the horizontal restraints, creating restraints against the impact of strike like the vertical component of earthquake, especially in the areas near to the fault for structures equipped with seismic bearing is of a particular importance.

9. References

[1] Tehrani T, Maalek S. The use of passive dampers and conventional strengthening methods for the rehabilitation of an existing steel structure, 4th International Conference on Earthquake Engineering, Taipei, Taiwan, Paper No. 133, 2006.

[2] Rahim Zadeh F, Zamani nouri A. Application of the base isolation method in seismic behaviour and retrofit of the 3D steel structure, The 4th National Conference on Civil Engineering, University of Tehran, Tehran, Iran, 2008.(In Persian).

[3] Takahashi Y. Damage of rubber bearings and dampers of bridges in 2011 greast east japan earthquake, Proceedings of the International Symposium on Engineering Lessons Learned from the 2011 Great East Japan Earthquake, Tokyo, Japan, 2012.

[4] Torunbalci N, Ozpalanlar G. Earthquake response analysis of mid-story buildings isolated with various seismic isolation techniques, The 14th World Conference on Earthquake Engineering, Beijing, China, 2008.

[5] Ashok S P, Mehta N, Wagh R, Padhiya M, Samare A, Patil Y. Response spectrum analysis of multi storeyed base-isolated building, International Journal of Civil, Structural Environmental and Infrastructure Engineering Research and Development, ISSN 2249-6866, 2012.

[6] Amiri Yekta A, Razani R. Assessment of the seismic performance of short buildings with FPS on the spherical concave foundation, The 2th National Conference on Structure- Earthquake- Geotechnical, Mazandaran, Iran, 2012. (In Persian).

[7] Mansouri S. An investigation of the effects of energy dissipation devices on the seismic behaviour retrofit of multiple-span reinforced concrete bridges, Department of Civil Engineering, «M.Sc» Thesis on Structural Engineering, Thesis Supervisor: DR. Shahrokh Maalek, Islamic Azad University, Dezful Branch, 2013. (In Persian).

[8] Tolani S., Sharma A. Effectiveness of base isolation technique and influence of isolator characteristics on response of a Base isolated building, American Journal of Engineering Research, Volume-5, Issue-5, pp-198-209, 2016.

[9] Ferraioli M., Mandara A. Base isolation for seismic retrofitting of a multiple building structure: evaluation of equivalent linearization method, mathematical problems in engineering, Volume 2016, Article ID 8934196, 17 pages, 2016.

[10] Kalantari A, Taghi Khani T. Guideline for design and practice of base isolation systems in buildings (No. 523), Islamic Republic of Iran, Vice Presidency for Strategic Planning and Supervision, Office of Deputy for Strategic Supervision, Bureau of Technical Execution System, 2010. (In Persian).

[11] Chen W F, Duan L. Bridge Engineering: Construction and Maintenance, CRC Press, Boca Raton London, New York Washington, D.C, Taylor & Francis Group, LLC, 2003.

[12] Pinho, R. Nonlinear Dynamic Analysis of Structures Subjected to Seismic Action, Courses and Lectures- No. 494, advanced earthquake engineering analysis, Springer Wien New York, ISBN 978-3-211-74213-6, page 63-89, 2007.

[13] Iranian cod of practice for seismic resistant design of building (standard 2800, 4th edition), road, housing and urban development research center, 2015.

[14] Pakniyat, S. & Pakniyat, E. Essential Analyses for Seismic Rehabilitation of Structures. Published by Motefakeran, Tehran, Iran, 2011. (In Persian).

Available online at www.CivileJournal.org

Civil Engineering Journal

Vol. 3, No. 3, March, 2017

Effects of Soil Modulus and Flexural Rigidity on Structural Analysis of Water Intake Basins

Hassan Akbari [a*]

[a] *Department of civil engineering, Tarbiat Modarres University, Tehran, Iran.*

Received 20 January 2017; Accepted 27 March 2017

Abstract

A water intake basin is a buried box that functions as a water reservoir near shorelines. Number of these structures has been increased in the recent years and for a safe design, it is necessary to know their behaviour under applied loads. In addition to common dead, live and seismic loads, the bottom of such a basin is usually located below sea water level and endures uplift pressure as well as reaction of supporting soils. Uncertainty of these special loads complicates the structural response of this buried basin to the applied loads. Therefore, the unreliability in the soil parameter and in the rigidity of the basin structure is studied in this research by calculating the generated internal bending moments. Different loads and load combinations have been taken into account and finite element analysis is carried out for modelling nonlinear behaviour of different types of supporting soils. It is concluded that the geometry and flexural stiffness of the basin affects the analysis more than the soil parameters because the contribution of the soil modulus in the total stiffness of the system is negligible than the structural rigidity of the basin structure. In addition, inner walls and geometry of the basin should be modelled in detail to obtain acceptable results.

Keywords: Soil Modulus; Water Intake; Rigidity; Bending Moment.

1. Introduction

In recent years, water consumptions have been increased due to development of industrial activities as well as extension of urban areas. Although demand of potable water has been expanded, the source of water is limited and its consumption should be done with special attentions. Desalination plants near seas are cost effective and reliable methods for establishing the required source of water [1]. In these systems, the sea water comes to a water intake basin through marine pipes and then the water is pumped from the basin to the required destination. Destination can be a plant or a crowded area with industrial or urban activities. Seawater intakes can be classified to submerged and buried intakes [2]. In a submerged intake, water comes to a basin through offshore pipes and in a buried intake system, water passes through screens and drilled wells. The capacity of the latter case is limited; however, a submerged system is applicable in different conditions and it is a common practice for providing required waters for industries. A chamber structure is usually used at offshore and water comes to inland basin through pipes. A desalination system has different parts including a water intake and an effluent outfall. There are some criteria and studies for the intake and outfall conditions [3, 4] and different shapes of the offshore chamber is investigated [5], but studies for the structural behavior of the intake basins is limited. This basin is actually a buried structure because its bottom level is under the sea level and the water comes to the basin by gravity. The basin acts as a box with interior walls and soil pressure as well as water pressures exert on the exterior walls. In addition, the bottom slab should resist against uplift force and soil reaction. Analysis of this structure is complicated because it is a combined system of solid, water and soil. The thickness of the bottom slab is usually uniform and the soil beneath the intake basin support the basin with reaction forces. In addition to the bearing capacity of the base soil, differential and total settlements also control the design [6]. Although the thickness of the bottom slab affects differential settlement and bending moments, its effect on the total

* Corresponding author: Akbari.H@modares.ac.ir

settlement is little. The maximum bending moment may be increased with increasing the slab thickness [7], but, the effect of the slab thickness on the maximum bending moment is decreased by increasing the slab thickness nearly more than 1.5 m [8].

Since modeling the soil beneath the basin structure can affect the total behavior of the basin, it is important to know the sensitivity of the analysis to the assumed soil parameters. It should be noted that there are usually considerable uncertainties in the soil parameters. Therefore, the effects of soil modulus on the behavior of an intake basin are investigated in this study by analyzing the basin under different loading conditions and by assuming different soil parameters. In addition, the effect of the rigidity of the bottom slab is studied. The soil beneath the basin is modeled via nonlinear springs and the results are also compared with the results of simplified models which assume a fixed support condition instead of nonlinear soil reactions.

2. Analysis Procedure

2.1. Geometry and Modelling

To study an actual case, the geometry of the basin is selected based on an actual case. The 3D geometry of the basin with two horizontal sections is presented in Figure 1. Plan view and dimensions are shown in Figure 2. As presented in this figure, Length, width and height of the analyzed sea water intake are 48.55 m, 22.3 m and 13.0 m, respectively. Inner walls of the basin act as separators for water flows and their lengths are different based on their locations. Sea water comes into the basin from the side with smaller width and pumps are located at the side with the larger width. The thicknesses of roof, floor, inner walls and outer walls are 0.8 m, 1.5 m, 0.6 m and 1.0 m, respectively, yet the thickness of the bottom slab is also changed to study the effect of the its rigidity. Four node, isotropic shell element are used in the utilized finite element software (Sap2000-14.2.4) for modeling both interior and exterior walls as well as roof and floor slabs. Dimensions of the Basin and modeling conditions are presented in Table 1.

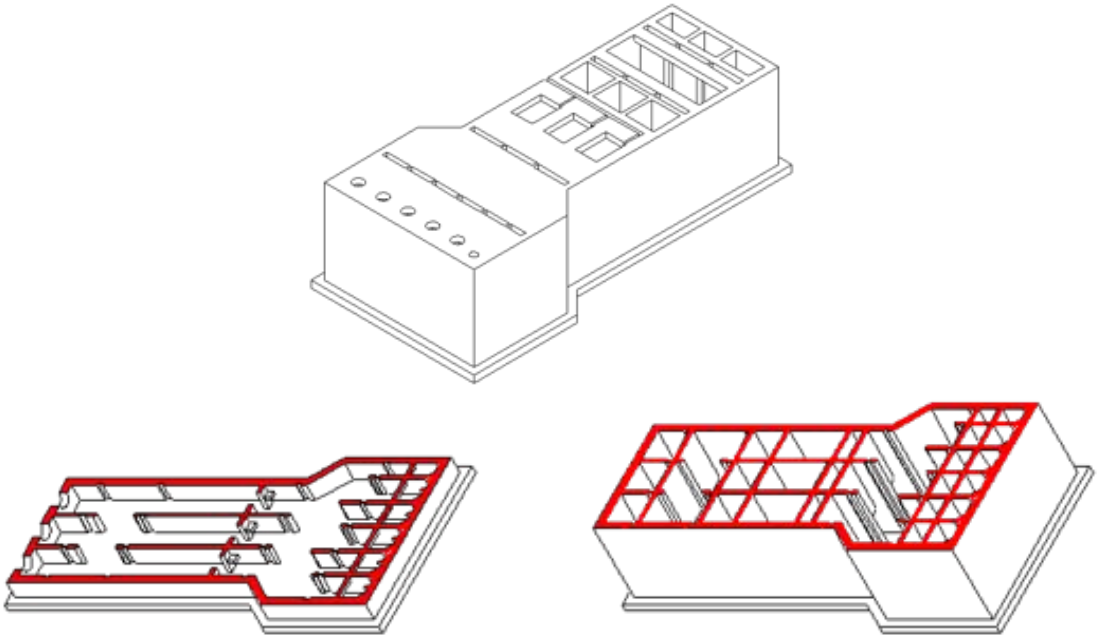

Figure 1. 3D geometry of the basin and two horizontal sections at different levels of the basin

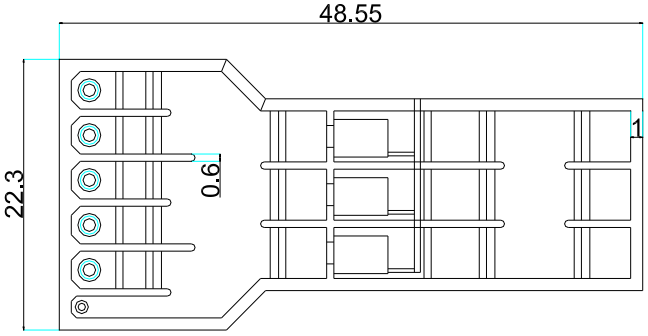

Figure 2. Plan view of the basin with dimensions

Table 1. Geometrical dimension of the basin and elements used for modeling

Geometry	**Length of sea water intake**	**48.55 m**	
	Width of sea water intake	22.3 m	
	Top of floor level	-7.0 m (CD)	
	Top of roof level	+5.5 m (CD)	
Model	Shell elements for modeling	Thickness	No. of elements
	Roof	0.8 m	9337
	Floor (supported on springs)	1.5 m	10481
	Inner walls	0.6 m	27185
	Outer walls	1.0 m	21521

Since the basin floor is located on the bed, the soil beneath the basin structure is modeled via nonlinear springs with a compressive behavior. According to the physical nature of contact between basin floor and bed, the springs can only endure the compressive forces and they cannot act in tension. The following Figures show the model geometry. To consider the effect of concrete cracking in analysis, module of elasticity has been decreased by a factor of 0.35 according to [9]. The model geometry is shown in Figure 3. and the applied classification for the shell elements i.e. inner walls, roof, exterior walls and foundation, respectively are shown in Figure 4.

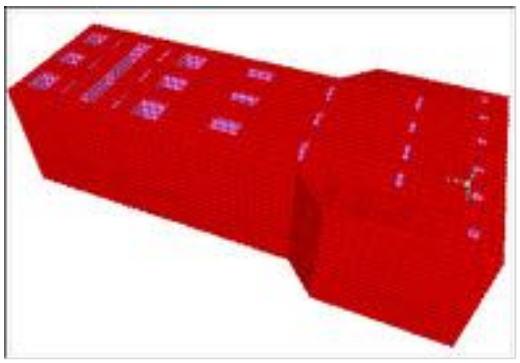

Figure 3. 3D modeled geometry of the basin

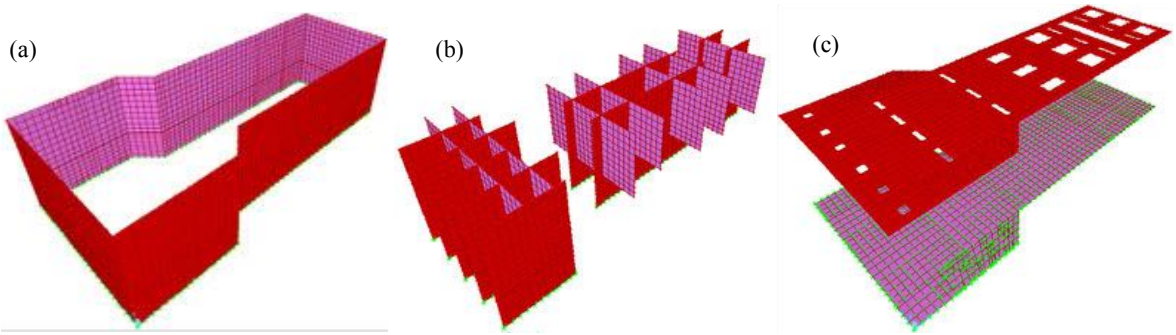

Figure 4. Classifications of shells in the modeled basin; a) outer walls, b) inner walls, c) roof and floor

2.2. Modulus of Soil Sub-grade Reaction

Soil beneath the basin supports the vertical and lateral movement of the structure. Assuming a fixed support is the simplest way for modeling the soil support. However, the better way is to model the actual behavior of the soil by making use of either nonlinear Winkler foundation or elastic continuum [10]. In Winkler model which is implemented in this study, the base soil assumes to behave like infinite number of springs that their stiffness is the modulus of subgrade reaction. By modeling the soil strata, the soil pressure beneath the basin will be obtained by analysis. Since assuming a rigid foundation is a common assumption in conventional modeling of mat foundations, the reliability of conventional methods is investigated in the present study for different soil parameters. To do this, the Finite element analysis is utilized as an effective and accurate way for analyzing the basin under applied loads. Since the sensitivity of the results depend on the soil parameters, different values of soil modulus have been taken into account. A wide range

of values has been recommended for the modulus of subgrade reaction for various soil types and, the exact value of subgrade module at each location should be determined by field test [11]. If not, it can be calculated based on the equations derived based on plate load test [12] and estimates the subgrade modulus as a function of soil parameters [13, 14]. Several equations have been suggested for evaluating subgrade modulus, one of them is the empirical equation recommended by [15] as $k = (40\ to\ 50) \times su$, for clay and $k = (70\ to\ 100) \times NSPT$, for sand. In these equations, k is subgrade modulus [t/m^3], su is undrained shear strength (t/m^2) and NSPT is value of Standard Penetration Test. Finally, typical values for different types of soils can be evaluated as the values in Table 2.

Table 2. Typical values of modulus of sub-grade reaction (ks) for different types of soils

Type of Soil	Loose sand	Medium dense sand	Dense sand	Clayey medium dense sand	Silty medium dense sand
ks (MN/m^3)	5 to 15	15 to 60	60 to 130	30 to 80	20 to 50

In this study, to consider uncertainty of soil condition, different values of soil modulus are modeled in a way to cover different types of soils. For this purpose and based on the typical values, soil modulus are selected as 10, 50, 100 and 130 MN/m^3. A fixed support condition is also modeled as the highest possible stiffness of the base soil.

2.3. Loading

Several combinations of dead, live, hydrostatic, seismic, soil pressure and thermal load act on the structure. Dead loads include the weight of basin structure, attached equipment and accessories. The weight was calculated based on the density of the reinforced concrete as 2400 kg/m^3. Live load is the load superimposed by the use and operation of basin. The following items were considered as live load: Maintenance and equipment hatch load (uniform load) = 1000 kg/m^2, Personal load (uniform load) = 500 kg/m^2. The Hydrostatic load varies linearly with height of the water and it acts perpendicular to the surfaces. The uplift pressure applied to the basin floor is the maximum water pressure with a uniform distribution. Seismic load is evaluated based on Iranian standards for marine structures [16].

Static method is utilized for calculating the inertia effects of earthquake on internal forces and displacements. For conditions of earthquake occurrence, it is considered that the basin is in operation state and it is full of water. The Earthquake coefficient for this condition is considered to be 0.16 ($= 0.13 \times 1.2 \times 1.0$) [17]. This coefficient cross the effective weight generates the earthquake force that is applied to the structure in two directions. Dead load plus 20% of live load is considered as the effective weight in calculating seismic load. In addition, seismic load may generate unbalanced water pressures inside the basin. To consider this effect, 30% of the dead weight is added to the above mentioned effective weight during earthquake and the total weight cross the earthquake coefficient is applied as the earthquake force. It should be noted that the weight of the water inside the basin is applied in the model in the seismic condition when the weight of the structure becomes important. Soil pressure around the basin is evaluated based on the supposed specific gravity and apparent gravity of the soil. Soil pressure is assumed equal in both seismic and ordinary conditions. The lateral soil pressure coefficient is assumed as k_0=0.45. Thermal Loads are defined as a force caused by variation of temperature and it is not considered in this study.

All the loads are combined based on [9] as presented in Table 3. An envelope combination is also determined to show the maximum stresses among different load cases. In addition to common load combinations, some special notes have been taken into account. For example, it may be required during operation to close the stop logs an empty the basin for maintenance or cleaning the basin. In this case, the uplift exerted on the bottom of basin can generate a critical state that governs design of the floor section of the basin foundation. In another case, the internal water pressure is not applied on the exterior walls and only the outer face of these walls are subjected to the hydrostatic pressure from the water outside the basin. In this manner, water pressure acting on the outer face of the exterior walls will not be balanced with the interior pressures and a critical condition is obtained that governs design of the exterior walls. To consider the worst case, MLHW level is considered for evaluating the lateral water pressure on the exterior and interior walls. Therefore, 3.0 m of the basin top is located above the sea water level. In a normal operating condition, hydrostatic pressures act on both sides of an interior wall and it do not generate a bending moment in the interior walls. However, when a section needs repair and it is done by closing the sluice gates, the hydrostatic water pressure is applied to the interior walls of the full sections of the basin. Meanwhile, the external forces applied to structure in this state are as same as the previous condition. The bending moment due to this condition can govern design of internal walls.

Table 3. Load combinations that are used for structural analysis of basin

Load Comb.	Dead Load	Live load	Water Pressure outside	Water Pressure inside	Uplift Pressure	Soil pressure	Earthq. X or Y Dir.
1	1.40						
2	1.40	1.70			1.70		
3	1.40	1.70	1.70		1.70		
4	0.90		1.275		1.275		
5	1.40	1.70	1.70		1.70	1.70	
6	1.40	1.70	1.70	1.70	1.70	1.70	
7, 8, 9, 10	1.05	1.275	1.275	1.70	1.275	1.275	±1.40
11, 12, 13, 14	0.90						±1.40
Envelope	Maximum output of all other combinations						

3. Effect of Soil Modulus

The structure of the basin is analyzed under different load combinations and the maximum bending moment in each element is obtained from the envelope combination. A sample output corresponding to the subgrade reaction modulus of 100 MPa/m is presented in Figure 5. that shows the distribution of the maximum bending moments in two perpendicular directions i.e. M11 and M22 in different elements of the bottom slab. As shown in this figure, the maximum bending moment per unit length of the bottom slab is nearly 200 tonf.m/m. The average value of the maximum bending moments as well as the standard deviation of these values can be calculated. The average value of the bending moment in this case is nearly 17 tonf.m/m and it can be useful in evaluating the adequacy of the thickness of the bottom slab. These maximum, averaged and standard deviations of the maximum bending moments in the bottom slab are calculated for different cases with different subgrade modulus.

The results are shown in Figure 6. According to these results, the averaged value of the bending moment is significantly less than the maximum value which is generated in a local point of the bottom slab. Since the soil modulus are selected based on loose to hard conditions, it can be concluded that the maximum bending moment in the bottom slab is not too sensitive to the soil modulus, however, a harder soil condition results in a lower bending moment value. The limit condition happens when a fixed support is modeled for the base reaction modeling. The averaged value is more sensitive to the changes in soil condition and it has been changed from the maximum value of 19 tonf.m/m in a loose soil to a minimum value of 10 tonfm/m in a hard soil condition. On the other hand, the standard deviation of a hard soil condition is clearly less than softer soil conditions. The effect of soil modulus on the averaged bending moment in different walls is presented in Figure 7. As shown in this figure, the bending moment in the bottom slab is clearly a function of soil modulus. The reason is that the slab is directly supported on soil and its behavior is more sensitive to the soil condition. However, the averaged bending moment in outer walls, inner walls and roof is independent to the soil modulus because stiffness of the intake is dominant to the soil condition.

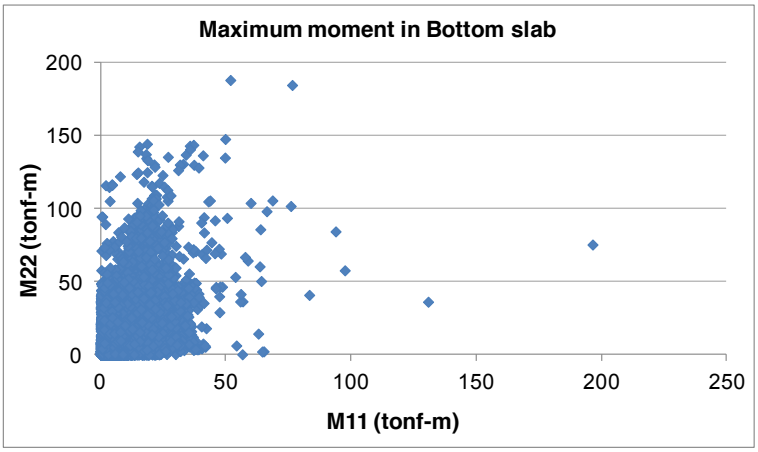

Figure 5. Bending moment in elements of the bottom slab in the envelope load combination

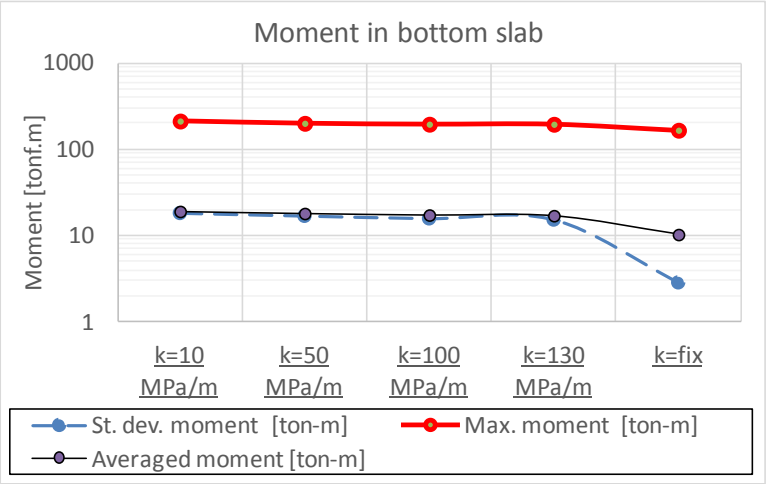

Figure 6. Averaged, standard deviation and maximum bending moment in the bottom slab with different subgrade modulus

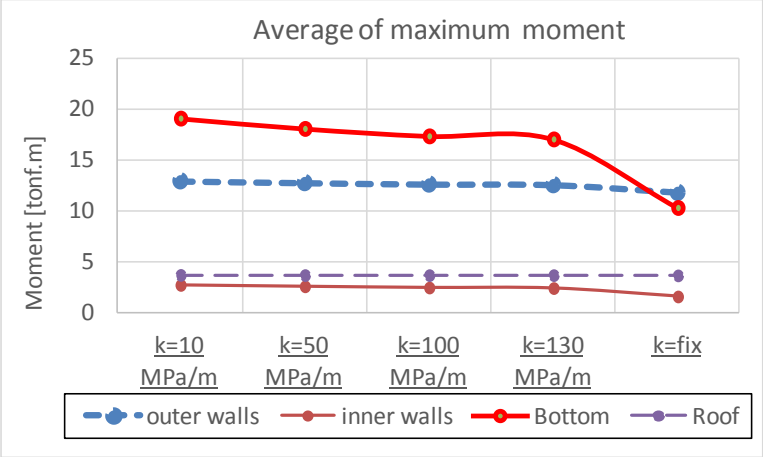

Figure 7. Averaged bending moment in different walls with different subgrade modulus

4. Effect of Bottom Slab Rigidity and Inner Walls

To study the effect of the existence of inner walls on the generated bending moment in the basin, two different structures with and without inner walls are analyzed by taking into account two different soil conditions with soil modulus of 10 and 100 MPa/m. The results i.e. averaged bending moment in different walls and slabs are presented in Figure 8. As shown in this figure, in the case of removing the inner walls, bending moment in all the shells (outer walls, roof and bottom slab) has been increased. The maximum effect is yet in the bottom slab where the averaged bending moment in the case of a structure without any inner wall is nearly twice the averaged bending moment in the case of existence of inner walls. The bending moment in the roof is also increased significantly by removing the inner walls. The minimum effect, however, has been occurred in the outer walls. Actually, the inner walls increase the rigidity of bottom slab and roof sections clearly and the length between the stiff supports will be decreased accordingly.

The outer walls are not supported on the inner walls and therefore, they experience fewer amounts of changes due to removing inner walls. On the other hand, the effect of soil stiffness on the averaged bending moment is little especially in outer walls and roof slabs. The bottom slab is the only shell element type that its bending moment is a function of soil stiffness. However, the effect of inner walls on the generated bending moment is clearly more than the effect of the soil condition. It is worth mentioning that the effect of soil condition on the averaged bending moment is limited only to the bottom slab and this effect is yet less than the effect of inner walls. In a soft soil condition, the existence of inner walls is more important in controlling the bending moment in bottom slab because the contribution of inner walls in the total stiffness is higher than its contribution in a stiff soil condition. As shown in Figure 9, the averaged bending moments in the bottom slab of a structure with inner walls are nearly the same for two soil conditions. However in the case of removing inner walls, the bending moment in the bottom slab has been increased nearly 30% in the case of the softer soil condition.

In addition to the inner walls, rigidity of the bottom slab depends on the thickness of the foundation. To evaluate this item, two different thicknesses i.e. 0.5 m and 1.5 m have been modeled for the shell elements at the bottom slab.

The results are presented in Figure 9. The thickness of the bottom slab does not affect the averaged bending moments in other walls and its effect is limited only to the bottom slab itself. A thicker slab absorbs a higher bending moment in a way that by increasing the thickness by three times, the generated averaged bending moment has been increased by the same order.

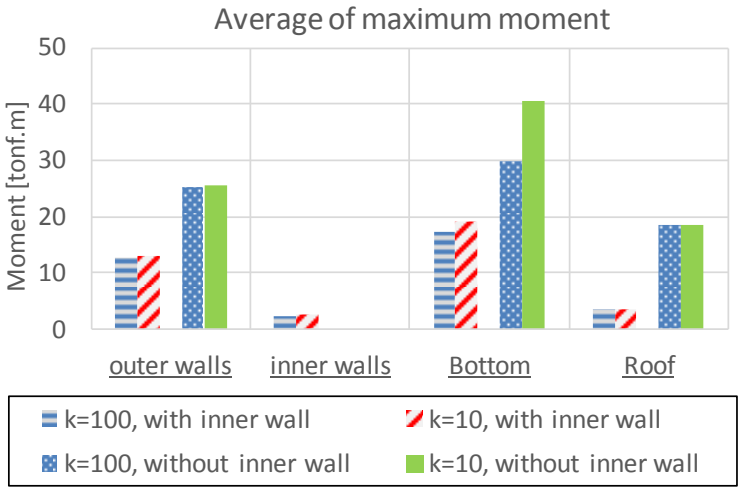

Figure 8. Averaged bending moment in different walls with and without inner walls and two different subgrade modulus

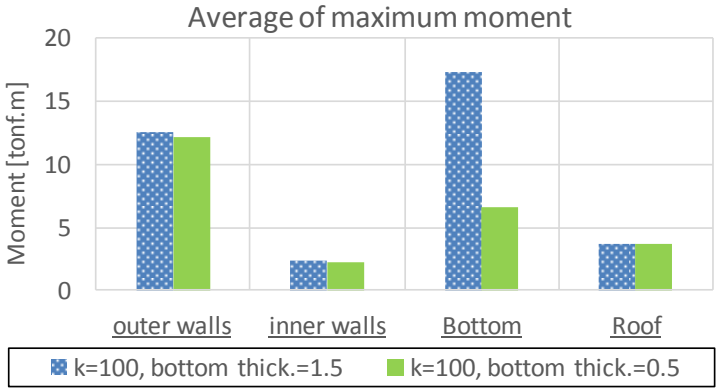

Figure 9. The effect of rigidity o the bottom slab on the averaged bending moment in different walls

5. Conclusion

The structural behavior of a water intake basin is studied under different applied loads. Since the basin is a buried structure which is supported vertically by the soil layers, the effect of the soil modulus on the internal bending moments is investigated by making use of a FEM analysis. Different soil parameters from a soft to a stiff condition have been taken into account to cover the unreliability of the soil parameters. In addition, the rigidity of the foundation is studied by making use of different thicknesses and removing inner walls. Based on the results, it is concluded that:

- The maximum bending moment in the basin structure is not too sensitive to the soil stiffness and the maximum effect of the soil modulus on the maximum bending moment is nearly 25% that occurs in the bottom slab located directly on the soil.
- In comparison with the maximum bending moment, the averaged bending moment in the bottom slab is more sensitive to the soil parameters and the averaged bending moment would be underestimated if a stiff soil condition was considered. In another word, the averaged bending moment in the bottom slab will be increased by assuming a softer soil condition. On the other hand, the averaged bending moment in other walls except the bottom slab is nearly independent to the soil modulus.
- The bending moment will be increased in all of the basin elements in the case of removing internal walls. Among the basin elements, the roof and bottom slabs are more sensitive because they are actually supported by inner walls.
- The effect of inner walls on the bending moment depend on the soil parameters and in a case of removing inner walls, the averaged bending moment in the bottom slab can be increased nearly 30% from a stiff to a soft soil condition. The effect of inner walls on the generated bending moment is more than the effect of the soil

condition and in a soft soil condition; the averaged bending moment in the bottom slab may be doubled in the case of removing internal walls.

- The thickness of the bottom slab defines its rigidity and by thickening the foundation slab a higher bending moment will be obtained. However, the bending moments in other walls i.e. outer wall, roof and inner walls are not a function of the foundation thickness.
- As a result, design of the basin walls based on the maximum bending moment can be done with making an acceptable assumption for the soil modulus. However, it is necessary to model the geometry of inner walls accurately when evaluating the structural behavior of a basin. It can be concluded that the contribution of the soil modulus in the total stiffness of the basin is less than the contribution of the geometry of the basin.

6. References

[1] Bleninger, T., G. H. Jirka, and S. Lattemann. "Environmental planning, prediction and management of brine discharges from desalination plants." Middle East Desalination Research Center (MEDRC): Muscat, Sultanate of Oman (2010)..

[2] Roscoe Moss Company. Designing buried seawater intake structured for enhanced corrosion resistance and prolonged durability. Technical memorandum 008-2. (2008).

[3] Mackey, Erin D., and Water Research Foundation. Assessing seawater intake systems for desalination plants. Water Research Foundation, 2011.

[4] Akbari, H., Ebrahimi, M.H., Near field mixing of Multi-Diffuser Dense Jets in Shallow water condition and Ambient Currents. 15th national hydraulic conference, Iran. (2016).

[5] Pita, E., and Isidro Sierra. "Seawater intake structures." In Proceedings International Symposium on Outfall Systems. Mar del Plata, Argentina. 2011.

[6] Pun, W. K., W. M. Cheung, and L. S. Lui. "Geotechnical standards in Hong Kong." In New Generation Design Codes For Geotechnical Engineering Practice—Taipei 2006.

[7] Poulos, H. G. "Methods of Analysis of Piled Raft Foundations. Report to Technical Committee TC 18 on Piled Foundations." (2001).

[8] Balasurbamaniam, S., and E. Y. N. Oh. "Parametric Study on Piled Raft Foundation in Sand Using Numerical Modelling." In Eleventh East Asia pacific Conference on Structural Engineering and Construction, pp. 19-21. 2008.

[9] ACI 318-2008: Building code requirements for structural concrete (2008). Standard code.

[10] Kame, G. S., S. K. Ukarande, K. Borgaonkar, and V. A. Sawant. "A parametric study on raft foundation." In 12th International Conference of International Association for Computer Methods and Advances in Geomechanics (IACMAG), Goa, India, pp. 3077-3085. 2008.

[11] Hussein, H. "Effects of flexural rigidity and soil modulus on the linear static analysis of raft foundations." Journal of Babylon University, Pure and Applied Sciences 19, no. 2 (2011).

[12] Moayed, Reza Ziaie, and Masoud Janbaz. "Foundation size effect on modulus of subgrade reaction in clayey soil." Electronic Journal of geotechnical Engineering 13 (2008): 1-8.

[13] Gagin, V. and Ivanilov P., Analysis of Lengthy Structures Resting on Multi-Layer Soil Foundation Taking Into Account Stochastic Behavior of Soil, Studia Geotechnica et Mechanica, Moscow, Russia, Vol. XXX, No. 3–4. (2008).

[14] Liao, S. S. C. "Estimating the coefficient of subgrade reaction for plane strain conditions." In Proceedings of the Institution of Civil Engineers: Geotechnical Engineering, vol. 113, no. 3. 1995.

[15] Widjaja, Budijanto. "Parametric Studies for Obtaining the Dimension of Soil Improved Area." Volume 8, No. 1, pp. 31–35. (2008).

[16] Iranian standard for design of coastal structures (1392-2013), (NO. 631: design conditions). Standard code.

Available online at www.CivileJournal.org

Civil Engineering Journal

Vol. 3, No. 3, March, 2017

Slope Remediation Techniques and Overview of Landslide Risk Management

Danish Kazmi [a], Sadaf Qasim [a*], I.S.H Harahap [b], Syed Baharom [b], Mudassir Mehmood [a], Fahad Irfan Siddiqui [c], Muhammad Imran [b]

[a] *NED University of Engineering & Technology, University Road, Karachi 75270, Pakistan.*

[b] *Universiti Teknologi Petronas, Seri Iskandar, Perak 32610, Malaysia.*

[c] *Mehran University of Engineering & Technology, Jamshoro76062, Pakistan.*

Received 5 February 2017; Accepted 22 March 2017

Abstract

Slope failures are common in many parts of the world which occur due to manifold reasons and they result in huge losses to the respective locals. This study evaluates the initiatives that can enhance the safety of slope by considering the remedial measures to deal with the factors causing slope instability and discusses the application of risk management strategies to address the problems that can cause the slope to fail. The methods for the remediation of slope include modification in slope geometry, drainage, use of retaining structures and internal slope reinforcement. This study also discusses the risk management process which is a hierarchical procedure that includes assessment and control of risk through different techniques in order to manage the uncertainties associated with the slope. It has been observed that the implementation of risk management strategy aids in the proper identification of risk and its severity which dictates the selection of appropriate remedial measure for the rectification of slope. For reducing the number of landslides, this study suggests the use of risk based strategies to curtail the chances of slope failure.

Keywords: Slope Failures; Slope Geometry; Drainage; Retaining Structures; Internal Slope Reinforcement; Risk Management Process.

1. Introduction

Landslides have resulted in the loss of human lives and properties in many parts of the world. To combat landslide risk, a wide range of risk mitigation measures are available. These range from hard engineering measures of slope stabilization and landslide protective works to soft community means of public education. Stabilization works aim at reducing the likelihood of failure of a slope whereas the other measure reduces the risk by minimizing the consequences of slope failures. The range of slope stabilization works may be categorized as follows [1]:

a. Surface protection and drainage
b. Subsurface drainage
c. Slope regarding
d. Retaining structures
e. Structural reinforcement
f. Strengthening of slope-forming material
g. Vegetation and bioengineering
h. Removal of hazards
i. Special materials and techniques

* Corresponding author: sadafqasim26@yahoo.com

It is a fact that slope failures account for enormous losses every year, both compensatory and non-compensatory. These failure events occur due to varying reasons which predominantly include design inaccuracies, lapses in construction, poor drainage system and lack of maintenance. It is observed that misperceptions towards the technical aspects of slope also contribute to the failure. Some of the misperceptions highlighted by Gue and Fong are given below [2].

1.1. Soil Tests Showed that Slope is Safe

It is irrational to rely solely on tests as soil is a very complex material and its properties can vary even at a very short distance. Remarkably detailed investigations are required to propose safety. In fact, they are the source of getting design variables used in analysis and designing of the slopes.

1.2. Heavy Rain Cause Slope Failures

It is not always the case because properly designed slopes will not fail unless water table and pore water pressure exceeds the design limit. Rainfall may catalyse the instability of slope but if the slope is designed as per requirement then the failure is unlikely.

1.3. Retaining Walls Always Prevents Slope Failures

This is only possible if retaining walls are designed according to required specifications, fulfilling every design criteria which is usually not satisfied in un-engineered walls.

1.4. Slopes Are Maintenance Free

Maintenance activities like clearing the debris from drains, covering up the erosion spots are essential. Blocked drains create excess water pressure which ultimately leads to slope failure. Poor maintenance or non-maintenance of slopes has significant contribution in decreasing the slope stability.

For slope stabilisation, Thompson et al., 2005 [3] proposes that slope reinforcement and the use of structural pile elements can be an effective slope remediation alternative when conventional remediation practices (e.g., improved drainage) fail to consider the causal factors leading to slope instability (e.g., strength loss due to weathering). An experimental research program was aimed at developing a rapid, cost-effective, and simple remediation system that can be implemented into slope stabilization practices for relatively shallow (<5 m) slope failure conditions. The results of the study shows that piles installed in failing slopes will arrest or slow the rate of slope movement.

The study of Ashour and Ardalan, 2012 [4], presents a new procedure for the analysis of slope stabilization using piles. The developed method allows the assessment of soil pressure and its distribution along the pile segment above the slip surface based on soil–pile interaction. The proposed method accounts for the influence of pile spacing on the interaction between the pile and surrounding soils and pile capacity.

The slope strengthening initiatives are taken on the basis of the factors that affect the stability of slope and the level of risk they are posing. In order to address the risk associated with the slope there is need to apply the risk management strategy for reducing the chances of failure. The risk management takes the output from the risk assessment, and considers risk mitigation, including accepting the risk, reducing the likelihood, reducing consequences e.g. by developing monitoring, warning and evacuation plans or transferring risk (e.g. to insurance), develops a risk mitigation plan and possibly implements regulatory controls. It also includes monitoring of the risk outcomes, feedback and iteration when needed. Landslide risk management involves a number of stakeholders including owners, occupiers, the affected public and regulatory authorities, as well as geotechnical professionals, and risk analysts. It is an integral part of risk management that the estimated risks are compared to acceptance criteria (either quantitative or qualitative). Geotechnical professionals are likely to be involved as the risk analysts, and may help guide in the assessment and decision process, but ultimately it is for owners, regulators and governments to decide whether the calculated risks are acceptable or whether risk mitigation is required [5].

Landslide risk management comprises an estimation of the landslide risk, deciding whether or not the risk is tolerable, exercising appropriate control measures to reduce the risk where the risk level cannot be tolerated. In a more global context, landslide risk management also refers to the systematic application of management policies, procedures and practices to the tasks of identifying, analyzing, assessing, mitigating and monitoring landslide risk [6].

2. Objectives of the Study

The objectives of the study are as follows:

1) To discuss the potential remedial works that can be employed for maximizing the stability of the slopes

2) To explore the approaches for risk based evaluation of slope and discuss the strategies for landslide risk management

3. Causal Factors of Landslides

There are two primary categories of causes of landslides: natural and human caused. Sometimes, landslides are caused, or made worse, by a combination of the two factors. The natural causes have three major triggering mechanisms that can occur either singly or in combination with water, seismic activity, and volcanic activity. Effects of all of these causes vary widely and depend on factors such as steepness of slope, morphology or shape of terrain, soil type, underlying geology, and whether there are people or structures on the affected areas [7] .

With regards to the human causes, populations expanding onto new land and creating neighborhoods, towns, and cities are the primary means by which humans contribute to the occurrence of landslides. Disturbing or changing drainage patterns, destabilizing slopes, and removing vegetation are common human-induced factors that may initiate landslides. Other examples include over steepening of slopes by undercutting the bottom and loading the top of a slope to exceed the bearing strength of the soil or other component material. However, landslides may also occur in once-stable areas due to other human activities such as irrigation, lawn watering, draining of reservoirs (or creating them), leaking pipes, and improper excavating or grading on slopes [7].

Table 1. A brief list of landslide causal factors [8]

1.	**Ground Conditions**
(1)	Plastic weak material
(2)	Sensitive material
(3)	Collapsible material
(4)	Weathered material
(5)	Sheared material
(6)	Jointed or fissured material
(7)	Adversely oriented mass discontinuities (including bedding, schistosity, cleavage)
(8)	Adversely oriented structural discontinuities (including faults, unconformities, flexural shears, sedimentary contacts)
(9)	Contrast in permeability and its effects on ground water contrast in stiffness (stiff, dense material over plastic material)
2.	**Geomorphological Processes**
(1)	Tectonic uplift
(2)	Volcanic uplift
(3)	Glacial rebound
(4)	Fluvial erosion of the slope toe
(5)	Wave erosion of the slope toe
(6)	Glacial erosion of the slope toe
(7)	Erosion of the lateral margins
(8)	Subterranean erosion (solution, piping)
(9)	Deposition loading of the slope or its crest
(10)	Vegetation removal (by erosion, forest fire, drought)
3.	**Physical Processes**
(1)	Intense, short period rainfall
(2)	Rapid melt of deep snow
(3)	Prolonged high precipitation
(4)	Rapid drawdown following floods, high tides or breaching of natural dams
(5)	Earthquake
(6)	Volcanic eruption
(7)	Breaching of crater lakes
(8)	Thawing of permafrost
(9)	Freeze and thaw weathering
(10)	Shrink and swell weathering of expansive soils

4. Man-Made Processes
(1) Excavation of the slope or its toe
(2) Loading of the slope or its crest
(3) Drawdown (of reservoirs)
(4) Irrigation
(5) Defective maintenance of drainage systems
(6) Water leakage from services (water supplies, sewers, storm water drains)
(7) Vegetation removal (deforestation)
(8) Mining and quarrying (open pits or underground galleries)
(9) Creation of dumps of very loose waste
(10) Artificial vibration (including traffic, pile driving, heavy machinery)

4. Remedial Measures for Slope

Slopes are all around us in the urban environment, and the soil on some of these slopes may be inherently unstable. Old, natural slopes in rural and forest areas have often developed a degree of stability over time. But artificial slopes within urban areas that are part of developments, or that are adjacent to infrastructure such as roads and railways, can be less stable, and may require stabilization [9].

Movement of soil and rock down unstable slopes due to gravity is called mass wasting; surface movement resulting from the effects of wind and water is called erosion. Both processes can affect the safety of people living or working on or near slopes, and on the quality of water for people living in the wider area. The expansion of urban areas, and associated deforestation and construction activities, are increasing the area of unstable or vulnerable slopes [9].

Decision on selecting an appropriate slope stabilisation method requires thorough evaluation of the existing slope conditions and assessment of the prevailing causes that are responsible for the instability of the slopes. Once the causes of slope stability are identified, the appropriate remedial measure for slope is selected on the basis of feasibility, stability and economy. These remedial measures are helpful in minimizing the chances of approaching slope failure by addressing its cause.

Precautionary action means detection of landslide prone area, early warning signs and slope assessment techniques to take necessary measure for their remediation. Government agencies put forward different policies while private sector also takes initiatives to prevent the consequences of slope failure by developing its own guidelines. The remedial methods proposed by Broms and Wong are divided into three main categories [10].

4.1. Geometrical Method

This method is simple and cheaper in cost but require sufficient space. Slope safety can be enhanced easily to convert steeper slopes into gentler ones. This method can be executed by trimming the slope or making the slope free from extra loading. Backfilling of toe also lies under this category.

By changing the geometry of a steep slope to a gentler slope either flatten the slope or backfill at the toe of slope, the stability of a slope can be increased. This method is easy and most cost effective. However, it depends very much on the site condition. As there are existing building at the site, this method cannot be adopted [11].

4.2. Drainage Method

This method usually works in combination with other methods. Drainage method is viable in those conditions where proper maintenance of surface and sub-surface drains is performed.

Saturation of subsoil and pore water pressure building up are major factors causing the instability of slope. With the proper design of surface and subsurface drainage system, the chances of building up pore water pressure and saturation of subsoil can be minimized and therefore the stability of slope can be increased. However, as a long term solution to increase the stability of slope, this method suffers greatly because the drainage systems must be maintained if they are to continue to function It is always easy to maintain the surface drains but very difficult for the subsoil drains. This method is generally used in combination with other methods [11].

4.3. Retaining Structures Method

This method is quite expensive but flexible in nature. In this method retaining structures are used to withstand against the pushing forces of the soil masses. Retaining structures have different varieties such as gravity and cantilever retaining wall, contiguous bored piles and sometimes method of soil nailing is also used to stabilize slopes.

Retaining structures include gravity types of retaining wall, cantilever retaining wall, contiguous bored piles, caisson, steel sheet piles, ground anchors, soil nails etc. This method is generally more expensive as compared with the other methods. However, it is always the most commonly adopted method in remedial works due to its flexibility in a constraint site. For this project, the remedial work can only be carried out within the boundary, a restrained structure is inevitable in order to stabilize and reinstate the failed slope [11].

The remedial works proposed by Popescu, [12] carry four groups namely slope geometry, drainage, retaining structures and internal slope reinforcement. The initiatives in the category of slope geometry involve fundamental changes that include removing material from the landslide driving area and reducing the slope angle. The remedial works in the class of drainage involve different methods which include providing boreholes, wells and water removal techniques. The category of retaining structures includes provision of different types of structure to give stability to the slope while the category of internal slope reinforcement includes providing anchors, micro piles and soil-nailing.

Table 2. Landslides Remedial Works [12]

Slope Geometry
Adding (counter weight berm or fill) material to stability maintain area
Removing material from landslide driving area (light weight fill)
Reducing the slope angle
Drainage
Surface drains for diversion of water (pipes and ditches)
Shallow or deep trench drains having filled with free draining Geo-materials
Vertical boreholes for self-draining
Vertical wells for gravity draining
Buttress counterforts of coarse grained materials
Sub vertical and sub horizontal boreholes
Drainage tunnels, galleries drainage by siphoning
Electroosmotic dewatering, Vacuum dewatering
Retaining Structures
Gravity retaining walls
Gabion walls, Crib-block walls
Passive piles, Piers, Cassions
Cast in situ reinforced concrete walls
Reinforced earth retaining structures
Buttress counterforts of coarse grained materials
Rock fall attenuation or stopping systems
Protective rocks or concrete blocks against erosion
Internal Slope Reinforcement
Rock bolts/ Anchors/Electroosmotic anchors Micro piles Soil nailing

5. Risk Based Planning of Slopes

The study of Li et al., 2009 [13] refers to the soil cut which are subject to deterioration and prone to failure especially during the monsoons and as a consequence of seismic activity. In this regard, risk based stabilized planning is developed to counter the deteriorating slopes.

Risk based stabilization planning is used as a tool in decision making to minimize the chances of slope failure and its consequences. The proper follow up of stabilization programme not only covers slope deterioration but also reduces

the maintenance expenditure. Level of risk (whether in in acceptable limits or not) can be easily estimated and reduction measures can be adopted through this risk based methodology in case of intolerable risk levels.

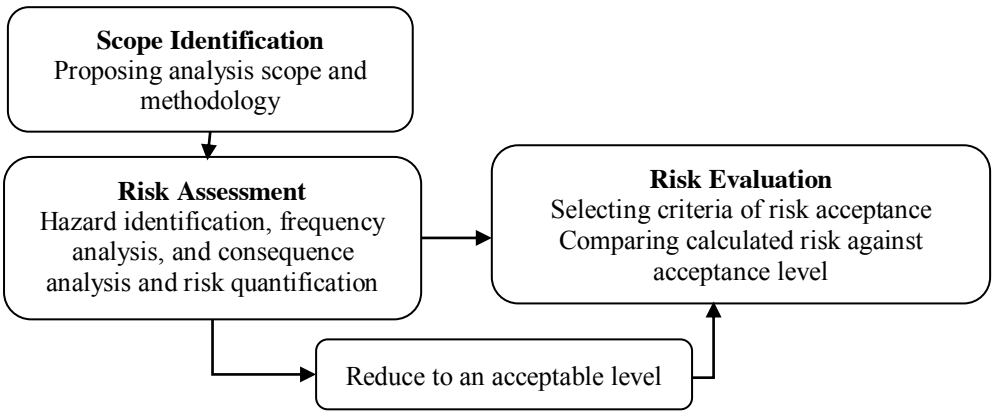

Figure 1. Risk based stabilization planning [13]

Landslide risk assessment and management encompasses the judgment of the level of risk [14]. Risk level has to be checked, whether if it is in an acceptable mode or not, and implement the correct controlling measures to minimize the risks. It needs the following issues to be discussed.

- Probability of land sliding
- Run out behaviour of landslide debris
- Vulnerability to people and property by the landslide
- Management strategies and decision-making.

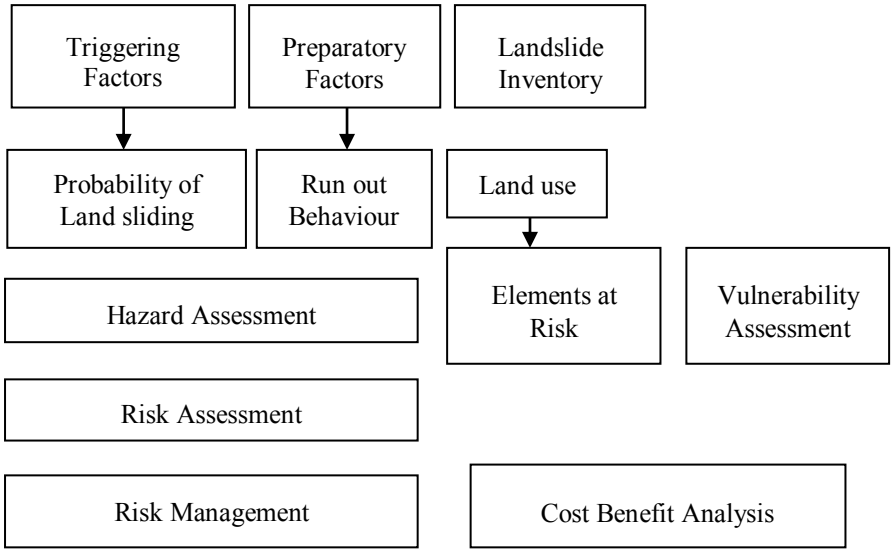

Figure 2. Landslide Risk Assessment and Management [14]

6. Risk Management Framework

A general risk management framework proposed by Shong [15] is shown in Figure 3. It involves four basic steps of:

- Planning
- Execution
- Review
- Improvement

In calculating the risks, equally important parameter of probability of slope failure has to be carried out first. Same is put forwarded by Shong [15] when discussing about the steps involved in determining slope stability assessment. In slope stability assessment, the major stages involved are given below:

- Evaluation of silhouette/shape with the condition of the slope.

- Weighing the external effect and their impact. For example surcharge, accidental loads on slopes or embankments.
- Determination of slope conditions for different time periods and selection of logical stability measures.

Figure 3. Risk Management framework [15]

A baseline approach for managing risks in developing countries is also proposed by Kjekstad [16]. The approach is divided into three pillars:

- Assessment or prediction of hazards and risks
- Mitigation measures for landsides
- Contribution of cooperation and support by other developed countries.

According to Nadim and Lacasse [17], the optimal risk mitigation strategy involves the following:

- Identification of possible landslide triggering scenarios, and the associated hazard level
- Analysis of possible consequences for the different scenarios
- Assessment of possible measures to reduce and/or eliminate the potential consequences
- Recommendation of specific remedial measure and if relevant reconstruction and rehabilitation plans
- Transfer of knowledge and communication with authorities and society

6. Probability of Slope Failure and Risk Management

The discussion on probability of slope failures as temporal and spatial probability has been done before by Van Westen et al., 2006 [18]. Spatial probability is directly concerned with static environmental factors of slope strength; material properties and depth while temporal are referring to dynamic factors such as rainfall intensities and drainage.

Another study discussed about the probability of failure of site specific slopes by Dai et al., 2005 [14]. In actual probability of failure is referring to the probability of the safety factor having value less than 1. The performance function $G(X)$ is the main function of the slopes which differentiates between the safety and the failure. If $G(X) > 0$ failure will not take place and $G(X) < 0$ shows that the safety level is alarming which means most probably it will fail. The performance function $G(X) = 0$ is a limit state boundary. It separates the two states. Once the performance function is established by taking all input variables involved in the stability analysis, the probability of failure can be calculated using statistical tools. Mathematically performance function is defined as:

$$G(X) = F(X) - 1 \quad (1)$$

or

$$G(X) = R(X) - S(X) \quad (2)$$

Where safety factor is denoted by $F(X)$, $R(X)$ is the resistance and $S(X)$ is the load.

Slope stability is one of the main controlling factors of landslide. Assessment of the existing slope in relation to risk is more meaningful in relation to the landslide issues. It is imperative to follow a risk management planning process which is a hierarchical procedure for the assessment of risk which indicates that the basic approach remains the same. In this connection, Canadian Standard Association [19] produced an extensive model about the assessment and the control of the risk which is given below.

Figure 4. Risk Management process [19]

7. Consequence Estimation of Slope Failure

It is one of the most significant components used to evaluate risk. Unlike the identification of hazard, it is performed quantitatively and provides information about the significance level of the probable effects. When consequence estimation is related to a particular accident, it is viable to decide from which aspect the safety and health of surrounding community can be affected. Consequence estimation can be performed by:

- Expert opinions/judgements
- Information about past incidences for comparison
- Consequence modelling

Wong et al., 1997 [20] proposed a consequence model which included slope features like slope angle and its height, landslide size and susceptibility to the affected amenities. The amenity is supposed to be at worst location and its degree of living is taken as below average. The anticipated consequences of failure (potential loss of life PLL) are measured according to real size/actual size of failure and the actual location of the facility.

Mathematically potential loss of life (PLL) can be defined as:

$$\text{PLL} = \sum \left\{ \begin{array}{c} \text{Expected no of fatalities directly by reference landslide} \end{array} \right\} \left\{ \frac{\text{Actual size of landslide}}{\text{Size of reference landslide}} \right\} \left\{ \begin{array}{c} \text{Vulnerability factor} \end{array} \right\} \quad (3)$$

The definition of vulnerability according to the glossary of risk-assessment terms of the International Society of Soil Mechanics and Geotechnical Engineering is the extent of losses to a specified element or combination of elements within the area hit by the landslide hazard. It is expressed on a scale of 0 (no loss) to 1 (total loss).

Vulnerability may perhaps be the propensity to loss (or the probability of loss) and not the degree of loss [21]. According to Li et al., [21] model definition of vulnerability is:

"Vulnerability (V) is defined as a function of the hazard intensity associated with exposed elements at risk and the resistance ability of the elements to withstand a threat".
Mathematically it can be summarized as:

$$V = f(I\ R) \quad (4)$$

Where:
I = intensity of risk exposed elements
R= ability of the elements to bear the threat

Basically the intensity refers to the two components including dynamic intensity factor taking velocity into consideration and geometric intensity factor which is governed with size related features of landslides. In the context of different localities, intensity can be modified with debris depth factor and deformation factor. Considering the resistance factor, it is indirectly dependent on construction material, age and height.

A study by Uzielli et al., 2008 [22] anticipated a univocal logical framework for quantitative evaluation of substantial vulnerability to landslides, which is expressed as a function of landslide intensity and susceptibility of vulnerable elements. Mathematically its definition is:

$$V = f(I\ S) \tag{9}$$

Vulnerabilities of persons, structures and persons in structures have also been estimated. Kaniya et al., 2008 [23] has shown the methodology for its estimation using first-order second-moment method. This method is mostly to be used for approximation of regional landslide risks because of the involvement of comprehensive indices such as impact spatial ratio, population density and per capita GDP.

8. Discussion

In slope stability analysis, risks and uncertainties related to properties of that particular soil has to be investigated in more rigorous manner. Uncertainties associated with the soil properties are basically the output of insufficient or inaccurate data, errors propagated by different testing techniques or different statistical operations. Due to composite nature of soils, the spatial variation in its properties are obvious and it is in actual the product of natural geological processes.

Risk of landslides can be quantified through likelihood of slope failure and the losses occurred. When slope stability problems are measured, the prime factor is to conclude the safety level of that particular slope. An accurate determination of safety level should appropriately deal three geotechnical basics that work with slope stability, geometry, pore pressure and strengths [24].

It is necessary to adhere to a proper risk assessment plan for managing the risks associated with landslides. It essentially comprises of evaluation of risk likelihood and its possible consequences which leads to the estimation of risk. In case, if the risk is found to be high compared to a limiting value, revision in the work is required to prevent the imminent failure.

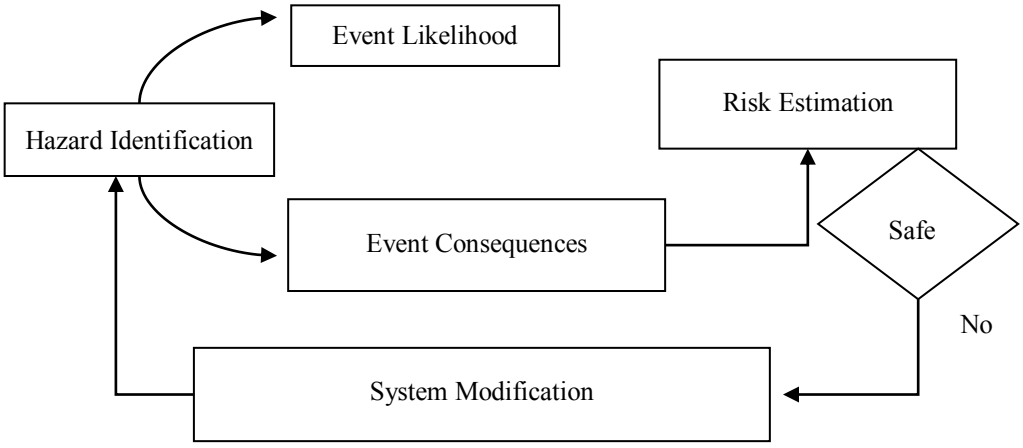

Figure 5. Risk Assessment Plan [24]

8. Conclusion

It has been established that landslides are responsible for prodigious losses every year which includes both compensatory and non-compensatory. Through various investigations it is clear that the landslides are triggered by several factors however, their chances can be minimized by employing a risk management strategy to cope with the factors causing slope instability and to take appropriate remedial measures for their rectification. The benefit of adhering to a risk based strategy is that it identifies the vulnerability to slope as a result of various factors by locating the risk and evaluating its intensity which leads to the selection of proper mitigation technique and reduction in the chances of slope failure. To curtail the landslide events, this paper suggests the use of risk based strategies to figure out appropriate solutions for the prevention of landslides.

7. References

[1] Pun, W. and G. Urciuoli. Soil nailing and subsurface drainage for slope stabilisation. in Proceedings of the Tenth International Symposium on Landslides and Engineered Slopes. 2008.

[2] Gue, S.S. and C.C. Fong, Slope safety: Factors and common misconceptions. Buletin Ingenieur, 2003. 19.

[3] Thompson, M.J., D.J. White, and M.T. Suleiman. Lateral load tests on small-diameter piles for slope remediation. in Proceedings of the 2005 Mid-Continent Transportation Research Symposium, Ames, Iowa. 2005.

[4] Ashour, M. and H. Ardalan, Analysis of pile stabilized slopes based on soil–pile interaction. Computers and Geotechnics, 2012. 39: p. 85-97.

[5] Fell, R., K.K. Ho, S. Lacasse, and E. Leroi, A framework for landslide risk assessment and management. Landslide risk management, 2005: p. 3-25.

[6] Ho, K. and F. Ko, Application of quantified risk analysis in landslide risk management practice: Hong Kong experience. Georisk, 2009. 3(3): p. 134-146.

[7] Highland, L. and P.T. Bobrowsky, The landslide handbook: a guide to understanding landslides2008: US Geological Survey Reston.

[8] Popescu, M.E. Landslide causal factors and landslide remediatial options. in 3rd International Conference on Landslides, Slope Stability and Safety of Infra-Structures. 2002. Citeseer.

[9] Slope stabilisation. 2006; Available from: https://www.forestry.gov.uk/fr/urgc-7evd56.

[10] Broms, B.B. and I.H. Wong, Stabilization of slopes with geofabric. Third International Geotechnical Seminar on Soil Improvement Methods, Singapore, 1985: p. 75-83.

[11] Chen, C. Stabilization of a failed slope with reinforced soil wall. in Proceedings of the 14th Southeast Asia Goetechnical Conference. 2001.

[12] Popescu, M., A Suggested Method for Reporting Landslide Remedial Measures. Bulletin of Engineering Geology and the Environment, 2001. 60(1): p. 69-74.

[13] Li, D., L. Zhang, C. Zhou, and W. Lu, Risk-based stabilization planning for soil cut slopes. Natural Hazards and Earth System Sciences, 2009. 9: p. 1365-1379.

[14] Dai, F.C., C.F. Lee, and Y.Y. Ngai, Landslide risk assessment and management: an overview. Engineering Geology, 2002. 64(1): p. 65-87.

[15] Shong, L.S. Slope Stability Assessment. in One-Day Short Course on Slope Engineering. 2010. Kota Kinabalu.

[16] Kjekstad, O. The Challenges of Landslide Hazard Mitigation in Developing Countries. in First North American Landslide Conference 2007. Vail, Colorado.

[17] Nadim, F. and S. Lacasse, Strategies for mitigation of risk associated with landslides. Landslides-Disaster Risk Reduction, 2008.

[18] Van Westen, C.J., T.W.J. Van Asch, and R. Soeters, Landslide hazard and risk zonation—why is it still so difficult? Bulletin of Engineering Geology and the Environment, 2006. 65(2): p. 167-184.

[19] CSA, Risk Analysis Requirements and Guidelines. Canadian Standard Association, CAN/CSA-Q634-91, 1991.

[20] Wong, H.N., K.K.S. Ho, and Y.C. Chan. Assessment of Consequence of Landslides. in Proceedings of the Landslide Risk Workshop, IUGS Working Group on Landslides,. 1997. Honolulu.

[21] Li, Z., F. Nadim, H. Huang, M. Uzielli, and S. Lacasse, Quantitative vulnerability estimation for scenario-based landslide hazards. Landslides, 2010. 7(2): p. 125-134.

[22] Uzielli, M., F. Nadim, S. Lacasse, and A.M. Kaynia, A conceptual framework for quantitative estimation of physical vulnerability to landslides. Engineering Geology, 2008. 102(3-4): p. 251-256.

[23] Kaynia, A.M., M. Papathoma-Köhle, B. Neuhäuser, K. Ratzinger, H. Wenzel, and Z. Medina-Cetina, Probabilistic assessment of vulnerability to landslide: Application to the village of Lichtenstein, Baden-Württemberg, Germany. Engineering Geology, 2008. 101(1-2): p. 33-48.

[24] Silva, F., T.W. Lambe, and W.A. Marr, Probability and Risk of Slope Failure. Journal of Geotechnical and Geoenvironmental Engineering, 2008. 134(12): p. 1691-1699.

Available online at www.CivileJournal.org

Civil Engineering Journal

Vol. 3, No. 3, March, 2017

State of the Art: Mechanical Properties of Ultra-High Performance Concrete

Mohamadtaqi Baqersad [a*], Ehsan Amir Sayyafi [a], Hamid Mortazavi Bak [b]

[a] *Ph.D. Student, Department of Civil and Environmental Engineering, Florida International University, Miami, FL, USA.*

[b] *Ph.D. Student, Department of Civil Engineering, Isfahan University of Technology, Isfahan, Iran.*

Received 7 February 2017; Accepted 25 March 2017

Abstract

During the past decades, there has been an extensive attention in using Ultra-High Performance Concrete (UHPC) in the buildings and infrastructures construction. Due to that, defining comprehensive mechanical properties of UHPC required to design structural members is worthwhile. The main difference of UHPC with the conventional concrete is the very high strength of UHPC, resulting designing elements with less weight and smaller sizes. However, there have been no globally accepted UHPC properties to be implemented in the designing process. Therefore, in the current study, the UHPC mechanical properties such as compressive and tensile strength, modulus of elasticity and development length for designing purposes are provided based on the reviewed literature. According to that, the best-recommended properties of UHPC that can be used in designing of UHPC members are summarized. Finally, different topics for future works and researches on UHPC's mechanical properties are suggested.

Keywords: Durability; Tensile Strength; Cracking; Fiber Reinforcement Polymer; Bond Properties.

1. Introduction

Concrete, along with steel, is the most widely used material in the construction of infrastructures. The reliable foundation provided by concrete makes it an appealing choice for traditionally non-concrete structures [1, 2], dams [3], pavement [4, 5] and bridges. However, the low tensile strength, flexural strength, and durability of concrete have been the main concern in designing of the elements. Therefore, the development of science and material in the recent decades has led to the production of Ultra-High Performance Concrete (UHPC). UHPC is a new class of concrete that exhibits remarkable mechanical and durability properties, as compared to the conventional concrete which is available commercially since 2000 [6]. The main components of UHPC which make UHPC properties special are an optimized gradation, fiber reinforcements, and its water to cementation ratio less than 0.25 which is less than conventional concrete [6, 7]. The special properties of UHPC cause the extensive interest in using UHPC in precast, pre-stressed, and field cast bridge connections. Bridge decks [8], movable decks [9], roof panels [10], precast piles and foundation of bridges on loose soils [11] are the structural elements that UHPC have been utilized to construct them.

Habel [12] demonstrated that UHPC has self-consolidation feature. This feature showed that UHPC could have a compressive strength over 150 MPa without applying any special curing during its casting. Moreover, the cost of UHPC mix design was investigated, and it was concluded that with the moderate cost it is possible to produce UHPC with enough workability [13]. Graybeal [14] investigated that the mixing procedure of conventional concrete can be implemented for UHPC mixing procedure. However, UHPC needed more input energy in its mixing procedure; therefore, ice should be used in the mixing of UHPC instead of water to produce no overheated mix.

The high energy absorption capacity is another unique feature of UHPC in high-rate loading which can prevent the collapsing of infrastructures during the earthquake and cycling loading [15]. To improve the energy absorption

* Corresponding author: mbaqe001@fiu.edu

capacity of UHPC, the concrete durability [16], the compressive encasing region of the concrete member [17], the percentage of steel reinforcement in the member [18] and the percentage of fibers in the concrete should be increased [19].

UHPC is a recently developed type of concrete which is desirable to be used in the construction of concrete members to improve design life, member strength and reduce the construction cost and weight. However, it needs more research to define its properties properly [20]. In this article the followings UHPC properties topics were discussed: UHPC constituent components, mechanical properties of UHPC such as compressive strength, compressive strain-stress behavior, tensile strain, modulus of elasticity, density, concrete cover, and bond properties of UHPC. Finally, some topics which need to be investigated were recommended.

2. UHPC Constituent Components

The UHPC was defined as concrete with a minimum 22 ksi compressive strength [21, 22]. The typical material composition of UHPC is represented in Table 1. In UHPC, fine aggregate instead of coarse aggregate combined with optimized granular mixture results homogenous, compact, and superior low porosity cementitious matrix, the same idea with epoxy grout [23]. These constituent components lead to improvement of mechanical performances, homogeneity, and ductility of UHPC in comparison with conventional concrete [24]. Implementation of fine aggregates in UHPC mix improves the homogeneity of concrete and results in different mechanical properties for UHPC [25]. UHPC's superior low porosity protects steel reinforcing bars from corrosion [26]. Fine aggregate also reduces the mixing time. As a result, the use of well-graded aggregate increased the dense packing and noticeably improves the mechanical properties of the material.

Table 1. Material Composition of Typical UHPC mix [21, 27]

Material	Amount (lb/yd^3)	Present by Weight
Portland Cement	1,200	28.5
Fine Sand	1,720	40.8
Silica Fume	390	9.3
Ground Quartz	355	8.4
Super Plasticizer	51.8	1.2
Accelerator	50.5	1.2
Steel Fibers	263	6.2
Water	184	4.4

As shown in Table 1, steel fiber as the most important constituent component is the main content that makes the UHPC properties exceptional from conventional concrete [28]. Fibers improve the mechanical properties as well as ductility of the material. Fibers act similar to the reinforcing steel in conventional reinforced concrete, but on the micro level [29, 30]. Fibers are distributed all over the mix uniformly, therefore provides consistency of tensile strength to the material. Thus, fibers content significantly promotes the tensile and shear strength, and thereby potentially eliminate or greatly reduce the need for flexural and shear reinforcements.

Moreover, fibers postpone the formation of micro-cracks, as well as controlling the crack widths and spacing [31]. These characteristics increase the stiffness of structural elements at service loads that eventually diminishes the service deflection. The high service stiffness is paramount to the design of structural elements for serviceability. The high service stiffness effectively helps engineers to design smaller sections with minimal service deflection, while still meets the deflection requirements of the building code in force.

Also, fibers content lead to non-brittle ductile behavior at ultimate capacity [32]. Ductility is the result of fibers pulls out mechanism at high loads. The gradual and controlled cracks reduce the risk of sudden failure [24]. The non-brittle ductile behavior of UHPC at ultimate loads provides a higher level of safety to the building users by showing large deflection before failure. Figure 1. summarizes how fibers content in UHPC enhance the mechanical properties and ductility, and how it affects the design.

Overall, fibers content enhance the mechanical properties and ductility of UHPC as follows:

- Increase the tensile strength and as result shear strength
- Decrease the needed reinforcement ratio
- Control cracks width
- Provide non-brittle behavior

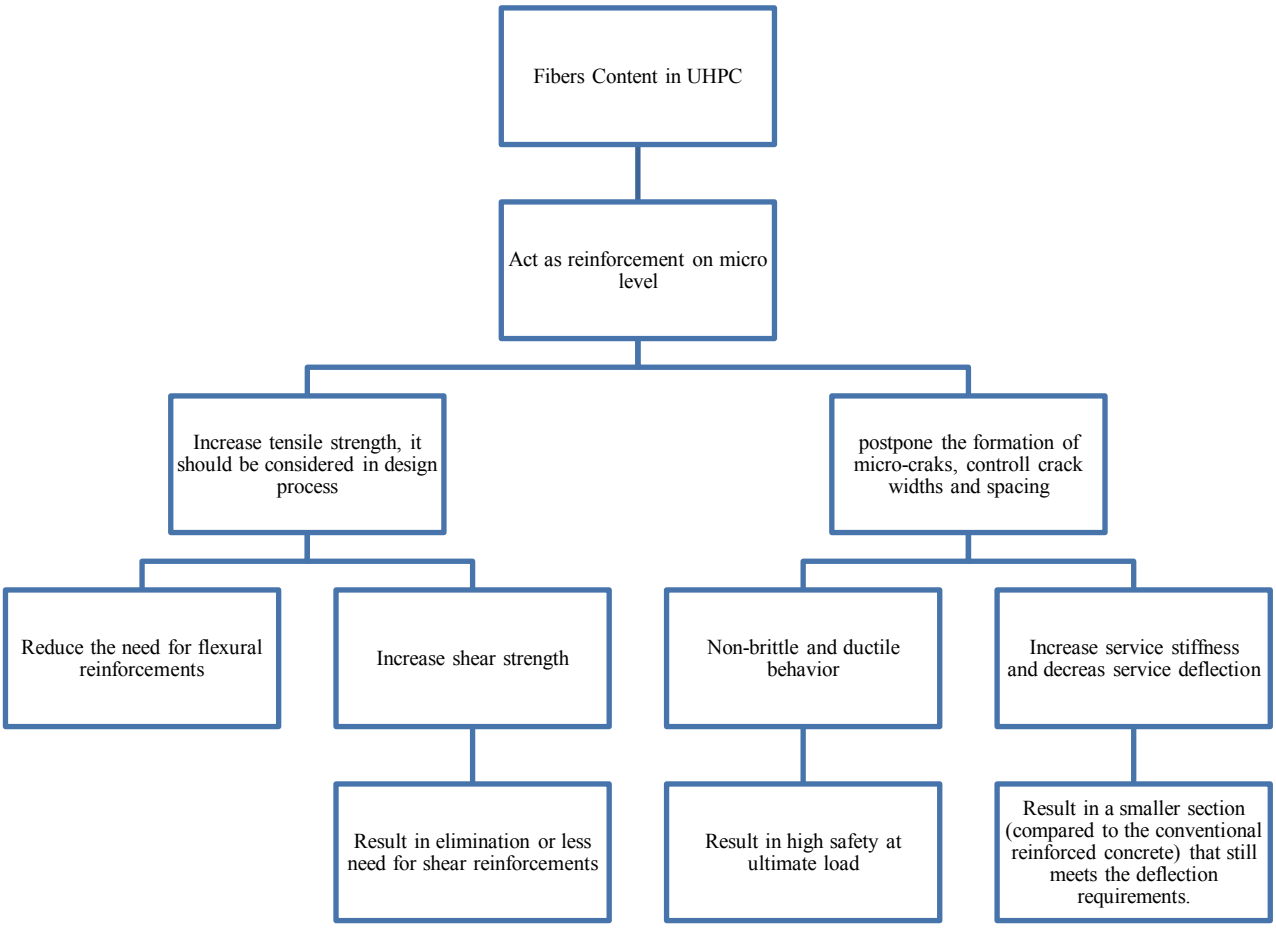

Figure 1. Fibers content in UHPC and its influence on the mechanical properties and characteristics of UHPC

3. Compressive Strength

The compressive strength of UHPC is one of the important features that are necessary for designing a member. As UHPC has different ingredients from typical concrete, it may show different behavior, especially due to the steel fibers content. Based on the research by Aaleti, Petersen [21], the 28-days compressive strength of UHPC (f'_c) depends on the curing type process. It was defied that for steam-cured and air-cured conditions, the compressive strength of concrete should be considered 24 ksi and 18 ksi, conservatively. It is even much stronger than epoxy grouts that are used in bridges cast-in field joints, and pourbacks of post-tensioned bridges [23].

Graybeal and Baby [33] recently developed an equation for UHPC which represents compressive strength gain at any age after casting cured under standard laboratory condition. By using Equation 1, it is possible to obtain concrete compressive strength by the age based on the concrete strength at 28 days.

$$f'_{ct} = f'_c \left[1 - \exp\left(-\left(\frac{t-0.9}{3}\right)^{0.6}\right)\right] \quad (1)$$

Where:

f'_{ct}: is UHPC compressive strength at age t days

f'_c: is UHPC compressive strength at 28 days

t: is time after casting in days.

To investigate the bond properties of UHPC, Graybeal [34, 35] performed an experimental test and identified that the average compressive strength of UHPC with 1 and 7 days age were 13.9 and 19 ksi, respectively. When the compressive strength of UHPC with 28 days age substitutes in the Equation 1, it cannot result in proper compressive strength for one day age concrete. Due to that, it can be concluded that this equation result may not be exact in some conditions. Thus, predicting the strength of UHPC from 28-days age concrete needs more research.

4. Compressive Strain-Stress Behaviour

For designing of members, knowing the compressive strain-stress behaviour of UHPC is essential. The strain at the peak of UHPC compressive strength is the key point in defining the concrete behaviour. It was assumed that the stress-strain behaviour of UHPC is linear and the compressive stress at the strain of 0.0035 and 0.004 can be used for air and steam-cured condition, respectively [21]. Moreover, French [36], Australian [37], and Japanese [38] UHPC designing manual recommend stress-strain behaviour as a trilinear curve, which is shown in Figure 2.

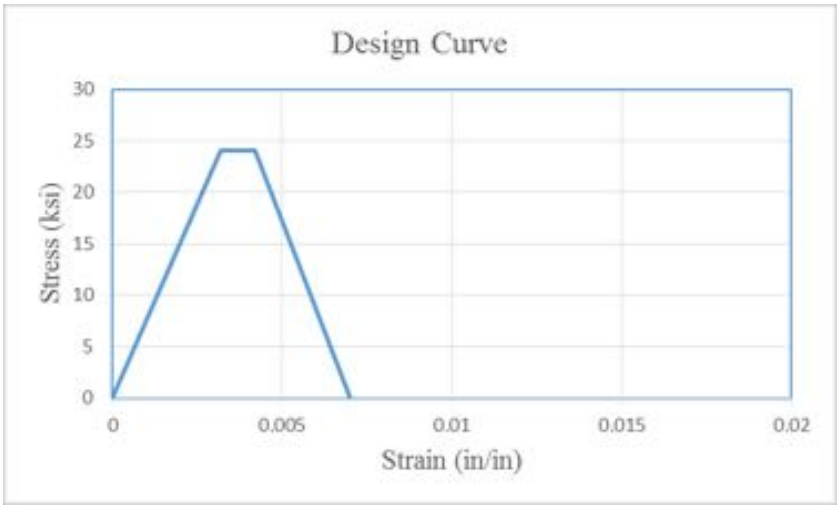

Figure 2. Trilinear stress- strain behavior [36-38]

5. Tensile Strength

As previously stated, steel fibers in UHPC act as reinforcing steel in a micro level and cause an improvement in tensile and shear strength of the concrete compare with the typical concrete. Another important factor that affects the tension strength of UHPC is the curing type and condition. Aaleti, Petersen [21] recommended that cracking tensile strength of UHPC should be taken 1.3 ksi and 0.9 ksi for steam and air-cured condition as shown in Figure 3. Graybeal and Baby [33] also obtained Equation 2. to compute the tensile strength of UHPC using measured compressive strength.

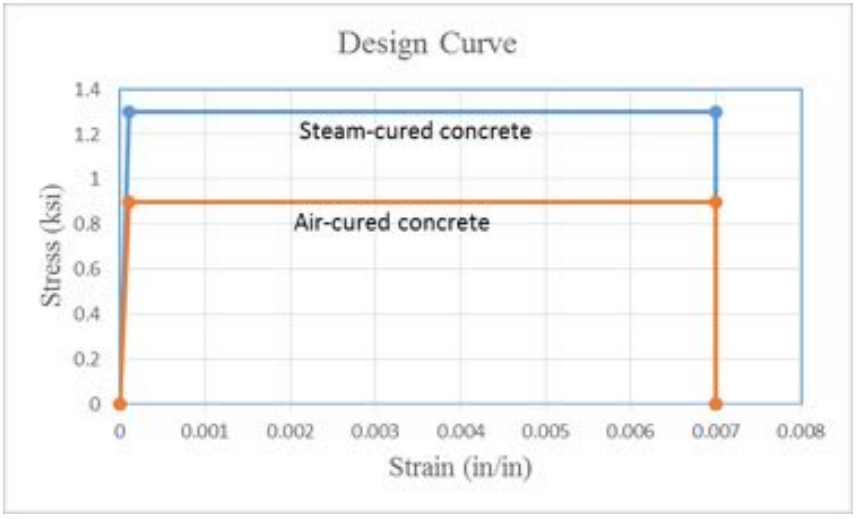

Figure 3. Tensile stress-strain behaviour [21]

$$f_t = K\sqrt{f'_c} \quad (2)$$

Where:

f_t: is tensile strength

f'_c: is compressive strength of 28 days age in psi unit

K: is a constant factor which is 6.7, 7.8 and 8.8 for the untreated, air-cured, and steam-cured specimen, respectively.

However, by comparing UHPC with conventional concrete, UHPC offers about a four-fold increase in tensile strength. In the designing of elements with conventional reinforced concrete, tensile strength is neglected due to its very low strength. However, it is totally different in UHPC in which high tensile is greatly beneficial in the design process of structural elements, and results in the magnificent lower need for reinforcing steel bars. As previously stated, the high tensile capacity of UHPC originated from the fibers used in UHPC. Accordingly, the tensile strength of UHPC is high enough to be considered in the designing of elements. Another difference in tensile strength is that UHPC showed very similar post cracking and pre-cracking capacity, as opposed to the conventional concrete that cannot carry loads after cracking [39]. This tensile capacity means UHPC still can almost maintain its ultimate capacity even after cracking. This phenomenon, high post-cracking strength, also brings a higher level of safety to the elements made by UHPC.

6. Modulus of Elasticity

As discussed, UHPC displays a linear stress-strain behaviour. There are some methods suggested to find the relationship between compressive strength and modulus of Elasticity. The best equation that meets the experimental results is suggested by Graybeal [39]. It is based on the general form of AASHTO equation and value of f'_c between 4 and 28 ksi. Also, it was suggested that in the absence of exact concrete strength, the value of 7,500 ksi can be used as the UHPC modulus of elasticity. Moreover, other studies suggest the value of 7,600 ksi [40], 8,100 ksi [41], and 7,300 ksi [42] as the UHPC modulus of elasticity.

$$E = 46{,}200\sqrt{f'_c} \tag{3}$$

Where:

E: is modulus of elasticity in psi unit

f'_c: is compressive strength at 28 days age in psi

7. Density

In the absence of coarse aggregates, UHPC has a self-compacted feature. It is much compacted than typical concrete. It is recommended that unit weight of UHPC should be considered between 155 lb/ft^3 and 160 lb/ft^3 [21, 27].

8. Concrete Cover

The concrete cover is important for durability and development of concrete bond strength. The Japanese Society of Civil Engineering [38] and Australian code for UHPC [37] require a minimum of 0.75 inches of concrete cover for uncoated concrete. The research performed by Aaleti, Petersen [21] suggested that the minimum concrete cover should be 1.5 times of the strand diameter for prestressing strands. They also suggested that reinforcement with strands should have a clear spacing of 3.25 times the reinforcement diameter or 1.5 inches, which one is greater.

9. Summary of Mechanical Properties of UHPC

Table 2. summarizes the mechanical properties of UHPC for designing purpose, based on the reviewed studies and comparison of different paper results.

Table 2. Summary of UHPC mechanical properties

Characteristic	Property
Compressive Strength	It depends on the percentage of fiber reinforcements in UHPC. For the designing purpose, using 18 and 24 ksi as 28-days age UHPC were recommended for the steam-cured and air-cured condition, respectively.
Tensile Strength	Its range is between 0.9 and 1.3 ksi. Using the following equation was conservative. $f_{ct} = 6.7\sqrt{f'_c}$
Modulus of Elasticity	$E(psi) = 46{,}200\sqrt{f'_c}(psi)$ or 7,300 to 7,500 ksi for 28-days age UHPC
Strain at peak compressive strength	Its range is between 0.0035 and 0.004. Using 0.0032 was recommended.
Density	Its range was between 155 lb/ft^3 and 160 lb/ft^3.
Poisson's ratio	0.2

As shown in Table 2, the UHPC has unique properties and high density in comparison with conventional concrete.

The high density of UHPC causes the small permeability of UHPC and leading the high durability of UHPC. Moreover, the maximum residual tensile strain of 0.13 in low permeability in tensile deformation test was observed [43].

10. Bond Properties of UHPC

As the ingredients of UHPC are different from conventional concrete, it shows different behavior and development length. The existence of fiber reinforcement in UHPC allows the material to have the tensile capacity beyond the cracking of cementations matrix, which can cause a reduction in development length of reinforcement bar. The amount of fiber reinforcement can be the important component that effects on the UHPC behavior and consequently represents different bond behaviour. The purpose of this section is an investigation on different factors that can influence the bond behaviour of UHPC and development length of rebars.

The term that is important in investigating bond properties of UHPC is the average bond strength at bond failure. This term exhibits the load transfer between reinforcement bar and surrounding concrete, which it is represented as equation bellow [21].

$$\mu_{Test} = \frac{f_{s,max}\ \pi\ {d_b}^2/4}{\pi\ d_b\ l_d} = \frac{f_{s,max}\ d_b}{4\ l_d} \quad (4)$$

Where:

l_d: Embedment length
μ_{Test}: Average bond strength of at bond failure
d_b: Bar size
$f_{s,max}$: Reinforcement stress at failure

Saleem, Mirmiran [44] investigated the development length of #10 and #22 reinforcing Grade 60 steel bars. They showed that #10 and #22 rebar require 12 and 18 times the rebar diameter development length. Another recent study represented that 20 to 40 times of rebar diameter is needed for development length of UHPC elements [45]. Also, it was concluded that casting orientation did not make an effect on the bond behavior of UHPC [34]. It was reported that increasing the embedment length improved the bond strength. Furthermore, bond strength and bond length relation are nearly linear.

Side cover C_{s0} is another factor that has effect on the development length. It is the factor that defines the failure mode of a member. The concrete failure may happen in concrete cover, if the side cover being less than half of the bar spacing (C_{si}). It was found that maximum bar stress at bond failure increased as side cover increases. When the side cover is large enough, the bar spacing controls the bond strength of UHPC [46].

Graybeal [34] reported that when bar spacing is less than half of the side cover ($2C_{si} \leq C_{s0}$), the bond strength controls by bar spacing ($2C_{si}$). If the bar spacing being between side cover and lap splice length l_s times ($tan\,\theta$), ($C_{s0} < 2C_{si} \leq l_s\ tan\,\theta$) -- θ is angle between diagonal cracks and testing bar -- the bond strength controls by side cover. Finally, if ($2C_{si} > l_s\ tan\,\theta$), the bond strength controls by mechanical properties of UHPC. Thus, the compressive strength, material properties, and compressive strength effect on the bond strength of UHPC should be considered, because the UHPC properties cannot be effectively represented by the μ_{Test} and f'_c [47].

Based on the Graybeal results, the minimum development length is $8d_b$ with minimum side cover of $3d_b$; bar spacing between $2d_b$ and $l_s\ tan\,\theta$; and minimum compressive strength of 13.5 ksi. For lap splice l_s a minimum of 75 percent of embedment length was suggested. In a situation, which the side cover is between $2d_b$ and $3d_b$, the minimum embedment length should increase to $10d_b$. Another recently conducted research also concluded that $8d_b$ development length is enough for rebars with $3d_b$ side cover [48]. The results indicated that bars with larger diameter have less bond strength in comparison to smaller bar size; therefore, larger bar diameter needs larger embedment length.

Saleem, Mirmiran [44] suggested that for #10 and #22 bars with compressive strength of 24 ksi in 28-days age, and a clear side cover of 0.51 inches, development length should be $12d_b$ and $18d_b$, respectively. Moreover, they indicated that ACI 318-08 and AASHTO are overestimated the development length; while ACI 408R-03 provided a reasonable development length. Another research showed that about $20d_b$ to $40d_b$ transfer length is needed for UHPC sections [49].

11. Discussion

Using UHPC in the construction of bridges and buildings has been in high interest. Due to its high strength and durability, UHPC is using wide-spread. However, regardless of needed special inspection in selecting the UHPC material, components, and curing process, it needs special techniques and attention for its designing. These critical inspections and attention are needed to be sure about the produced elements strength and durability which can cause different mechanical properties for produced UHPC. One of the UHPC constituent components which play an

essential role in the mechanical properties of UHPC is the fiber. The using fibers percentage in the UHPC can change the UHPC properties significantly. Fibers should be uniformly distributed in the mixing process. Therefore, the effect of different percentage of fibers in the UHPC on the required development length and bond properties of UHPC can be one of the interesting topics that need more research.

Based on the review of published and experimental works on mechanical properties and bond behaviour of UHPC, UHPC provides two major exceptional mechanical characteristics: (1) High compressive strength, and; (2) High tensile strength, compared to the typical concrete [50]. In addition, UHPC's high tensile strength and strain hardening properties improve serviceability performance through the increased stiffness, reduced deflection, and postponement of formation of localized macro-cracks [12]. As compared to conventional reinforced concrete, it is clear that there is no general information about the mechanical properties, bond behavior, and especially the required development length and bond properties of UHPC. Moreover, UHPC which has amended properties shows high early compression strength, durability, and ease of placement. Several technical papers were reviewed, and the typical UHPC properties that can be used in designing the members constructed by UHPC was recommended. It should be noted that UHPC with the different component may represent different properties. However, these topics need more research. For example, the effect of different rebar size on the bond behaviour and development length of UHPC. As UHPC has high strength capacity, using High Strength Steel (HSS) in UHPC is valuable to increase the strength capacity of the member [10, 51]. Thus, determining the required development length of HSS bar in the UHPC sections is worthwhile.

The UHPC has a compressive strength of 22 ksi and greater, which is four to eight times of the conventional concrete, and high tensile strength of 0.9 to 1.3 ksi [35, 39], opposed to the 0.3 to 0.7 ksi of normal concrete. Both pre and post-cracking strength of UHPC are noticeably greater than the conventional concrete [39]. These significant improvements, especially tensile strength, considerably enhance the design of flexural elements made of UHPC. Unlike the approach utilized in the design of traditional reinforced concrete-- that neglects the tensile strength of conventional concrete -- the tensile strength of UHPC should be considered in the design process. High compressive strength significantly reduces the size of compressive elements (e.g. columns), while tensile strength greatly affects the size of flexural elements and members subjected to shear forces. Thus, UHPC's high compressive and tensile strength result in superior structural elements in a small section size.

12. Conclusion

In this article, the mechanical properties of UHPC and its differences with the conventional concrete is reviewed, and the recent developments in the defining the properties of UHPC are reported. It is obvious that there are no globally acceptable properties for the UHPC to be used in the designing of the members with UHPC. In this case, according to the reviewed researches, the acceptable properties of UHPC by different researchers which can be used in the designing of the UHPC members are recommended. Moreover, some special topics which need more research are identified.

13. References

[1] Fesharaki, M. and A. Hamedi, EFFECTS OF HIGH-SPEED RAIL SUBSTRUCTURE ON GROUND-BORNE VIBRATIONS. 2016. Florida Civil Engineering Journal, 2016. 2: p. 38–47.

[2] Fesharaki, M. and T.-L. Wang, The Effect of Rail Defects on Track Impact Factors. Civil Engineering Journal, 2016. 2(9): p. 458-473.

[3] Hamedi, A., Ketabdar, M., Fesharaki, M., & Mansoori, A., Nappe Flow Regime Energy Loss in Stepped Chutes Equipped with Reverse Inclined Steps: Experimental Development. Florida Civil Engineering Journal, 2016. 2: p. 28-37.

[4] Ali, H. and Mohammadafzali, M. , Asphalt Surface Treatment Practice in Southeastern United States, Louisiana Transportation Research Center. 2014.

[5] Ali, H. Massahi, Aidin, Hesham Ali, Farshad Koohifar, and Mojtaba Mohammadafzali. Analysis of pavement raveling using smartphone. In Transportation Research Board 95th Annual Meeting, no. 16-6155. 2016.

[6] Russell, H.G. and B.A. Graybeal, Ultra-high performance concrete: A state-of-the-art report for the bridge community. 2013.

[7] Azizhemmatlou, Y., Hamedi, A., Farbehi, H., Iranyar, D. The Optimum water to cement ratio for designing impermeable water storage tanks. in 1st International Conference on Non Osmosis Concrete(1st ICNOC)-Water Storage Tanks. Guilan, Iran. 2011.

[8] Ghasemi, S., et al., Novel UHPC-CFRP Waffle Deck Panel System for Accelerated Bridge Construction. Journal of Composites for Construction, 2015. 20(1): p. 04015042.

[9] Ghasemi, S., et al., A super lightweight UHPC–HSS deck panel for movable bridges. Engineering Structures, 2016. 113: p. 186-193.

[10] Amir-sayyafi, E., A.G. Chowdhury, and A. Mirmiran. A supper Lightweight Hurrican-Resistant Thin-Walled Box-cell

Roofing System. in International Symposium on Structural Engineering, 2016, in press.

[11] Baqersad, M., Haghighat, A. E., Rowshanzamir, M., & Bak, H. M., Comparison of Coupled and Uncoupled Consolidation Equations Using Finite Element Method in Plane-Strain Condition. Civil Engineering Journal, 2016. 2(8): p. 375-388.

[12] Habel, K., et al., Ultra-high performance fibre reinforced concrete mix design in central Canada. Canadian Journal of Civil Engineering, 2008. 35(2): p. 217-224.

[13] Holschemacher, K. and D. Weiße, Economic Mix Design Ultra High-Strength Concrete. Seventh International Symposium on the Utilization of High-Strength/High-Performance Concrete, 2005. Vol. II: p. 133–1,144.

[14] Graybeal, B.A., Characterization of the behavior of ultra-high performance concrete. 2005.

[15] Tran, N.T., et al., Fracture energy of ultra-high-performance fiber-reinforced concrete at high strain rates. Cement and Concrete Research, 2016. 79: p. 169-184.

[16] King, K.W., J.H. Wawclawczyk, and C. Ozbey, Retrofit strategies to protect structures from blast loading This article is one of a selection of papers published in the Special Issue on Blast Engineering. Canadian Journal of Civil Engineering, 2009. 36(8): p. 1345-1355.

[17] Aboutaha, R.S. and R. Machado, Seismic resistance of steel confined reinforced concrete (SCRC) columns. The Structural Design of Tall Buildings, 1998. 7(3): p. 251-260.

[18] ALlexander, S. and S.H. Simmonds, Punching shear tests of concrete slab-column joints containing fiber reinforcement. Structural Journal, 1992. 89(4): p. 425-432.

[19] Kim, J.J., et al., High-rate tensile behavior of steel fiber-reinforced concrete for nuclear power plants. Nuclear Engineering and Design, 2014. 266: p. 43-54.

[20] Abbas, S., M. Nehdi, and M. Saleem, Ultra-High Performance Concrete: Mechanical Performance, Durability, Sustainability and Implementation Challenges. International Journal of Concrete Structures and Materials, 2016. 10(3): p. 271-295.

[21] Aaleti, S., B. Petersen, and S. Sritharan, Design Guide for Precast UHPC Waffle Deck Panel System, Including Connections. 2013.

[22] Saleem, M.A., et al., Ultra-high-performance concrete bridge deck reinforced with high-strength steel. ACI Structural Journal, 2011. 108(5): p. 601.

[23] Ahmad, I., Suksawang, N., Sobhan, K., Corven, J., Sayyafi, E. A., Pant, S., & Martinez, F., Develop Epoxy Grout Pourback Guidance and Test Methods to Eliminate Thermal/Shrinkage Cracking at Post-Tensioning Anchorages: Phase II. 2015.

[24] Richard, P. and M. Cheyrezy, Composition of reactive powder concretes. Cement and concrete research, 1995. 25(7): p. 1501-1511.

[25] Ma, J., et al. Comparative investigations on ultra-high performance concrete with and without coarse aggregates. in Proceedings of international symposium on ultra high performance concrete, Germany. 2004.

[26] Scheydt, J.C. and H. Müller. Microstructure of ultra high performance concrete (UHPC) and its impact on durability. in The 3rd International Symposium on UHPC and Nanotechnology for High Performance Construction Materials, Kassel, Germany. 2012.

[27] Yuan, J. and B.A. Graybeal, Bond behavior of reinforcing steel in ultra-high performance concrete. 2014.

[28] Barnett, S.J., et al., Assessment of fibre orientation in ultra high performance fibre reinforced concrete and its effect on flexural strength. Materials and Structures, 2010. 43(7): p. 1009-1023.

[29] Perry, V. and D. Zakariasen. Overview of UHPC technology, materials, properties, markets and manufacturing. in Proceedings of the 2003 Concrete Bridge Conference. 2003.

[30] Harris, D.K. and C.L. Roberts-Wollmann, Characterization of the punching shear capacity of thin ultra-high performance concrete slabs. 2005.

[31] Reda, M., N. Shrive, and J. Gillott, Microstructural investigation of innovative UHPC. Cement and Concrete Research, 1999. 29(3): p. 323-329.

[32] AFGC-SETRA, U.H.P.F., Reinforced Concretes. Interim Recommendations, AFGC Publication, France, 2002.

[33] Graybeal, B.A. and F. Baby, Development of Direct Tension Test Method for Ultra-High-Performance Fiber-Reinforced Concrete. ACI Materials Journal, 2013. 110(2).

[34] Graybeal, B.A., Splice length of prestressing strands in field-cast UHPC connections. Materials and Structures, 2015. 48(6): p. 1831-1839.

[35] Graybeal, B., Design and construction of field-cast UHPC Connections. 2014.

[36] BFUP, A., Ultra-High Performance Fibre-Reinforced Concretes. Interim Recommendations, AFGC publication, France, 2002.

[37] Gowripalan, N. and R. Gilbert, Design Guidelines for Ductal Prestressed Concrete Beams. Reference Artical, The University of NSW, 2000.

[38] Rokugo, K., Recommendations for design and construction of High Performance Fiber Reinforced Cement Composites with multiple fine cracks (HPFRCC). 2008: Japan Society of Civil Engineers, Concrete Committee.

[39] Graybeal, B.A., Material property characterization of ultra-high performance concrete. 2006.

[40] Standard Test Method for Static Modulus of Elasticity and Poisson’s Ratio of Concrete in Compression. 2014, ASTM International.

[41] Graybeal, B.A., Flexural behavior of an ultrahigh-performance concrete I-girder. Journal of Bridge Engineering, 2008. 13(6): p. 602-610.

[42] Hassan, A. and S. Jones, Non-destructive testing of ultra high performance fibre reinforced concrete (UHPFRC): A feasibility study for using ultrasonic and resonant frequency testing techniques. Construction and Building Materials, 2012. 35: p. 361-367.

[43] Cheyrezy, M. and M. Behloul, Creep and shrinkage of ultra-high performance concrete. Creep, Shrinkage and Durability Mechanics of concrete and other Quasi-Brittle Materials", édité par F.-J. Ulm, ZP Ba. ant and FH Witmann, Elsevier, Cambridge, 2001: p. 527-538.

[44] Saleem, M.A., et al., Development length of high-strength steel rebar in ultrahigh performance concrete. Journal of Materials in Civil Engineering, 2012. 25(8): p. 991-998.

[45] Ronanki, V.S., D.B. Valentim, and S. Aaleti, Development length of reinforcing bars in UHPC: An experimental and analytical investigation.

[46] Vic Perry, F., et al., Innovative Field Cast UHPC Joints for Precast Bridge Systems–3-span Live Load Continuous. 2010.

[47] Hassan, A., S. Jones, and G. Mahmud, Experimental test methods to determine the uniaxial tensile and compressive behaviour of ultra high performance fibre reinforced concrete (UHPFRC). Construction and building materials, 2012. 37: p. 874-882.

[48] Ronanki, V.S., D.B. Valentim, and S. Aaleti, Development length of reinforcing bars in UHPC: An experimental and analytical investigation. 2016.

[49] John, E., et al., Transfer and development lengths and prestress losses in ultra-high-performance concrete beams. Transportation Research Record: Journal of the Transportation Research Board, 2011(2251): p. 76-81.

[50] Prem, P., B. Bharathkumar, and R.I. Nagesh, Mechanical properties of ultra high performance concrete. World academy of Science, Engineering and Technology, 2012(68): p. 1969-1978.

[51] Ghasemi, S., Innovative Modular High Performance Lightweight Decks for Accelerated Bridge Construction. 2015.

Civil Engineering Journal

E-ISSN: 2476-3055

Civil Engineering Journal is a multidisciplinary, an open-access, internationally double-blind peer -reviewed journal concerned with all aspects of civil engineering, which include but are not necessarily restricted to:

Building Materials and Structures, Coastal and Harbor Engineering, Constructions Technology, Constructions Management, Road and Bridge Engineering, Renovation of Buildings, Earthquake Engineering, Environmental Engineering, Geotechnical Engineering, Highway Engineering, Hydraulic and Hydraulic Structures, Structural Engineering, Surveying and Geo-Spatial Engineering, Transportation Engineering, Tunnel Engineering, Urban Engineering and Economy, Water Resources Engineering, Urban Drainage.

Mailing Address: Dr. Kavianpour office, 3rd Floor of Civil Engineering Faculty, K. N. Toosi University of Technology, No. 1346, Vali Asr Street, Mirdamad Intersection, Tehran, Iran

Phone: +98-21-88779475-ext. 258 **Fax:** +98-21-88779674

Email: kavianpour@civilejournal.org